



<https://theses.gla.ac.uk/>

Theses Digitisation:

<https://www.gla.ac.uk/myglasgow/research/enlighten/theses/digitisation/>

This is a digitised version of the original print thesis.

Copyright and moral rights for this work are retained by the author

A copy can be downloaded for personal non-commercial research or study,
without prior permission or charge

This work cannot be reproduced or quoted extensively from without first
obtaining permission in writing from the author

The content must not be changed in any way or sold commercially in any
format or medium without the formal permission of the author

When referring to this work, full bibliographic details including the author,
title, awarding institution and date of the thesis must be given

Enlighten: Theses

<https://theses.gla.ac.uk/>
research-enlighten@glasgow.ac.uk

**PREPARATION, CHARACTERIZATION AND
TESTING OF NICKEL CATALYSTS FOR THE
AMINATION OF ETHANOL**

THESIS

SUBMITTED TO THE UNIVERSITY OF GLASGOW

FOR THE DEGREE

OF

MASTER OF SCIENCE

BY

ACHMAD HANAFI SETIAWAN

DEPARTMENT OF CHEMISTRY

AUGUST, 1993

ProQuest Number: 10992245

All rights reserved

INFORMATION TO ALL USERS

The quality of this reproduction is dependent upon the quality of the copy submitted.

In the unlikely event that the author did not send a complete manuscript and there are missing pages, these will be noted. Also, if material had to be removed, a note will indicate the deletion.



ProQuest 10992245

Published by ProQuest LLC (2018). Copyright of the Dissertation is held by the Author.

All rights reserved.

This work is protected against unauthorized copying under Title 17, United States Code
Microform Edition © ProQuest LLC.

ProQuest LLC.
789 East Eisenhower Parkway
P.O. Box 1346
Ann Arbor, MI 48106 – 1346

Thesis
9597
copy 1



Acknowledgements

My special gratitude goes to my supervisors, Prof.G.Webb and Dr.D.Stirling who encouraged me and gave me all the support during the research and all the assistance I could have asked for .

Special thanks and appreciation go to the Foreign and Commonwealth Office Scholarships and Awards Scheme(FCOAS) through the British Council for their financial support ; Prof.D.W.A. Sharp and the Research and Development Centre for Applied Chemistry for encouragement and also to the technological deputy of the chairman of Indonesia Institute of Science for the recommendation of my subject for research study.

I should also like to thank my colleagues in the surface chemistry group for their helpful comments and guidance in the laboratory .

I am deeply grateful to all technicians for all their help in the maintenance of the equipment in the surface chemistry laboratory at Glasgow University .

Summary.

Three types of nickel metal catalyst supported on silica gel have been prepared using impregnation, ion exchanged sodium hydroxide and ion exchanged ammonia methods, in order to investigate the influence of preparation methods on metal dispersion and catalyst structure. All the catalyst samples had a nominal nickel loading of 5 percent(w/w). After preparation, the catalysts were activated by a drying stage followed by calcination and reduction. Various spectroscopic techniques were then used to characterize the catalyst precursors and the amination of ethanol was used to test the activity of each reduced catalyst.

The result of transferring the nickel salt to the support phase has shown that the impregnation method was the most efficient, the least efficient being the ion exchanged sodium hydroxide method where 0.09 percent sodium was left in the precursor.

Elemental analysis, uv-vis spectroscopy, thermogravimetry and X-ray diffraction have been used to identify the phases present in each precursor. Temperature programmed reduction has been used to investigate the reducibility of each calcined catalyst and carbon monoxide chemisorption used to determine the percentage dispersion and to estimate the total nickel metal surface area for each reduced catalyst. The results from the characterization experiments have shown that the nickel species obtained by the impregnation method interacted weakly with the silica support whereas the ion exchanged nickel interacted strongly with the support.

XRD analysis of the calcined catalysts showed that nickel(II) oxide (bunsenite) was formed as the predominant component in the impregnated sample. However, analysis of the ion exchanged sample did not show any evidence for nickel(II) oxide although it was present in very small concentrations as indicated by TPR studies.

Carbon monoxide chemisorption studies showed that the nickel is poorly dispersed in the impregnated sample, and highly dispersed in the ion exchanged sample prepared by the ammonia method. The dispersion was lower for the catalyst prepared by the sodium hydroxide method due to the formation of sodium nickel silicates which were difficult to reduce.

Thermogravimetry and temperature programmed reduction showed that the nickel(II) ions in the ion exchanged sample not only exchanged with hydrogen on the silica surface but also partially combined with the support to form a hydrosilicate type compound. Non-interacting nickel(II) oxide present in the impregnated sample was easily reduced, while strongly bound or combined nickel(II) oxide present in the ion exchanged sample contained three nickel species, that is, an easily reduced species, a less easily reduced form and a very difficult to reduce species.

The amination of ethanol over these catalysts has been found to take place at 503 K with methane being formed as a by-product. The ion exchanged sample prepared by the ammonia method gave the highest yield of ethylamine although its specific activity/m² nickel metal was similar to the sample prepared by the impregnation method. The retained sodium in the ion exchanged sodium hydroxide catalyst poisoned metal sites for ethanol amination.

Contents.

ACKNOWLEDGEMENTS

SUMMARY

CHAPTER ONE I N T R O D U C T I O N .

- 1.1. General introduction.

- 1.2. Catalyst preparation.
 - 1.2.1. Silica gel as the support material.
 - 1.2.2. Preparation techniques.

- 1.3. Catalyst activation .
 - 1.3.1. Drying.
 - 1.3.2. Calcination.
 - 1.3.3. Reduction.

- 1.4. Catalyst characterization .
 - 1.4.1. Bulk composition.
 - 1.4.2. Electronic properties.
 - 1.4.3. Infrared spectroscopy.
 - 1.4.4. Bulk structure.
 - 1.4.5. Thermal characterization.
 - 1.4.6. Chemisorption.

- 1.5. Catalyst testing .
 - 1.5.1. Amination of ethanol
 - 1.5.2. Optimum condition.
 - 1.5.3. Mechanism.
 - 1.5.4. Catalyst deactivation.

CHAPTER TWOO B J E C T I V E S

CHAPTER THREEEXPERIMENTAL

- 3.1. Catalyst preparation .
 - 3.1.1. Impregnation method.
 - 3.1.2. Ion exchange sodium hydroxide method.
 - 3.1.3. Ion exchange ammonia method.

- 3.2. Catalyst characterization.
 - 3.2.1. Determination of metal content by atomic absorption spectroscopy and flame photometry.
 - 3.2.2. Determination of nitrogen and hydrogen content by elemental analysis.
 - 3.2.3. Determination of the electronic ground state by uv-vis and diffuse reflectance spectroscopy.
 - 3.2.4. Infrared studies.
 - 3.2.5. X-ray diffraction studies.
 - 3.2.6. Thermogravimetry
 - 3.2.7. Temperature programmed reduction.
 - 3.2.8. Determination of nickel metal surface area by carbon monoxide chemisorption.

- 3.3. The amination of ethanol.
 - 3.3.1. Introduction.

- 3.3.2. **Materials.**

- 3.3.3. **Apparatus.**
 - 3.3.3.1. **The microcatalytic reactor system.**
 - 3.3.3.2. **The feed system.**
 - 3.3.3.3. **The analytical system.**

- 3.3.4. **Preparation of the catalysts.**

- 3.3.5. **Setting the gas chromatography PE 8500.**

- 3.3.6. **Test reaction.**

- 3.3.7. **Products analysis.**

CHAPTER FOUR..... RESULTS AND DISCUSSION

- 4.1. **Chemical analysis of the precursors.**
 - 4.1.1. **Studies of the precursors by atomic absorption spectroscopy.**

 - 4.1.2. **Studies of the eluents from the ion exchange column by uv-vis spectroscopy.**

 - 4.1.3. **Studies of the precursors by elemental analysis and flame photometry.**
 - 4.1.3.1. **Calcined silica gel as a reference sample.**
 - 4.1.3.2. **Impregnated sample.**
 - 4.1.3.3. **Ion exchanged sodium hydroxide sample.**
 - 4.1.3.4. **Ion exchanged ammonia sample.**

- 4.2. **The electronic ground state of dried precursors.**

- 4.2.1. Impregnated precursors.
- 4.2.2. Ion exchanged sodium hydroxide precursors.
- 4.2.3. Ion exchanged ammonia precursors.

- 4.3. Studies of the precursors by FTIR.
 - 4.3.1. Reference spectra.

 - 4.3.2. Impregnation method.
 - 4.3.2.1. Dried sample.
 - 4.3.2.2. Calcined sample.

 - 4.3.3. Ion exchanged sodium hydroxide method.
 - 4.3.3.1. Dried sample.
 - 4.3.3.2. Calcined sample.

 - 4.3.4. Ion exchanged ammonia method.
 - 4.3.4.1. Dried sample.
 - 4.3.4.2. Calcined sample.

- 4.4. The bulk structure of the dried, calcined and reduced precursors.
 - 4.4.1. Impregnated sample.
 - 4.4.2. Ion exchanged samples.

- 4.5. The decomposition of the dried precursors.
 - 4.5.1. Impregnated sample.
 - 4.5.2. Ion exchanged sodium hydroxide sample.
 - 4.5.3. Ion exchanged ammonia sample.

- 4.6. The reducibility of the calcined precursors.
 - 4.6.1. Impregnated sample.
 - 4.6.2. Ion exchanged sodium hydroxide sample.

4.6.3. Ion exchanged ammonia sample.

4.7. Determination of the nickel metal surface areas of the catalyst by CO chemisorption.

4.8. The amination reaction.

CHAPTER FIVECONCLUSIONS.

R E F E R E N C E S.

CHAPTER ONE

INTRODUCTION

1.1. General Introduction.

Catalytic processes play a vital role in the production of a wide variety of raw materials for both the chemical and petroleum industries. The majority of these processes are heterogeneous in nature (1,2). In the U.S.A. in the 1980s nearly half the total production of main chemical products depended upon catalytic processes, 85 percent of which were heterogeneous processes (2). The advantage of the heterogeneous catalyst is its ability to maximise the formation of a desired product compared with the undesirable by-products (1). A general classification of the selectivities of catalysts to particular types of reaction was proposed by G.C.Bond (3) as illustrated in table 1.1 . It can be seen from the table that nickel metal can function as a hydrogenation, dehydrogenation, hydrogenolysis or oxidation catalyst. In industrial processes, for example, nickel based catalysts are used in the hydrogenation of vegetable oil to produce margarine (2) and the dehydroamination of alcohols to produce amines which are the main raw materials in producing fabric softeners, emulsion stabilizers and corrosion inhibitors (4) .

The ability of a substance to act as a catalyst in a specific system depends on its chemical nature i.e. the specific chemical properties of the surface of the catalyst (5). The development of the catalyst is highly dependant on its precursor structure and this is largely determined by the method of

Table 1.1.: Classification of catalysts.

CLASS	REACTIONS	EXAMPLES
Metal	hydrogenation dehydrogenation hydrogenolysis oxidation	Fe, Ni, Pd, Pt, Ag ..
Semiconducting oxides and sulphides	oxidation dehydrogenation desulphurization hydrogenation	NiO, ZnO, MnO ₂ , Cr ₂ O ₃ , Bi ₂ O ₃ -MoO ₃ , WS ₂ .
Insulator oxides	dehydration	Al ₂ O ₃ , SiO ₂ ., MgO .
Acids .	polymerisation isomerisation cracking alkylation	H ₃ PO ₄ , H ₂ SO ₄ SiO ₂ -Al ₂ O ₃ .

preparation (4). The usefulness of an industrial catalyst includes the ability to resist deactivation by sintering processes. Sintering is a condition in which metal particles agglomerate to form larger crystallites (6). In an effort to avoid this condition, it is common practice to disperse the active ingredient on the support surface. Typical support materials include silica gel, alumina and zeolites (7). For a catalytic reaction to proceed, there must be some surface interaction between the catalyst and the reactant but this interaction must not permanently change the chemical nature of the catalyst (6,7). A knowledge of the nature of the active component(s) of the catalyst, their interaction with the support and their capacity to adsorb reactants and desorb products is necessary in order to meet these requirements.

Various spectroscopic techniques can be used to obtain this information (6,8). The usefulness of the catalyst is often determined by its selectivity. Selectivity is the term used to describe the ability of catalysts to direct the conversion to the formation of one or more desired products (2). It is expressed as the percentage of the consumed reactant that forms the desired product (8).

1.2. Catalyst Preparation.

Catalyst preparation techniques include impregnation, precipitation, and ion exchange (2,9). These techniques involve contact of the support with a solution containing a soluble salt of the metal being added. The impregnation

technique involves filling the pores of the support with the metal salt solution (9,10). The precipitation technique involves precipitation of a salt or hydroxide of the active component of the catalyst onto the support (10), and the ion exchange technique involves exchange of the ions in the salt solution with acidic protons on the support surface (9,11).

1.2.1. Silica gel as the support material.

Porous silica is commonly produced through the polymerisation of silicic acid (9). Molecules of silicic, disilicic and trisilicic acid are condensed to form a macromolecular silicic acid, which then grows into a polymeric particle in the colloidal state. During the condensation, gelation occurs and an interaction between the hydroxyl groups of different particles takes place to form a "hydrogel" which forms a porous silica gel called a "xerogel" after washing and drying .

The properties of the silica are influenced by every step of its preparation such as pH conditions during condensation process, surface tension of water contained in the hydrogel and aging of the gel (12,13). Gasil 35 is one example of the wide pore silicas which contain primary, secondary and tertiary particles and their related pore structure (figure 1.1). These units are contained within quaternary particles whose size varies from 100 μ in unmicronised to 5 μ in the micronised silica. The pores within the secondary particles (primary pores) are

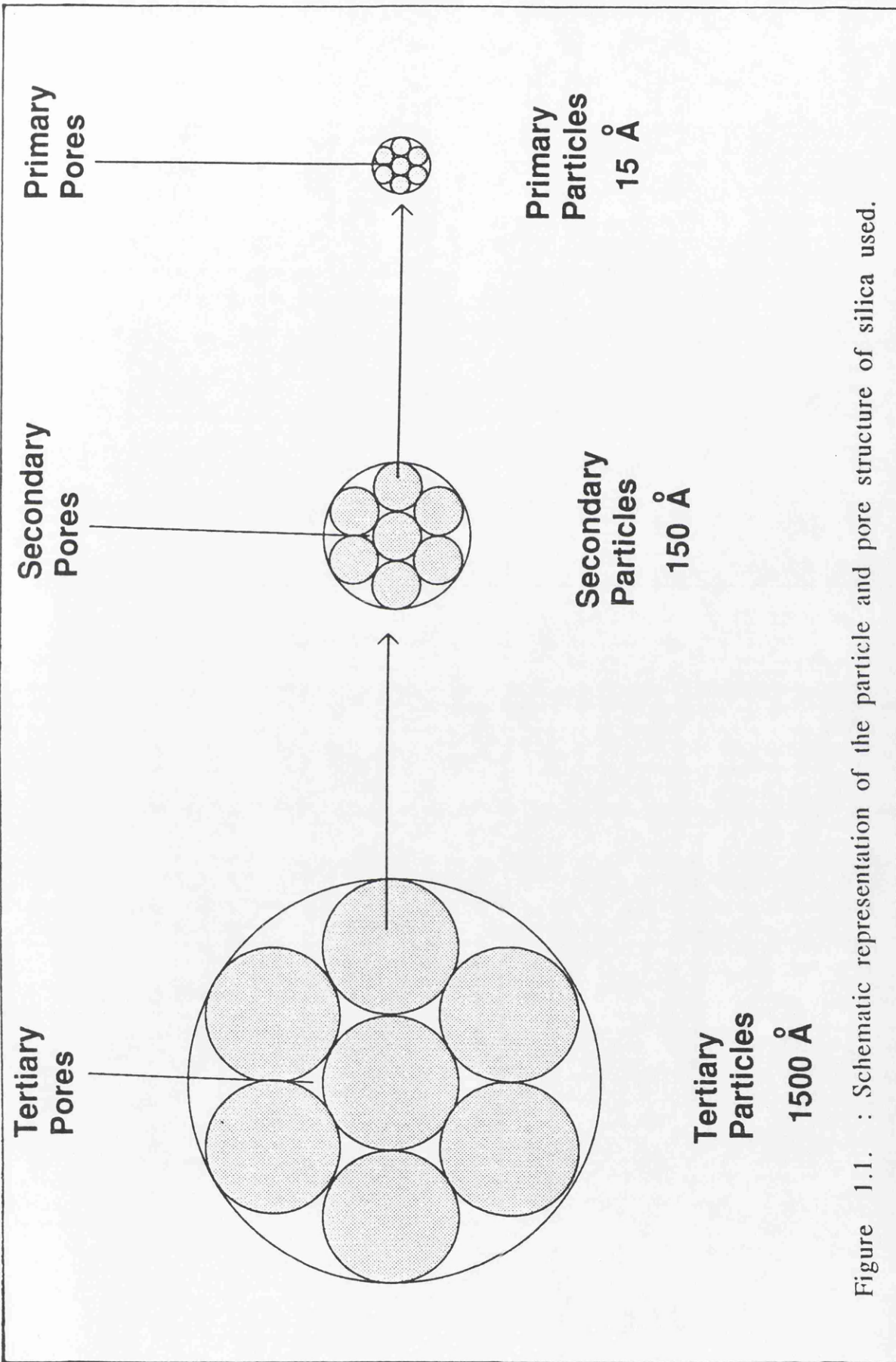
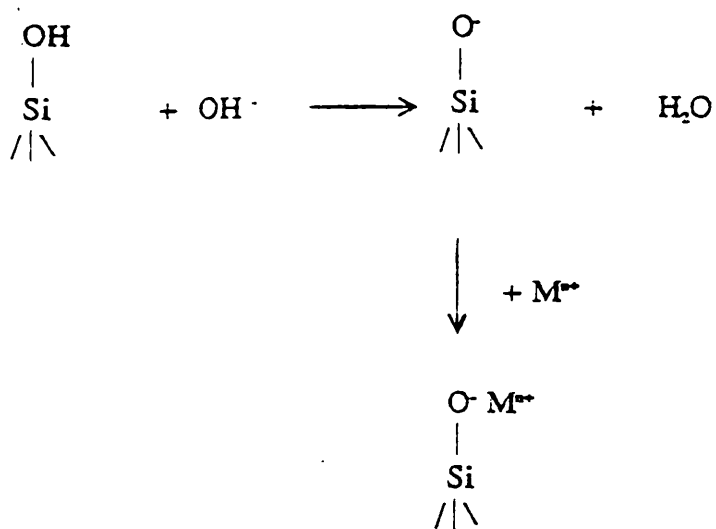


Figure 1.1. : Schematic representation of the particle and pore structure of silica used.

impenetrable owing to extensive particle aggregation. 80 percent of the surface area is in the secondary pores. Typical samples have a pore diameter of 140-160 Å and a surface area of 300 m² g⁻¹ (13,14). The active sites on the silica gel are the surface hydroxyl groups, that is silanol groups (9,12). The population of the surface by these groups is between 4.6 and 8 per 10 nm²(9,15).

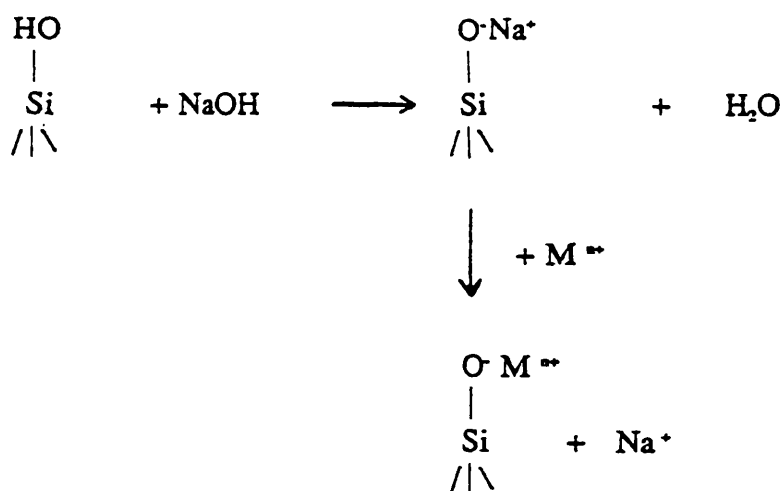
Representation of silica gel as a condensation polymer of silicic acid implies that the bulk structures are interlinked SiO₄ tetrahedra and their surface is covered with silanol groups. The surface silanol groups are strong hydrogen ion donors and they strongly adsorb molecules containing groups which are hydrogen-ion acceptors (16). The probable negative surface sites on silica-gel are ≡Si-O⁻ to which adsorbed cations are weakly bound (9). The silica gel can behave as a weak acid ion exchanger with the pK_a of the first ionization of free silicic acid being 9.9 (17) where the negative sites are readily exchangeable (9). Silica gel can therefore be classified as a weak acid cation exchanger where multivalent ions are adsorbed more easily than monovalent ions (18). Burwell et.al. (9) suggested that cations could be adsorbed onto silica gel by two methods:

(i). The silica gel is exposed to a basic solution containing a cation where the hydroxide ion from the solution reacts with the surface of silica gel to form negative sites to which the cation is bound as shown in scheme 1.1:



Scheme 1.1.

(ii). The silica gel is treated with a dilute solution of sodium hydroxide and then washed to near neutrality. The gel adsorbs cation from a metal solution, replacing the sodium ion with a metal ion (M^{++}) as shown:



Scheme 1.2.

A pH of about 9 is recommended (17) due to the dissolution of silica at a pH of about 10.7 (15). Silica gel is widely used as a catalyst support since the high area porous supports are often used to give optimum activity and stability. When using high area porous supports, the reaction occurs inside the pores and the initial products then undergo further reaction before diffusing out of the pores (9). A. Wheeler (19) proposed a mechanism for gas transport in catalyst pores. Molecules are transported into the inner pore structure of a catalyst by Knudsen flow. The actual rate of diffusion is many orders of magnitude slower than this due to two reasons: (i) collisions with the pore walls and (ii) collisions with other molecules. The molecule will start down a pore mouth with a high velocity but after travelling a short distance will collide either with the pore wall or with a second molecule. With a catalyst containing small pores of 1000 Å, in diameter, the mean free path between intermolecular collision will be greater than the pore diameter. As a result a molecule within the pore structure will strike a pore wall before it strikes a second molecule. Intermolecular collisions may therefore be neglected, and so the molecule travels randomly within the pore interrupted by a series of collisions with the pore wall. A highly active catalyst will cause reactant molecules to react before they can diffuse very far into the pellet (fast reaction), whereas in a relatively inactive catalyst, they can penetrate deeply into the pore structure before they undergo a further reaction (slow reaction). Figure 1.2.a and 1.2.b illustrate the very active and inactive catalyst respectively (13,19).

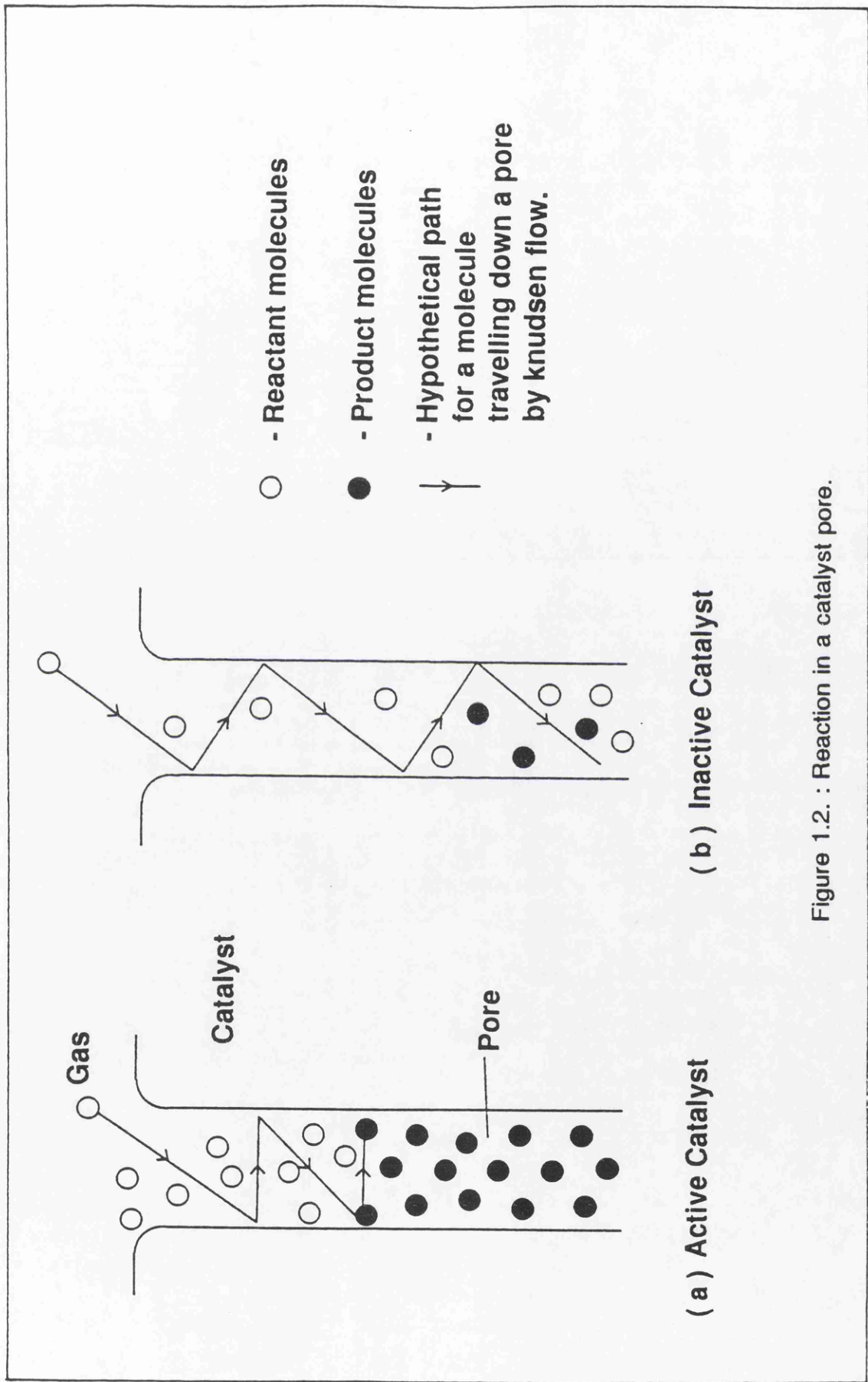
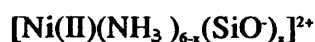


Figure 1.2. : Reaction in a catalyst pore.

1.2.2. Preparation techniques :

In impregnation, the pores are filled by the metal solution being added (10) and it is therefore advantageous to use a high area porous support. Sufficient contact time between the support and the solution is required to allow the support to reach an equilibrium with the solution. At equilibrium both the support and the solution contain the metal ion. In ion exchange techniques, the extent of ion exchange is determined by the ability of the support to exchange the acidic proton with the metal ion in solution (9,20). Burwell et.al. proposed two ion exchange methods in basic media: one using sodium hydroxide and the other ammonium hydroxide (9). In the ammonium method, the nickel ion was first treated with ammonia as discussed on page 5, scheme 1.1. The resulting nickel amine complex was then ion exchanged for the acidic proton on the silica surface, where some of the ammonia molecules are replaced by surface $\equiv\text{SiO}^-$ groups producing the adsorbed species:



In the sodium hydroxide method, the support was initially treated with diluted sodium hydroxide before the ion exchange process with the metal ion had taken place as discussed on page 6, scheme 1.2. Sodium ions from the solution adsorbed onto $\equiv\text{Si-O}^-$ sites and could exchange with hexaaquanickel(II) ions from solution. It was suggested that the surface $\equiv\text{Si-O}^-$ groups could enter

the coordination sphere of the nickel by displacing some of the water molecules to form the adsorbed species of:



It is clear that the exchange capacity of the support determines the loading that can be obtained by ion exchange. Samuelson (18) proposed that the following ion exchange conditions are required to reach the optimum exchange capacity: i) the process must be operated under irreversible conditions by continuously removing one of the compounds from the system; ii) the system must never be allowed to reach overall equilibrium to prevent complete penetration of the solution to the bulk of the support; iii) the washing treatment must be handled carefully to remove all excess salt solution in order to gain a higher efficiency (1,9,10,18). The efficiency of the method may be defined as the amount of metal ion which can be taken up quantitatively by the ion exchanger under the preparation conditions (18,20).

The selection of a suitable metal salt is an important factor. Nitrate salts are often chosen for making the mother solution because the use of salts such as chlorides or sulphates can poison the catalyst if retained in the final product (1). Poisoning can be represented by any process in which the catalyst is deactivated by adsorption of impurities onto catalytically active sites on the supported metal catalyst (10).

Labile nickel complexes can be adsorbed by silica gel (7,9). The precise

composition of the complex incorporated into the gel is governed by its equilibrium constant. Logarithms of the stepwise equilibrium constants (K_n) for nickelamine formation in aqueous solution (2M) at 303 K are : $K_1=2.79$; $K_2=2.26$; $K_3=1.69$; $K_4= 1.25$; $K_5=0.74$ and $K_6=0.03$ where the overall formation constant, $\beta_6 = 8.01$ (21).

1.3. Catalyst Activation.

After preparation the catalyst is activated by a drying stage followed by calcination and reduction of the supported precursors.

1.3.1. Drying

Drying is a dehydration process in which the physically adsorbed water is eliminated and partial decomposition may occur (10). Metal supported silicas were usually dried at 383 K for up to 16 hours. This slow drying provided a uniform moisture concentration and resulted in the completion of the dehydration process.

1.3.2. Calcination.

Calcination is an oxidation process in which the supported metal salt is fully decomposed to its oxide under carefully controlled time-temperature regimes and atmosphere (10,22). Metal supported on silicas are usually calcined at the decomposition temperature of the supported salt. The calcination temperature and atmosphere controls the chemical nature of the resultant bulk oxide and the rate of sintering of the active phase. Tamman (23) suggested that sintering occurred at a temperature around half the melting point of the solid in degrees Kelvin. The degree of sintering will increase by increasing either the temperature or the duration of heating.

1.3.3. Reduction.

Reduction is a process in which a metal oxide is converted to its metallic form in the presence of a reducing gas such as hydrogen (10). The reduction of metal oxides in hydrogen can be interpreted by either a nucleation or a contracting sphere model (13, 24).

In the contracting sphere model, the reaction interface decreases continuously from the beginning of the reaction when it has its maximum value. This can be explained in terms of a very rapid nucleation which results in total coverage of the oxide grain with a thin layer of the product in the initial stage

of the reaction. The reaction interface then decreases as the reaction proceeds.

In the nucleation model, oxygen ions contained within the lattice are removed during the reduction. When the removal of these oxygen ions reaches a certain level the metal nuclei will be formed. Oxygen removal takes place by diffusion either from the metal oxide to the metal/gas interface or from the hydrogen ion to the metal/metal oxide interface. The creation of new metal nuclei and the growth of the existing nuclei rapidly increases the interface between the nuclei and the metal oxide. At some stage during the reduction, the metal nuclei will come into contact with each other. This leads to a decrease in the reaction interface. This process continues until the metal oxide is completely reduced to the metal (figure 1.3). N.W.Hurst et.al. (24) postulated that the concept of a contracting sphere would seem to be inappropriate in the case of metal oxides supported on inert carriers such as silica gels. Therefore reduction may involve instantaneous nucleation across the whole area of the supported oxide. The nucleation processes may be hindered by metal/support interactions reducing the mobility of metal atoms. Even though the reduction temperature of a supported catalyst is usually high, the sintering process is inhibited by the distribution of the metal on the support material, the support hindering the formation of an agglomerate (25). The exact reduction temperature of a catalyst can be obtained by a temperature programmed reduction experiment.

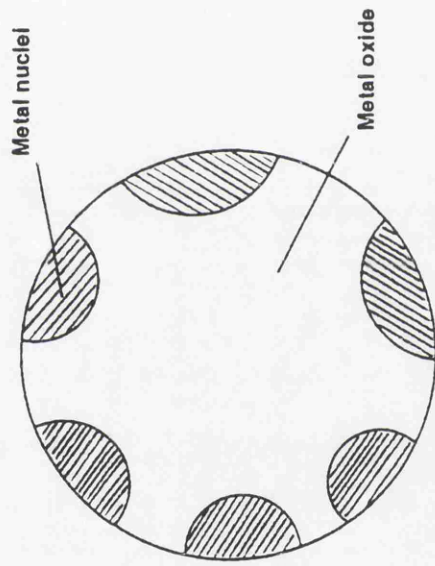


Figure 1.3. : Creating a metal nuclei on the metal oxide.

1.4. Catalyst Characterization.

The prepared catalysts and their precursors are characterized to obtain information on the nature of the active sites. Catalysts are usually characterized in terms of both their bulk composition and surface reactivity. Bulk characterization includes determining the composition of the phases present, the size and shape of the catalyst particles and the surface area, porosity and acidity of the catalyst. The surface structure and chemical state at the surface is determined from the dispersion of the active component and its coordination geometry (8). The processes occurring during catalyst preparation can be monitored and used to provide useful information on the state of the catalyst. The techniques used in this work for catalyst characterization include atomic absorption spectroscopy, elemental analysis, flame photometry, diffuse reflectance, UV-vis and near infrared and infrared spectroscopies, X-ray diffraction, thermogravimetry, temperature programmed reduction and carbon monoxide chemisorption . The following discussion relates the use of these techniques to the characterization of supported nickel catalysts and their precursors.

1.4.1. Bulk composition.

Atomic absorption spectroscopy and flame photometry can be used to

investigate the total metal concentration in the catalyst. Atomic absorption can also be used to assess the efficiency of the different preparation methods by comparing the nickel content in the solid precursor with that in the precursor salt solution. The main principle of this instrument is that the metal in solution is atomized by aspiration into a flame (usually an acetylene/air flame which achieves temperatures between 2398 and 2673 K). The molecules are decomposed and converted to gaseous elementary particles in the flame. The subsequent absorption of the atomized element gives rise to a small number of discrete lines at a wavelength that is characteristic of that element (26).

Elemental analysis can be used to investigate the hydrogen and nitrogen content (27, 28) in every stage of the preparation and thus identify the environment of the catalysts and their precursors. This analysis is based on combustion.

1.4.2. Electronic properties.

The electronic ground state of the catalyst precursor can be investigated by diffuse reflectance spectroscopy. This method studies the diffuse reflectance of uv-visible radiation ($5000 - 50.000 \text{ cm}^{-1}$) by finely divided solids. The environment of transition metal atoms within the solid may be studied by the position of the reflectance bands.

Ni^{2+} is the most common oxidation state for nickel (11). The energy

diagram in the weak crystal field approximation for a d^8 species showing the allowed ground state transitions are shown in figure 1.4. In a cubic field three spin-allowed transitions are expected. Spectra of octahedral nickel(II) usually consist of three bands which are accordingly assigned as:

$$\nu_1 = {}^3T_{2g}(F) \longleftarrow {}^3A_{2g}(F)$$

$$\nu_2 = {}^3T_{1g}(F) \longleftarrow {}^3A_{2g}(F)$$

$$\nu_3 = {}^3T_{1g}(P) \longleftarrow {}^3A_{2g}(F)$$

It is well documented that nickel complexes have covalent bonds between the metal and the ligand. The bonding involves an electron-pair donation from the ligand to the metal ion (29). The electronic spectra of aqua and amine complexes of octahedral nickel(II) are shown in table 1.2:

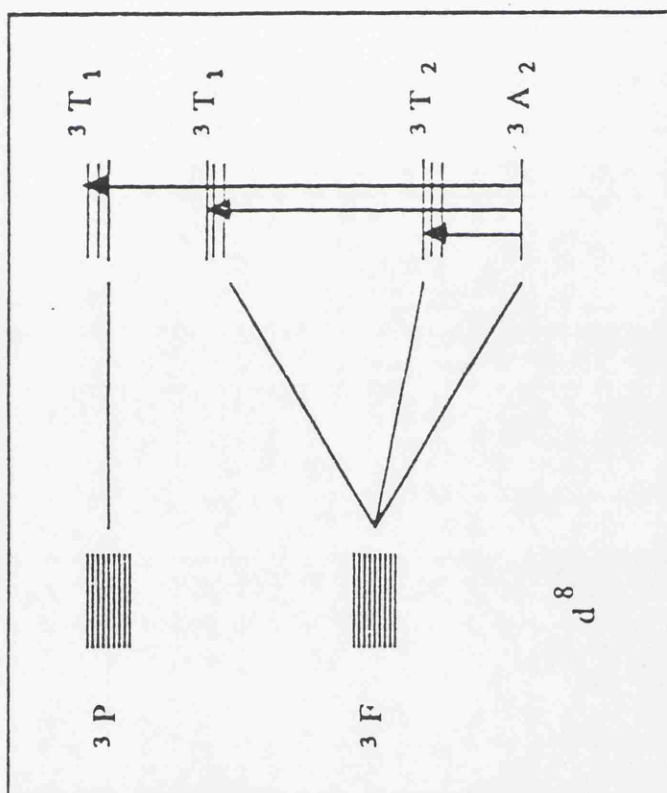


Figure 1.4. : Energy diagram of the weak crystal field approximation for a d^8 species showing the allowed ground state transitions.

Table 1.2. : Wavenumber for allowed transitions for two different ligands on nickel.

Nickel complexes	ν_1/cm^{-1}	ν_2/cm^{-1}	ν_3/cm^{-1}
$[\text{Ni}(\text{H}_2\text{O})_6]^{2+}$	8 500	13 800	25 300
$[\text{Ni}(\text{NH}_3)_6]^{2+}$	10 750	17 500	28 200

1.4.3. Infra-red spectroscopy:

Infrared spectroscopy (30) can be used to investigate the metal environment in the precursor state by studying the characteristic vibrational frequencies of the surrounding ligands. The ligands are often identified by comparison of observed infrared frequencies with known group frequencies, but surface interactions can shift the band frequencies to a higher or lower value

depending on their environment and thus provide information on the composition of the supported precursor resulting from each preparation route. The use of adsorbates as "probe" molecules (31, 32, 33), besides demonstrating the surface location of hydroxyl or other groups, can also provide information on the nature and environment of atoms and ions exposed on the surface, even though such atoms or ions cannot be studied directly by infrared spectroscopy. The use of probe molecules such as carbon monoxide and ammonia provide important information. Changes in both the frequencies and intensities of the infrared bands on surface sites can be used to elucidate the number and nature of the probe molecules on surface sites. Subtle differences in surface sites can readily be demonstrated by changes in the spectra of adsorbed molecules.

1.4.4. Bulk structure.

The phase composition of the precursors and catalysts can be investigated by X-ray powder diffraction (XRD). X-rays are electromagnetic radiation of wavelength 1 \AA (10^{-10} m). They occur in that part of the electromagnetic spectrum between γ -rays and ultraviolet. The principles of the powder method are that a monochromatic beam of X-rays strikes a finely powdered sample that has crystals randomly arranged in every possible orientation. Some crystals must be oriented at the Bragg angle, θ , to the incident beam, and diffraction occurs for these crystals and planes. The diffracted beams may be detected by using a

movable detector that is connected to a chart recorder (34). Since the catalyst activation includes drying, calcination and reduction (section 1.3), the form of nickel species at each stage can be identified by comparison to that on an unsupported catalyst/ pure metal salt. By definition, Ni^{2+} , NiO and Ni metal are the nickel species present on the dried, calcined and reduced precursors respectively. Line positions of pure metal compound are well documented in the powder diffraction file. Comparing the line positions with the reference file, the bulk structure of the precursors can be identified. This identification could also indicate the strength of interaction between the metal and the support.

1.4.5. Thermal characterization.

Thermal characterization is a fundamental property of a catalyst since heating is used during preparation, activation and use. This yields information on the nature of the phase/composition under a specific atmosphere as a function of temperature. Thermogravimetry (TG) and temperature programmed reduction (TPR) are two analytical techniques which use thermal characterization methods. TG is used to observe the change in weight of a substance as a function of temperature and time under a specific atmosphere, and TPR to observe the hydrogen consumption of a metal oxide as a function of temperature (35).

TG can be used to investigate catalyst precursor decomposition (36) since changes in sample weight as a function of temperature are directly related to the

specific stoichiometries of the reaction. Nickel(II) nitrate, the initial salt for catalyst preparation, has a multistep solid phase decomposition to form nickel(II) oxide. B.Mile et.al. (37) reported that three main stages can be distinguished as the decomposition of bulk nickel(II) nitrate at heating rate of 10 K/minute. Heating from 366 to 398 K (stage I) resulted in the loss of one water molecule to form nickel(II) nitrate 5 hydrate. Further heating to 538 K (stage II) affected the loss of $3/2$ waters and one nitric acid molecule to form nickel(II) hydronitrate $5/2$ hydrate. Finally, heating from 538 to 698 K resulted in complete decomposition of the nickel salt to form nickel(II) oxide. C.Duval (38) found that with 3 K /min heating rate, the black nickel(II) oxide formed on increasing the temperature to 613 K.

The technique of temperature-programmed reduction (TPR) can be used to characterize the reduction process associated with each catalyst. This technique involves the measurement of the hydrogen consumption due to the reduction of the metal oxide surface while the catalyst sample is heated up at a constant rate. This technique is very sensitive to the presence of reduced species and has been extensively applied to the study of supported metal catalysts (24). Nickel(II) oxide supported on a silica catalyst (5 wt percent), prepared by impregnation method, was studied by E.E.Unmuth et.al. (39). The catalyst produced three main peaks. The first peak appeared at a temperature less than 600 K. He assumed that this peak was due to an endothermic phase transition occurring simultaneously with the reduction. The second peak, produced at 600 K, was interpreted as the reduction of nickel(II) oxide to the

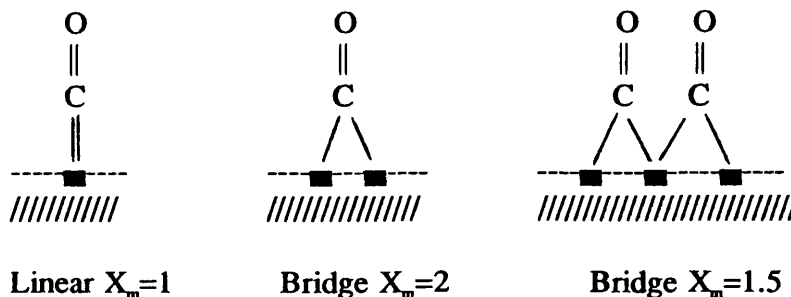
nickel metal and the third peak, at more than 600 K, was thought to arise from the reduction of very small oxide particles or possible silicates.

1.4.6. Chemisorption.

Adsorption is usually defined as being physical or chemical. In physical adsorption, the molecules are held to the surface by dispersion forces. The process is random, non-activated and usually occurs at temperatures near the boiling point of the gas (8).

Chemisorption involves the breaking and reforming of chemical bonds and is the mode of adsorption which is important in heterogeneous catalysed reactions (8, 10, 30). Chemisorption of small molecules is often used as a test for the surface properties of supported transition metals. The information is deduced from experimental measurement of the adsorption isotherms, the heats of adsorption, the thermal desorption spectra, and the vibrational spectra of the adsorbate (30,40). The chemisorption of carbon monoxide has been commonly used to probe the surface of a transition metal ion. The use of chemisorption for metal surface area measurement requires the measurement of gas uptake under conditions where the chemisorption stoichiometry is well defined, so that the number of metal surface atoms and thus the metal surface area may be estimated.

Figure 1.5. : Carbon monoxide chemisorbs onto the surface of a metal in a variety of forms:



X_m = the average number of surface metal sites associated with the adsorption of one carbon monoxide molecule.

The various forms are bound to the surface with different energies and their X_m values are different. The relative proportions of the various forms are temperature, pressure and metal particle size dependent (8). Both the linear and bridged forms of carbon monoxide have been found adsorbed on nickel metal but the linear form is generally more intense in the spectrum than the bridged form (8, 31).

1.5. Catalytic Testing.

For catalysis to proceed, there must be some surface interaction between the catalyst and the reactant but this interaction must not permanently change the chemical nature of the catalyst (7). Therefore, in catalytic testing, the catalytic activity of the prepared and characterized catalysts is determined for a model reaction to obtain information on catalyst selectivity for the desired products. The ability of a substance to act as a catalyst in a specific system depends on the specific chemical properties of the surface of the catalyst (41).

Consider a simple scheme in which a reactant A undergoes a variety of reactions, one of which yields a particular product B. Selectivity to B (S_b) is defined as:

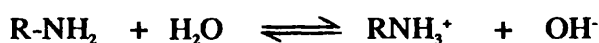
$$S_b = \frac{\text{Number of moles of A converted to B}}{\text{Total number of moles of A consumed}} \times 100\%$$

Additional information from the testing experiment includes the determination of the rate of conversion, which allows the selection of operating conditions so that the reaction can be conducted within a realistic contact time (2).

1.5.1. Amination of ethanol:

In the amination of ethanol it is necessary to know which product will be obtained. Aliphatic amines are important products of the chemical industry and find applications in most fields of modern technology, agriculture and pharmaceuticals (42).

All amines have a lone pair of electrons and reactions involving the lone pair are generally the dominant reactions of amines. Amines are moderately strong bases, being stronger bases than water and alcohols but weaker than the hydroxide ion (43). Aqueous solutions of amines are therefore alkaline. The amine is partly protonated in water:



equation1.1.

and is completely converted into the ammonium ion by strong acid:



equation1.2.

Amines may be prepared by aminating alcohols, aldehydes and ketones in the presence of ammonia and hydrogen over a suitable catalyst at elevated temperatures and pressures (44). Silver, copper and nickel supported catalysts

result in a good selectivity for amines (45). Primary, secondary and tertiary amines are preferentially formed in these processes and hydrocarbons, nitriles and ethers are commonly formed as by-products.

1.5.2. Optimum Conditions:

The amination of alcohols in the presence of ammonia and hydrogen is referred to as dehydroamination. Optimum conditions for the dehydroamination reaction depend on the type of reactor used (42). Even though a continuous fixed-bed reactor may perform more efficiently, many patents have used a batch or semi batch reactor (46). The most important parameters which influence the optimum conditions are the type of catalyst used, the reaction temperature, the molar ratio and the total pressure (42). Supported copper catalysts containing 10-65 percent(wt) copper show a high yield for the dehydroamination of aliphatic alcohols (47). Silica supported materials have been used in this reaction. The support itself shows no dehydroamination activity (46).

A reaction temperature of 473-513 K is suitable for supported copper catalysts in a continuous reactor whereas in a batch reactor the optimum temperature was found to be considerably higher (46). The conditions used in the alcohol amination process, over a nickel metal catalyst, are temperatures of between 373 and 523 K and pressures of 1-280 bar (42) where the activity and selectivity of the catalyst is about 60 percent (45).

The molar ratio of reactants plays a vital role in the selectivity of dehydroamination products (48). For the dehydroamination of dodecanol, a ratio of primary amine to dodecanol of 2/5 and secondary amine to dodecanol of 3/1 were preferred for synthesizing secondary and tertiary amines respectively.

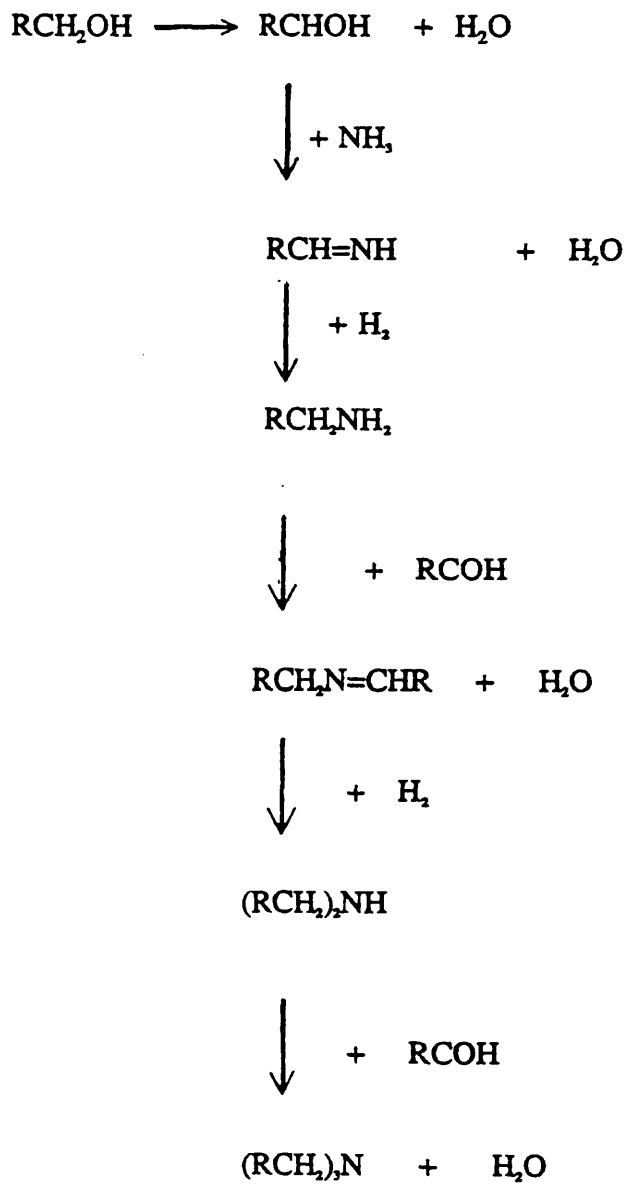
The selectivity for dehydroamination can be affected by the total pressure of reactants (42). 12 wt percent of the by-product N,N-didodecylmethylamine was obtained at 50 bar total pressure and 1-wt percent of this by-product was formed at pressures below 50 bar for the dehydroamination of dodecanol with dimethylamine.

A comparative study of the dehydroamination reaction using silica supported nickel(II) oxide and copper(II) oxide catalysts showed that both catalysts gave selectivity to N,N-dimethyldodecylamine of more than 60 percent (49). This indicates that similar operating conditions may be adopted for supported copper(II) oxide and nickel(II) oxide catalysts.

1.5.3. Mechanism.

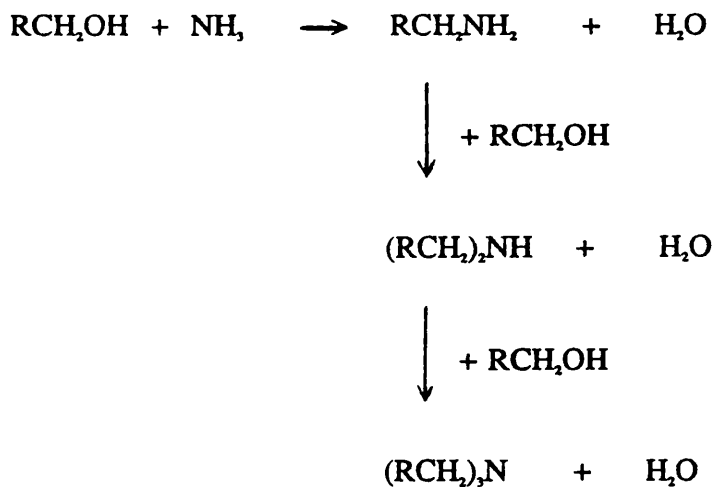
The mechanisms proposed by many workers are specific to a particular catalyst. However, three general mechanisms have been proposed by L.Baum, E.D.Schwegler and H.Adkins, and Popov.

E.D.Schwegler and H.Adkins(51) suggested that the amination followed the sequence of alcohols-aldehydes-imines-amines and they assumed that the aldehyde was the active intermediate.



Scheme 1.4.

It has been shown that amines are formed in the amination of alcohols by direct substitution of the alcoholic hydroxy-group by the amino group:

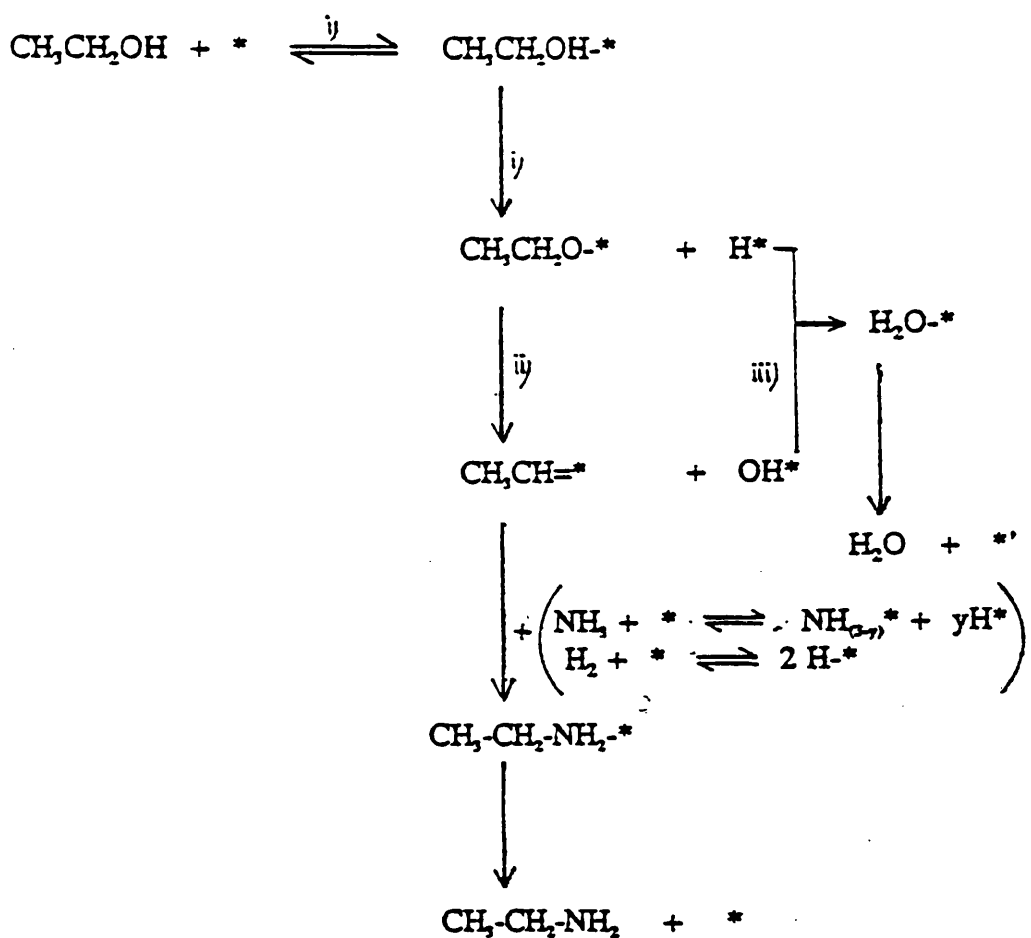


Scheme 1.6.

Recently, A. Sharatt (52) has suggested that $\text{CH}_3\text{-CH=}$ * is the intermediate species in the amination of ethanol using a 10 percent nickel supported on silica catalyst. He found that this catalyst could convert ethanol to ethanal in a helium atmosphere and to hydrocarbons in a hydrogen atmosphere. He assumed that this indicated that the surface intermediate did not contain an oxygen atom, to which the addition of hydrogen dehydrated ethanol to form a hydrocarbon. His assumption was proved using isotopic labelling. When D_6 - and (^3H) labelled ethanol was aminated, the labelled amine was observed and the methylene group label was still detectable in the residual alcohol. However, amination in the presence of ^3H produced a labelled amine but no label was

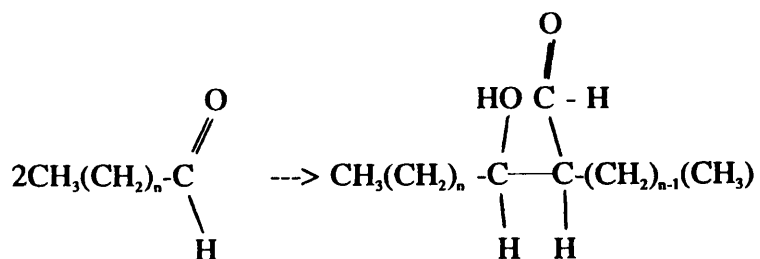
detectable in the residual alcohol. He proposed that the intermediate is formed by the dehydration of ethanol in three stages as shown in scheme 1.7 :

i) Ethanol is bound to the surface and this is followed by the loss of the hydrogen from the hydroxyl group; ii) This ethoxy species then loses a hydroxyl group to form the intermediate; iii) The hydroxyl group is then converted to water. The intermediate then reacts with an ammonia species and hydrogen to form an amine.



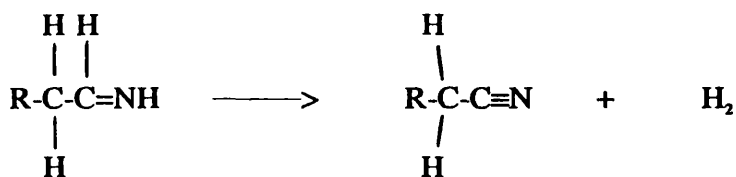
Scheme 1.7.

The condensation of aldehydes by an aldol condensation reaction may occur during dehydroamination (47,48):



equation 1.3.

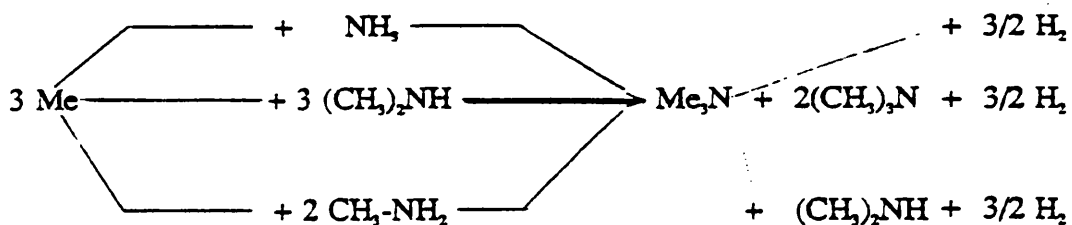
The formation of nitriles may also be produced through dehydrogenation of the corresponding imines:



equation 1.4.

Nitrile formation is favoured at temperatures greater than 570 K and at low hydrogen partial pressures. Card and Schmitt (55) reported that a 90% yield of acetonitriles is obtained from the reaction of ammonia with ethanol at 598 K on 15 percent copper supported on an aluminium(III) oxide catalyst.

Metal nitrides can be formed by the reaction of ammonia or amines with metal:



Scheme 1.9.

Since the reactions are reversible, if sufficient hydrogen is present in the reaction mixture, catalyst deactivation may not occur (53). A basic requirement is that the supported catalyst particles are thermally stable and do not sinter under the conditions used. Silica and alumina were found to be the most suitable supports (49).

CHAPTER TWO

OBJECTIVES

Objectives.

From chapter 1, it is clear that the preparation method, characterization and selectivity of a catalyst are dependent upon each other. It has been well documented that the method of preparation influences the selectivity of products for a chosen reaction. The different preparation methods may result in the catalysts having different surface properties. These differences can be determined by the characterization of each catalyst.

The principle objective of the work presented in this thesis was to obtain information on the preparation, characterization and selectivity of silica supported nickel catalysts for the amination of ethanol. Catalysts were prepared by impregnation and ion exchange techniques in order to investigate the influence of preparation methods on metal dispersion and catalyst morphology.

The catalyst precursors were then characterized by various techniques such as: atomic absorption spectrometry (AAS), elemental analysis, uv-vis spectroscopy, diffuse reflectance spectroscopy (DRS), fourier transform infra red (FTIR), X-ray diffraction (XRD), thermogravimetry (TG), temperature programmed reduction (TPR) and carbon monoxide (CO) chemisorption. The activities and selectivities of the reduced catalyst precursors were then investigated using the amination of ethanol as the model reaction .

CHAPTER THREE

EXPERIMENTAL

3.1. Catalyst Preparation.

Nickel supported on silica catalyst precursors were prepared using either impregnation or ion exchange methods. Ion exchanged samples were prepared using either sodium hydroxide or ammonium hydroxide as the base. Nickel(II)nitrate hexahydrate, molecular weight of 290.81, supplied by Jansen Chimica, and silica gel, Gasil 35, supplied by Crosfield Chemicals, were used as the starting materials. The impurity levels of Gasil 35 are 1000-2000 ppm Al; <100 ppm of Mg, Ca and K; 10-100 ppm of Fe, Cu, Zn, Sr, Ba, P, S, Cl and F. The silica has a surface area of $300 \text{ m}^2\text{g}^{-1}$; mean pore diameter of 16 nm and pore volume of $1.55 \text{ cm}^3\text{g}^{-1}$ (37). All catalyst samples had a nominal nickel loading of 5 percent (w/w) i.e. : 2.5 g of nickel salt was used per 10 g of silica gel.

3.1.1. Impregnation method.

An impregnated nickel supported on silica catalyst was prepared by pore volume impregnation of the silica support with hexaaquanickel(II) ions. Silica gel (10 g) was mixed with distilled water to make a homogeneous slurry and 30 cm^3 of 0.28 M nickel salt solution in water was then added to the slurry. The mixture was stirred for 30 minutes and was then left standing for about 120 minutes to allow both materials to reach equilibrium. Excess water was then

removed on a rotary evaporator and the catalyst precursor was dried in an oven at 383 K. Finally, the precursor was calcined at 673 K for 4 hours in furnace.

3.1.2. Ion exchange sodium hydroxide method:

A second catalyst precursor was prepared by a sodium hydroxide ion exchange technique. In this method, the ion exchange column (Figure 3.1) was prepared by pouring a slurry (a mixture of one part silica gel^{10g} and two parts water) along the wall of the column allowing the particles to settle forming the ion exchange bed. During this stage water was constantly passed through the column with the excess solution being drained off at 2 cm³ /minute. The column was then treated with dilute sodium hydroxide solution (pH about 9) for about 30 minutes and washed with distilled water until the filtrate neared neutrality. Afterwards, the ion exchange column was eluted with 30 cm³ of a 0.28 M nickel salt solution in water as used in the impregnation method and the excess solution was drained off at a flow rate of 2 cm³ /minute. The column was then washed with distilled water to remove all the free metal salt. The solid obtained was dried at 383 K overnight and the retained eluate from the column was transferred to a 100 cm³ volumetric flask for analysis. Finally, the dried sample was calcined at 673 K in an oven for 4 hours.

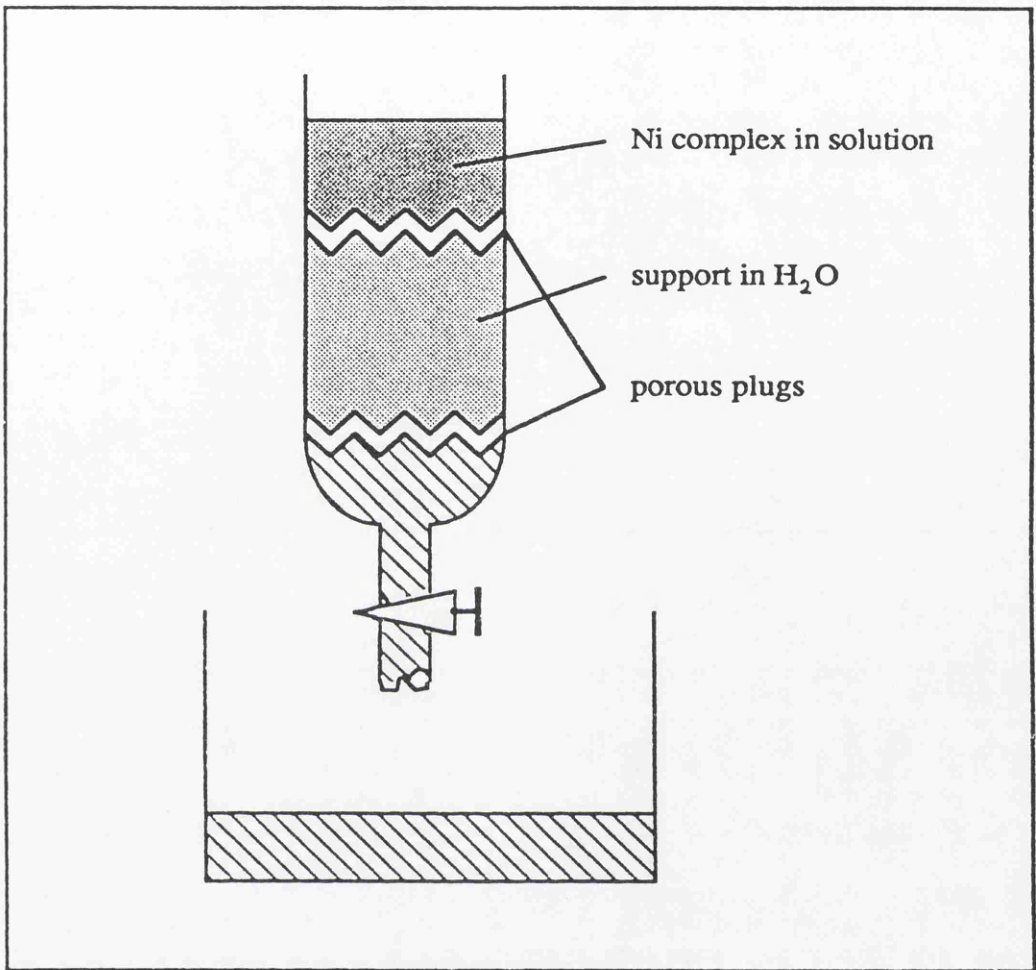


Figure 3.1. : The ion exchange column and its process .

3.1.3. Ion exchange ammonia method:

A third nickel catalyst precursor was prepared by ion exchange using nickel hexaammine as the initial solution. A 0.28 M nickel hexaammine solution was prepared by dissolving nickel(II) nitrate hexahydrate in 30 cm³ of 3 M ammonia solution. This nickel salt solution was then passed through the ion exchange bed which was prepared as in the sodium hydroxide technique and the excess solution was again drained off at 2 cm³ /minute. Next, the column was washed with distilled water to remove all free metal salt. The solid precursor was then dried overnight at 383 K and the eluate collected in a 100 cm³ volumetric flask for further analysis. The dried precursor was then calcined at 673 K in an oven for 4 hours.

3.2. Catalyst Characterization.

The catalyst precursors were characterised using spectroscopic techniques to obtain information on the bulk composition, the electronic ground state, the interaction of nickel(II) oxide with the support and its subsequent reduction and the metal dispersion of the catalyst.

3.2.1. Determination of metal content by atomic absorption spectroscopy and flame photometry.

The bulk composition of the catalyst was investigated by atomic absorption spectroscopy (type: Perkin-Elmer, M 1100, wavelength: 232.1 nm). In order to obtain a calibration curve, 1 to 5 ppm nickel standard solutions in 1 percent nitric acid were prepared and their absorbances were studied by atomic absorption spectroscopy. The absorbances obtained were plotted against their corresponding concentrations as shown in figure 4.1.

The dried catalyst precursors, the eluent from the ion exchange columns and the precursor salt solutions were all analysed by atomic absorption. The dried samples were prepared in the following way. A 100 mg sample was weighed out and then transferred to a 100 cm³ beaker. 10 cm³ of aqua-regia was added to the beaker and the mixture was heated for 15 minutes to extract the metal salt from the support. It then was evaporated on a hot plate until dryness. The dried sample was dissolved in 50 cm³ of 2 percent nitric acid and was then filtered to remove the residual support. The filtrate was transferred to a 100 cm³ volumetric flask and made up to volume with distilled water for analysis by atomic absorption spectroscopy. The ion exchange column eluents and precursor salts were evaporated to dryness and then dissolved in 50 cm³ of 2 percent nitric acid and diluted to 100 cm³ in a volumetric flask for analysis by atomic absorption spectroscopy. The absorbances obtained for each solution were matched with the calibration curve to find the corresponding concentration.

In order to calculate the metal content in the samples, the formula below was used:

$$\% \text{ metal content} = \frac{\text{ppm} \times \text{volume} \times \text{dilution}}{\text{sample weight} \times 10^6} \times 100\%$$

Furthermore, the efficiency of each preparation method was calculated by the formula:

$$\% \text{ efficiency} = \frac{\text{Nickel content in the catalyst precursor}}{\text{Nickel content in the initial solution}} \times 100\%$$

The results are compiled in table 4.1.

The yield of the ion exchange techniques was also evaluated by comparing the nickel content of the catalyst precursors with that in the eluents.

The percentage of sodium retained in the ion exchanged sample using the sodium hydroxide method was determined by flame photometry using a Corning 410 flame photometer. A calibration curve of absorbance against concentration was run using 1 to 4 ppm sodium standard solutions in 1 percent nitric acid. The sodium content in the samples was then determined by matching their measured absorbances to those on the calibration curve as in the atomic absorption analysis.

The curve is shown in figure 4.3.

3.2.2. Determination of nitrogen and hydrogen content by elemental analysis.

The elemental analyzer MOD-1106 (Carlo Erba) was used to analyse the hydrogen and nitrogen contained within the dried and calcined precursors. A calcined pure silica support was used as a reference.

A mg sample was loaded onto the combustion tube and then placed in a furnace. This furnace contained a mixture of cobalt(II) oxide, copper(II) oxide and chromium(III) oxide, and was heated to about 1273 K. This oxidizing atmosphere results in any nitrogen or hydrogen present in the sample being converted to water and nitrogen oxides. The sample is then transferred to a second furnace containing hot copper metal which converts the oxides and water to nitrogen and hydrogen. The gases were then analysed by a katharometer detector connected to an integrator and chart recorder.

3.2.3. Determination of electronic ground state by uv-vis and diffuse reflectance spectroscopy.

The electronic ground state of nickel in the catalysts was investigated by uv-visible near infrared diffuse reflectance spectroscopy . A Perkin Elmer, Lambda-9 spectrometer, was used in reflectance mode using an integrating sphere attached and barium sulphate as a reference, to investigate the dried precursors

over the wavelength range of 100 to 1300 nm. The results are shown in figure 4.5. The obtained spectra were evaluated by comparing them with the spectra of the initial solution (Figure 4.4.) which was measured by uv-vis spectroscopy in transmission mode over the wavelength range from 200 to 1400 nm.

3.2.4. Infrared studies.

A Philips analytical PU9800 FTIR spectrometer was used to analyse the environment of the nickel(II) cation in the dried and calcined precursors. A pure calcined silica gel was used as the reference spectra.

A few mg of the finely ground sample were mixed with about 100 mg of dried potassium bromide powder on a mortar. The mixture was pressed for 3 minutes in a die of 1.5 cm diameter at 10 kg/cm² under vacuum to yield a transparent disk. The disk was then held in the instrument beam for spectroscopic examination in the range of 400 - 4000 cm⁻¹. The spectra are shown in figure 4.6, 4.7 and 4.8.

3.2.5. X-ray diffraction :

A Phillips X-ray diffractometer (XRD) using Ni filtered Cu α radiation (λ :1.5405 Å) in the range of 10 to 90 ° 2 θ , was used to identify the phases

present in dried, calcined and reduced catalyst precursor samples. The results are presented in figure 4.3, 4.4 and 4.5, and they were compared against standard data in the powder diffraction file-JCPDS (Joint Committee on Powder Diffraction Standard).

3.2.6. Thermogravimetry:

A Du Pont thermobalance was used to measure the weight loss of the prepared precursors with increasing temperature. Initially, 10 mg of each dried precursor was weighed and mounted to the sample holder. The instrument was then ramped from room temperature to 923 K at 10 K per minute in air at a flow-rate of 50 cm³ per minute. The results are shown in figure 4.11. The decomposition steps were then evaluated by comparing the observed weight loss with that calculated for the decomposition of the nickel salt in the dried precursors to nickel(II) oxide. The formula for estimating the percentage decomposition of this sample is:

$$\% \text{ decomposition} = \frac{M_{(i)} - M_{(f)}}{M_{Ni}} \times \% \text{ Ni load}$$

where : $M_{(i)}$ = the molecular weight of nickel salt in the dried precursors.

$M_{(n)}$ = the molecular weight of the nickel(II)oxide

M_{Ni} = 58.69 gmol⁻¹

Ni load = the nickel content in the dried precursors from the results of atomic absorption spectroscopy analysis.

3.2.7. Temperature programmed reduction :

Temperature programmed reduction (TPR) was used to study the reduction of the catalyst as a function of temperature. A schematic flow diagram of the line is shown in figure 3.2.

A mixture of 6 percent hydrogen in nitrogen was introduced at a flow rate of 34 cm³ /minute and the temperature was then ramped to 983 K at 20 K/minute. Water produced during reduction was removed by an acetone trap, cooled by dry ice, and located before the thermal conductivity detector (TCD). The rate of hydrogen removal was calculated as a function of temperature and time, and the total hydrogen consumption was obtained by integration of the curve. The output signal was calibrated by pulsing 50 µl of hydrogen into the helium carrier gas passing through the detector.

Figure 4.12 shows the results of these experiments.

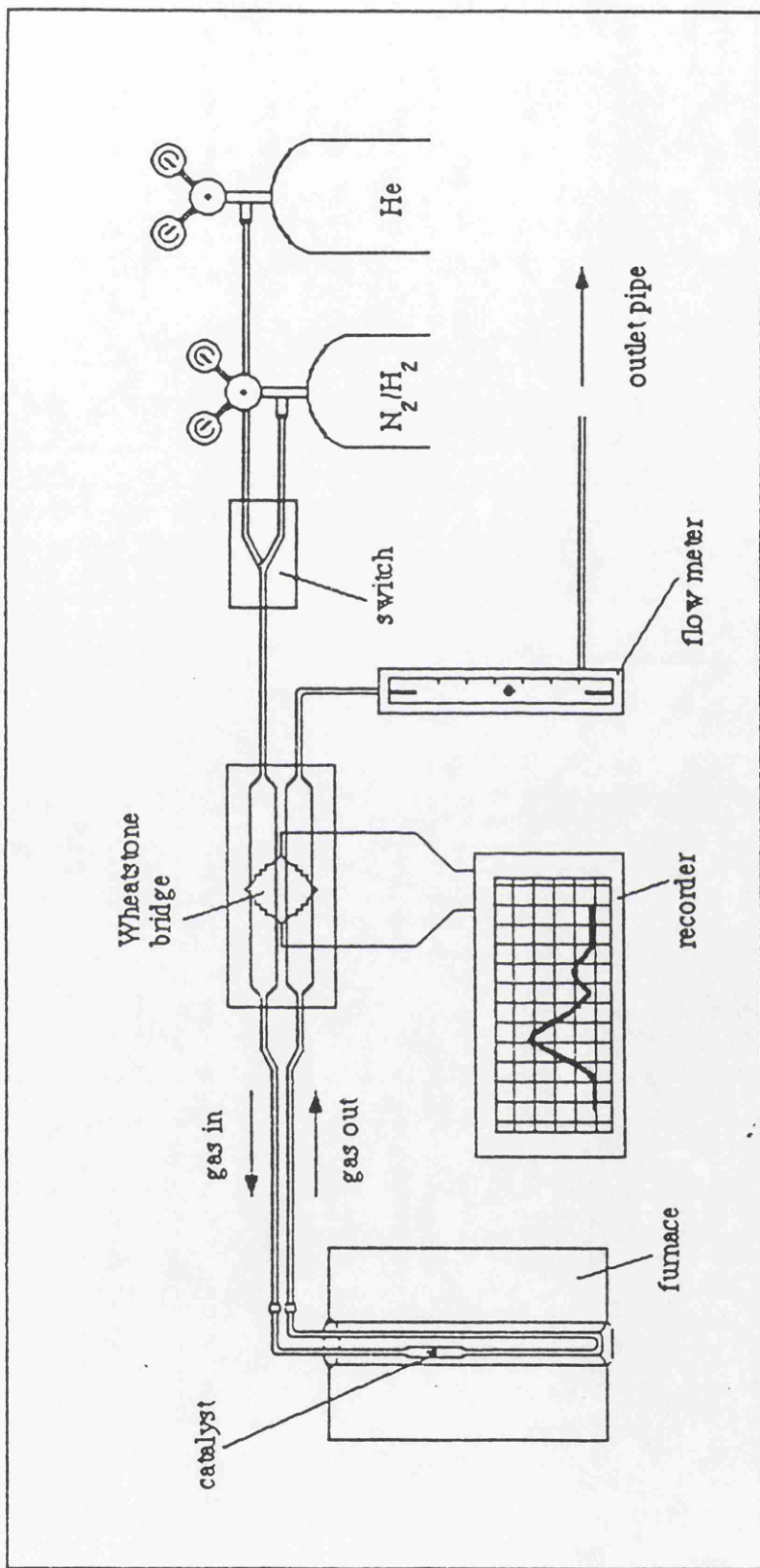


Figure 3.2. : Schematic diagram TPR apparatus.

The nickel present on the catalyst surface can be calculated by the equation :

$$\frac{A_p \times S_p}{A_c \times S_c} \times N(H_2) = N(Ni)$$

Where : S_p = sensitivity of recorder for sample (=8)

S_c = sensitivity of recorder for calibration (=64)

A_p = area under sample peak

A_c = area under calibration peak

$N(H_2)$ = number of moles of hydrogen in the calibration
sample (=2.0660 x 10⁴ moles hydrogen).

$N(Ni)$ = number of moles of nickel formed on reduction

The results are shown in table 4.7.

3.2.8. Determination of nickel metal surface area by carbon monoxide chemisorption :

Carbon monoxide chemisorption was used to investigate the metal surface areas of the supported nickel catalysts. The apparatus used is shown schematically in figure 3.3. Prior to the chemisorption studies, 0.2 g of each catalyst was reduced in pure hydrogen at a flow rate of 80 cm³/min at the

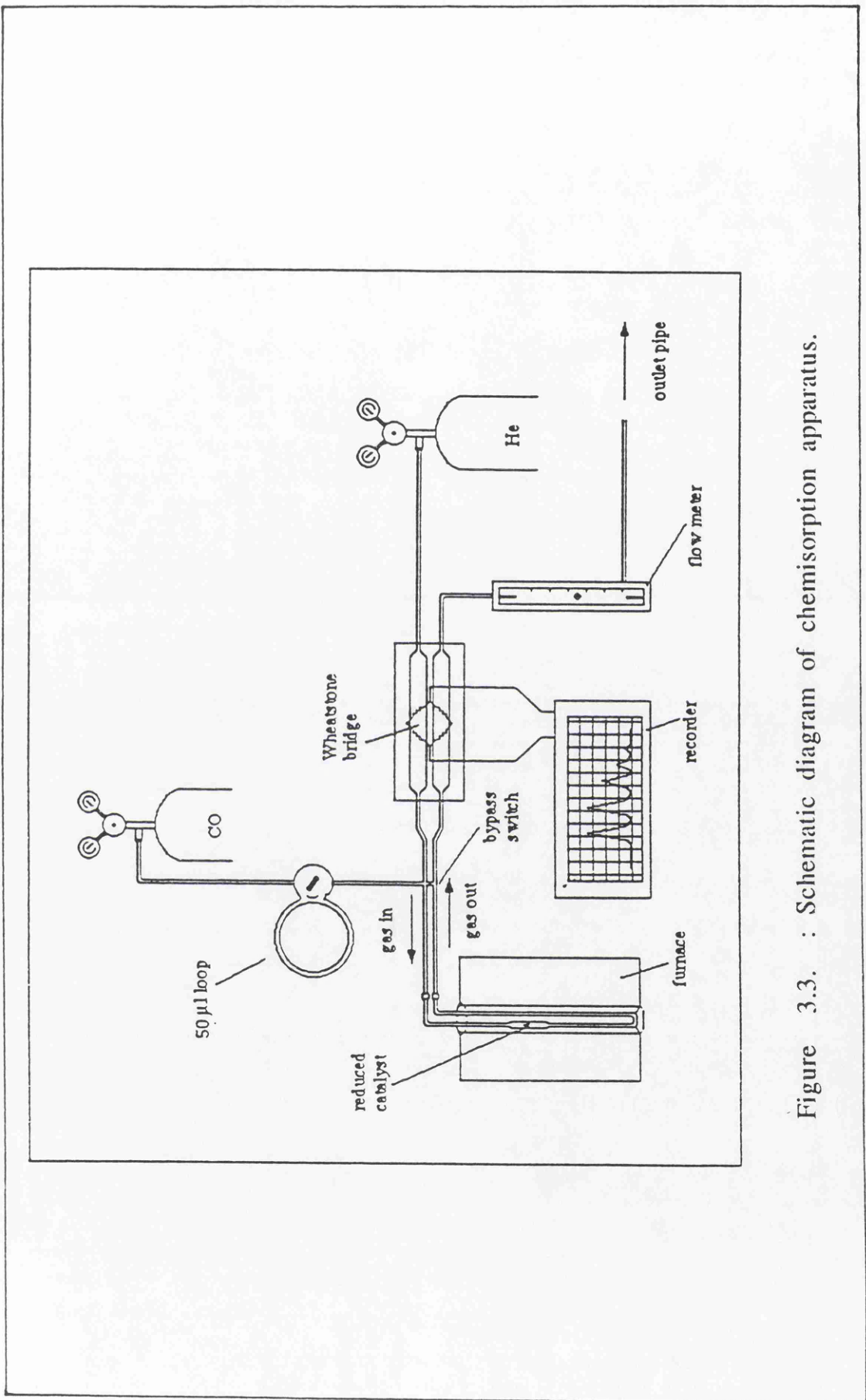


Figure 3.3. : Schematic diagram of chemisorption apparatus.

temperature of the maximum reduction of each catalyst (based on the result of TPR experiments) for three hours. The catalyst was cooled to room temperature in hydrogen and carbon monoxide was then pulsed via a sample loop of volume 4.18 cm³ into a stream of helium which passed over the catalyst. Several pulses were applied until the catalyst surface was saturated with carbon monoxide.

The numbers of moles of carbon monoxide per pulse (=n) was calculated by the equation :

$$n = \frac{P \times V}{R \times T}$$

where : P = Carbon monoxide pressure (=20 mm mercury)

V = Volume of carbon monoxide/pulse (=4.18 cm³)

R = Gas constant (=0.08205 atm dm³/mol K)

T = Temperature (K)

Then, the total carbon monoxide adsorbed was calculated using the formula :

$$n_{\text{COads}} = \sum_{i=1}^{i=n} n_{\text{CO}} (1 - A_i/A_{\text{sat}})$$

where : n_{CO} = no of moles carbon monoxide per pulse
(=4.61 x 10⁶ mol/pulse)

A_i = area of peak i

A_{sat} = area of saturated peak n

The total metallic surface area, A , is given by the equation:

$$A = (n_m/n_s) \times (\% \text{ Ni loading})$$

where : n_m = the number of surface atom which can be
calculated by :

$$n_m = 6.022 \times 10^{23} \times n_{CO_{ads}}$$

n_s = the number of surface atoms per unit area of
polycrystalline surface.

(For nickel metal = 1.54 x 10¹⁹ atom/m²)

The results are reported in table 4.8.

The percentage dispersion was accounted for by having the fraction of the carbon monoxide in linear (one carbon monoxide molecule per one nickel atom) and in bridged (one carbon monoxide molecule per two nickel atoms) orientations using the formula :

$$\% \text{ Dispersion} = (n_{CO_{ads}}) / X_m \times n_{Ni}$$

where : $n_{\text{CO}_{\text{ads}}}$ = the total carbon monoxide adsorbed

X_m = the average number of surface nickel metal sites associated with the adsorption of one carbon monoxide molecule.

n_{Ni} = no of atoms of nickel metal in the sample (w/w)

The results are reported in table 4.9.

3.3. The Amination of Ethanol.

3.3.1. Introduction:

The initial part of this study was concerned with the design, construction and calibration of a microreactor operating at a temperature of 383 K and pressure of approximately 20 psi. Since ammonia and amines are corrosive, stainless steel tubing and fittings were used for the main apparatus.

3.3.2. Materials:

Helium (BOC Ltd) was used as the carrier gas for gas chromatography;

Hydrogen (BOC Ltd) was used to reduce the catalyst and as the supply for the flame ionisation detector (FID); Air (BOC Ltd) was also used for FID analysis; 5 percent ammonia in hydrogen (G&E, Union carbide Ltd) and ethanol (BDH) were used as reactants.

3.3.3. Apparatus:

An apparatus was designed to allow the catalyst to be tested under the desired conditions and the products were monitored by an analytical system. It is shown schematically in figure 3.4. The system therefore consisted of three sections: (i) The microcatalytic reactor system; (ii) the feed system and (iii) the analytical system.

3.3.3.1. The microcatalytic reactor system:

A microcatalytic reactor system coupled to a gas chromatograph was used throughout this study. It is illustrated in figure 3.5. This system could be operated in either continuous flow or a circulating mode by manipulation of three-way taps A and B. In the circulating mode the system was connected to a peristaltic pump via silicone tubing. Three way taps, C and D, allow the system to operate either through the sample or bypass tube. A (30 psi) pressure

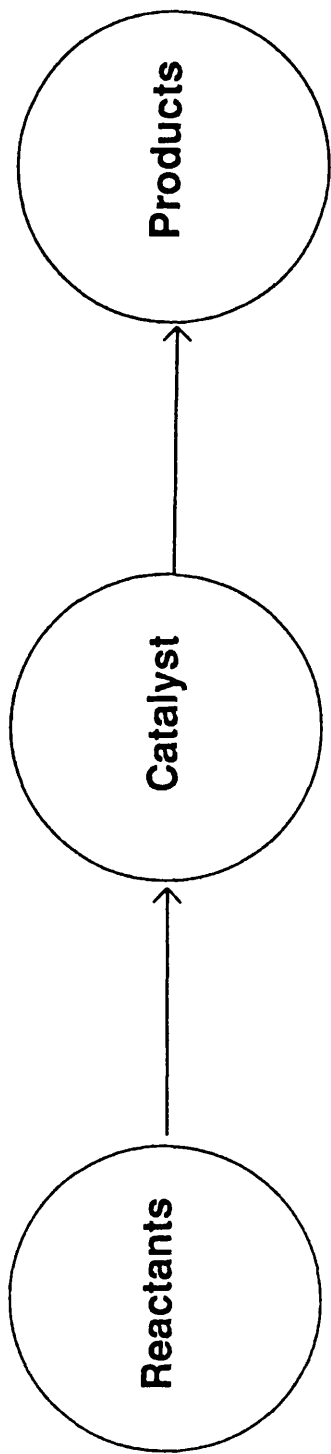


Figure 3.4. : A simple diagram of the apparatus used.

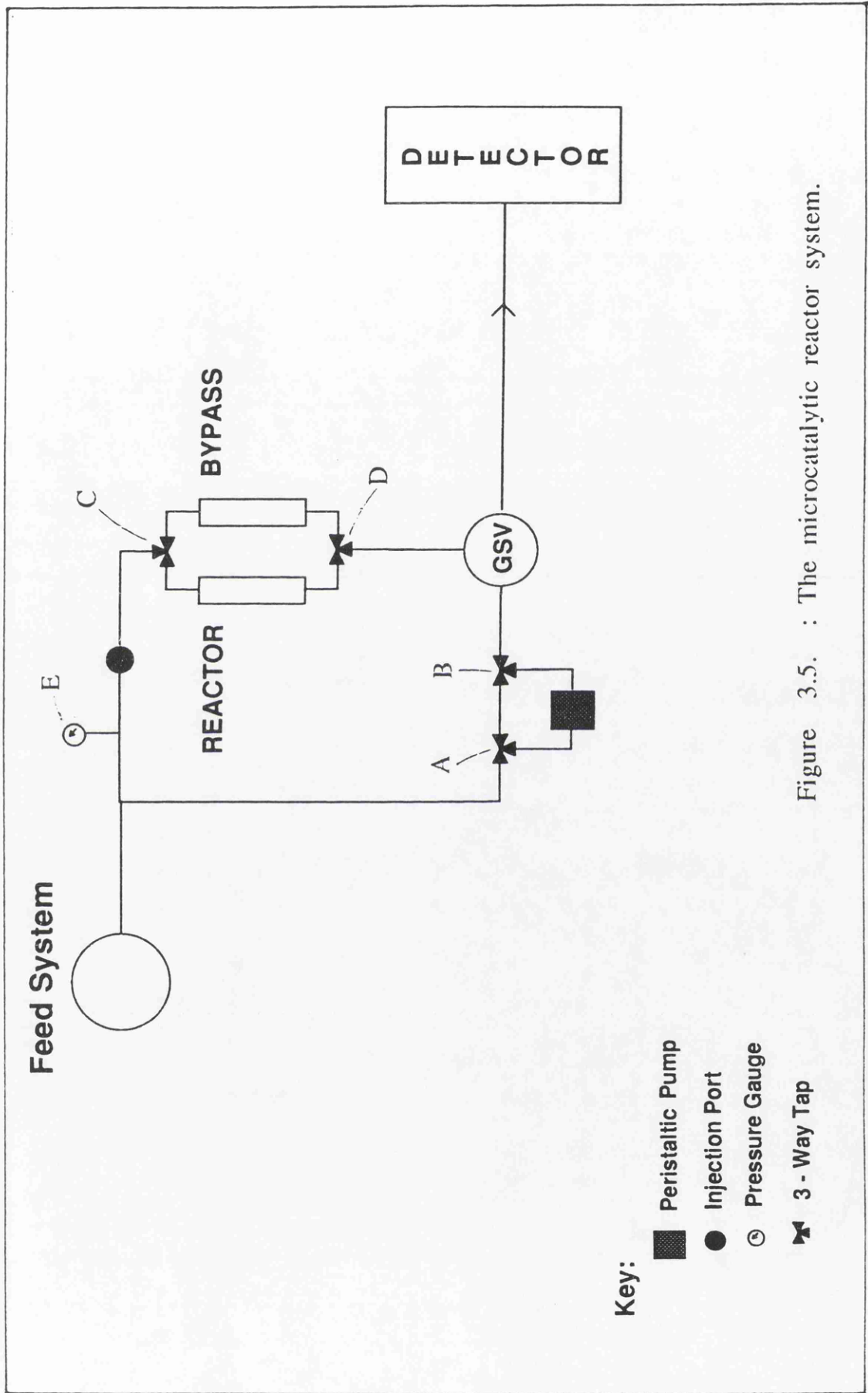


Figure 3.5. : The microcatalytic reactor system.

gauge, E, was connected to the system to monitor the pressure and a manual gas sample valve, H, was used for sampling the microreactor exit onto the GC. The metal tubing in the system was maintained at approximately 383 K using heating tape controlled by a 3A-variatic in order to prevent condensation of reactants or products.

The reactor itself (figure 3.6.) consisted of two 30 cm sections of 0.6 cm i.d. glass lined stainless steel tubing. One was used to hold the catalyst sample and the other as a bypass. This enabled reaction conditions to be attained before putting the catalyst on line. Catalyst samples (0.2 g) were held in the centre of the reactor vessel by glasswool plugs.

The temperature of the catalyst bed was maintained at the desired value by means of a 2 kw ceramic furnace which surrounded the reactor vessel. The temperature was controlled by a 5A variatic. The temperature was measured using a thermocouple placed in the centre of the furnace.

3.3.3.2. The feed system :

This system was designed to feed a gaseous mixture to the reactor system during reduction and reaction. To achieve this, separate gas streams were combined through a T junction. A schematic diagram of the feed system is shown in Figure 3.7. Gas flow rates through the system were controlled by pressure regulators ($B_{(1,3)}$) and fine ($C_{(1,3)}$) needle valves. Two way switch valves

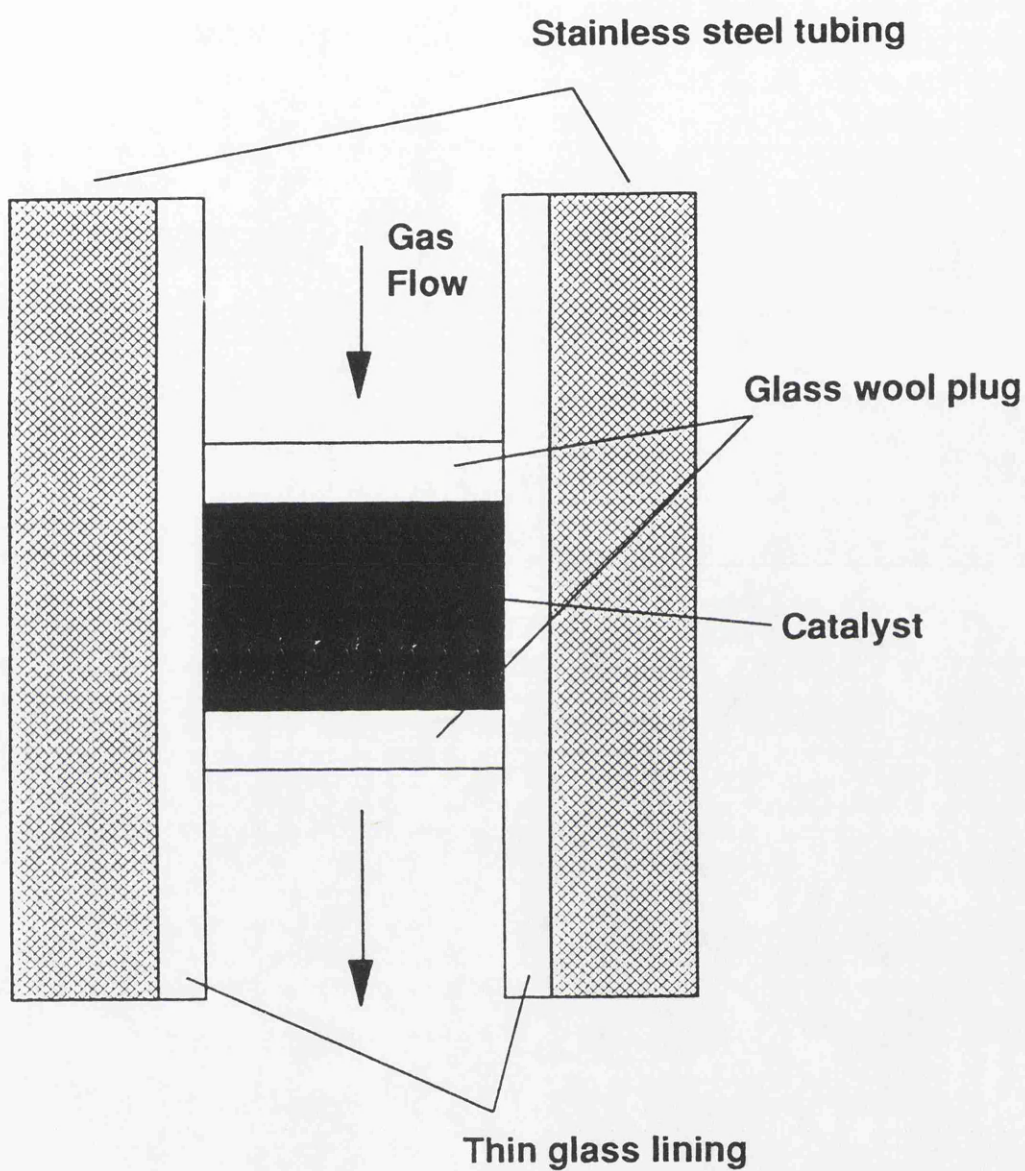


Figure 3.6. : The microreactor.

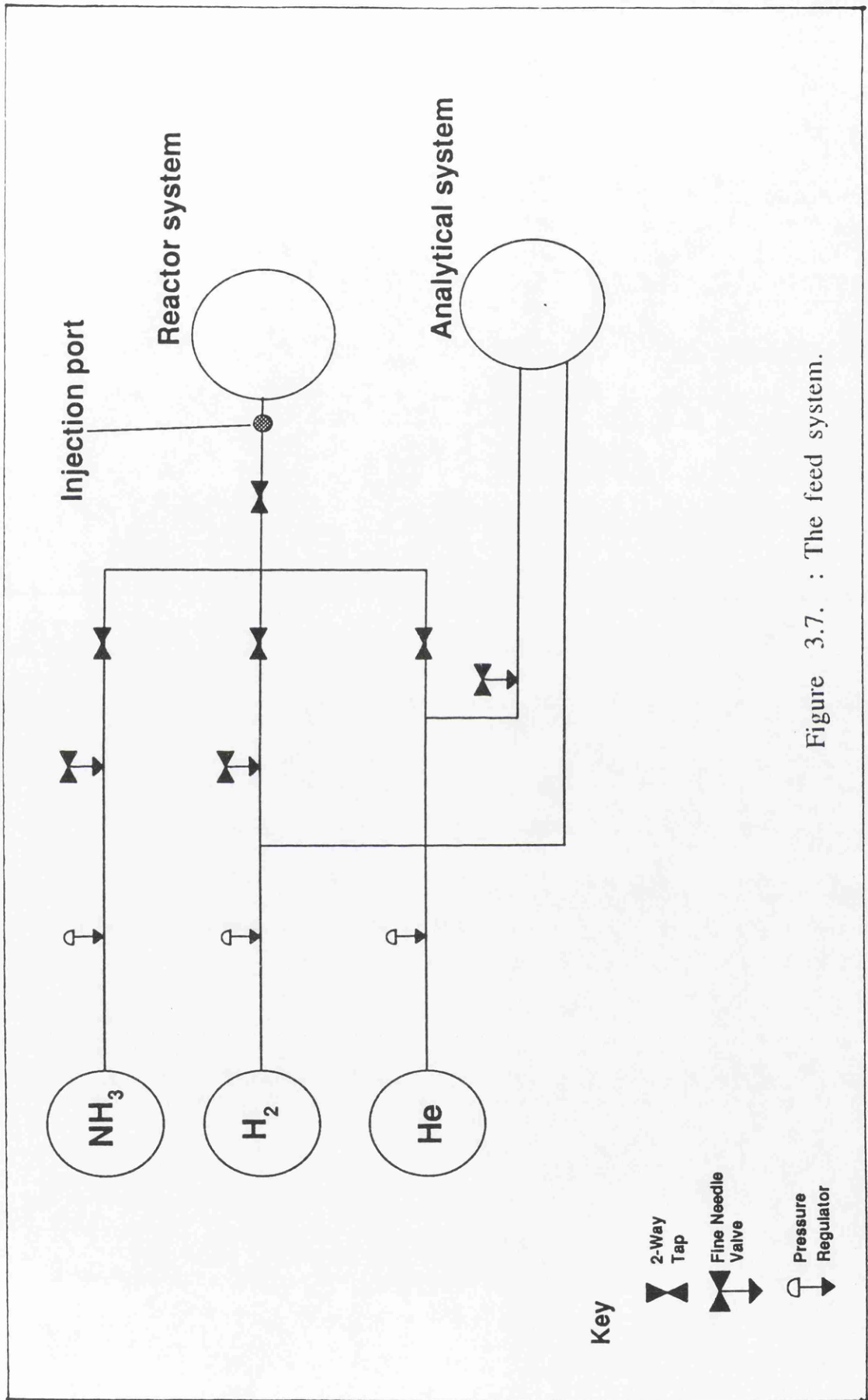


Figure 3.7. : The feed system.

(D_(1,4)) were used to control the input of reactant and carrier gases. Ethanol was introduced into the gas flow by injection using a syringe into injection port (E) which was heated to 383 K by heating tape.

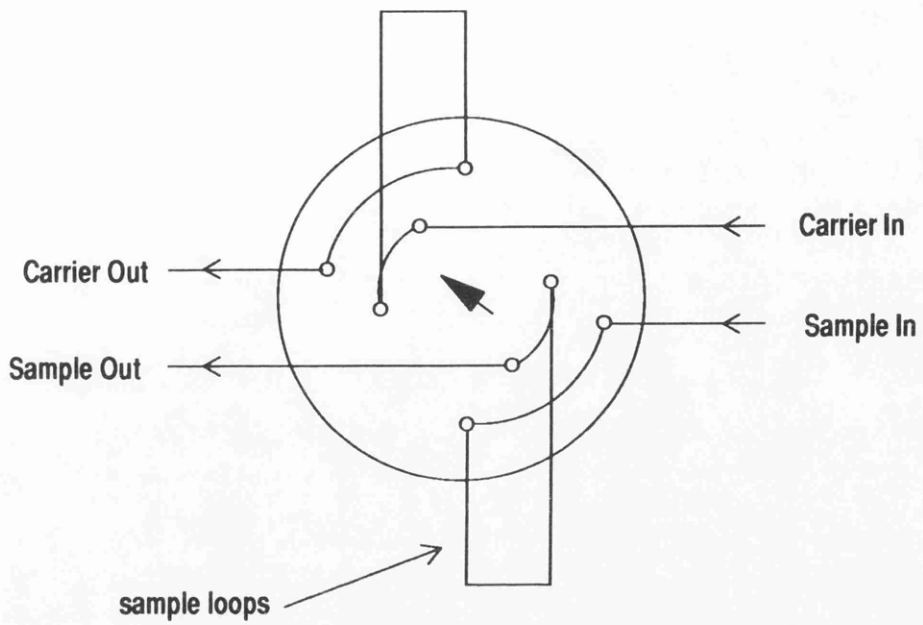
3.3.3.3. The analytical system :

The analytical system consisted of two sections, namely, the gas sampling system and gas chromatographic system.

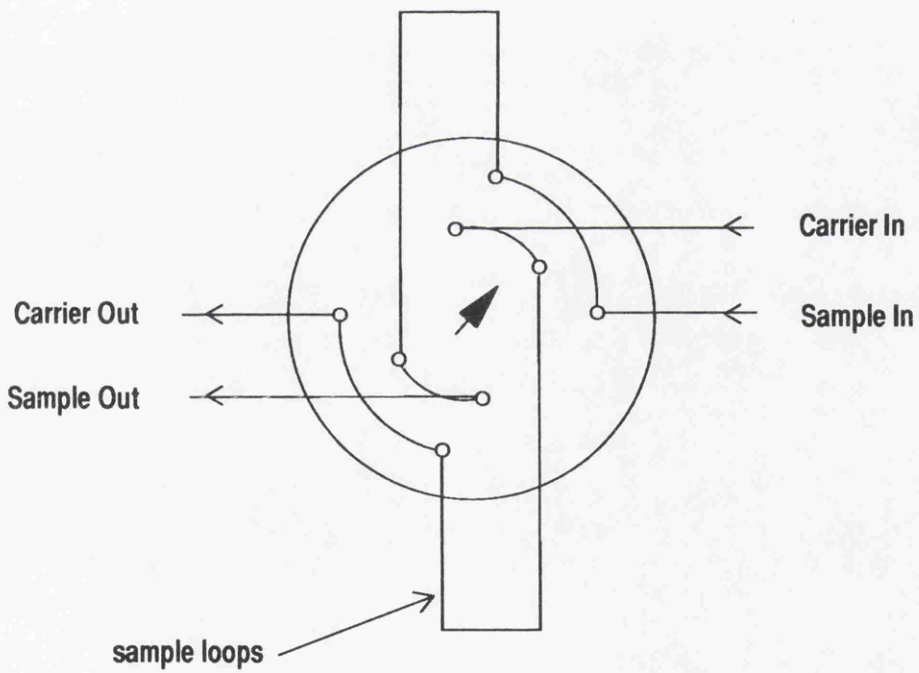
(a). Gas sampling system :

A manual gas sample valve attached to the gas chromatograph was used to withdraw samples at regular time intervals. Its schematic diagram is shown in figure 3.8. The figure shows that in position A, sample gas will flow through a sample loop. In position B, the sample gas in the sample loop will then be swept by the carrier gas into the column.

A trap, cooled by dry ice in acetone, was used to condense various fractions of the reaction products for NMR and MS analysis, and its schematic diagram is shown in figure 3.9.



Position A



Position B

Figure 3.8. : Schematic diagram of the gas sampling valve.

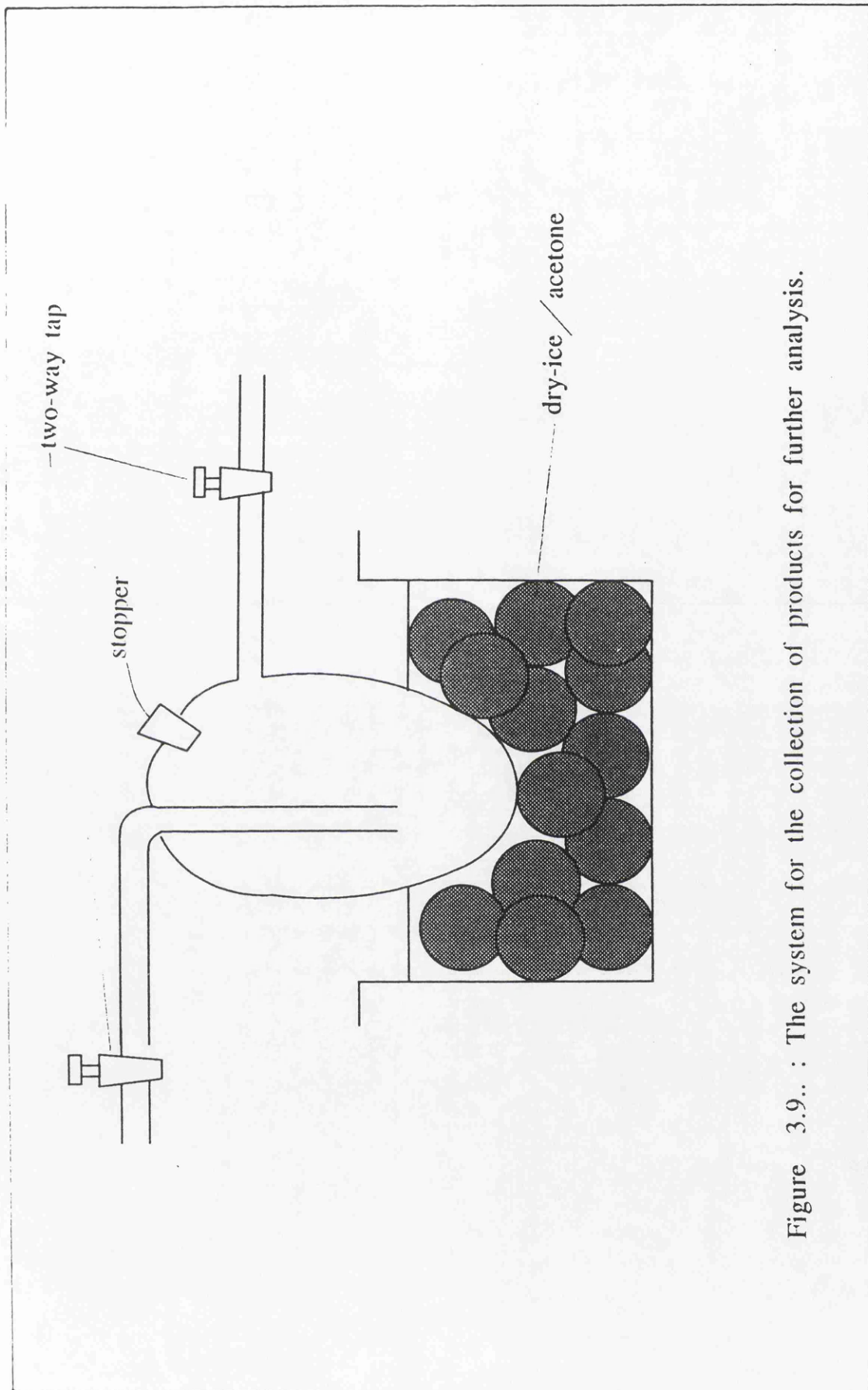


Figure 3.9.: The system for the collection of products for further analysis.

(b). Chromatographic system:

Analysis of the products from the reaction between ethanol and ammonia was achieved using a Perkin Elmer 8500 series gas chromatograph fitted with a flame ionization detector (FID). The gas chromatograph was coupled to the microcatalytic reactor system via a sample valve fitted with a 100 μl sample loop. Reactant/product separation was carried out using a stainless steel column, 6 m in length and 0.6 cm in diameter, packed with chromosorb 103 (mesh size 80-100) at 373 K. Helium was used as the carrier gas at a flow rate of 25 cm^3/min . The reactor and analysis system are shown schematically in Figure 3.10.

3.3.4. Preparation of the catalysts.

The calcined impregnated and ion exchanged catalysts described in section 3.1 were pressed into disks and then crushed and sieved to a particle size of 355 to 840 μm before being loaded into the 6 mm reactor used for catalyst testing. 200 mg of the calcined catalyst precursors were used in each run. Each catalyst was initially purged with He gas at 25 cm^3/min for one hour prior to reduction in hydrogen at 25 cm^3/min , programming from room temperature to its reduction temperature (from TPR experiment). The temperature was maintained for 3 hours and then the catalyst was cooled in flowing hydrogen. The reactor was

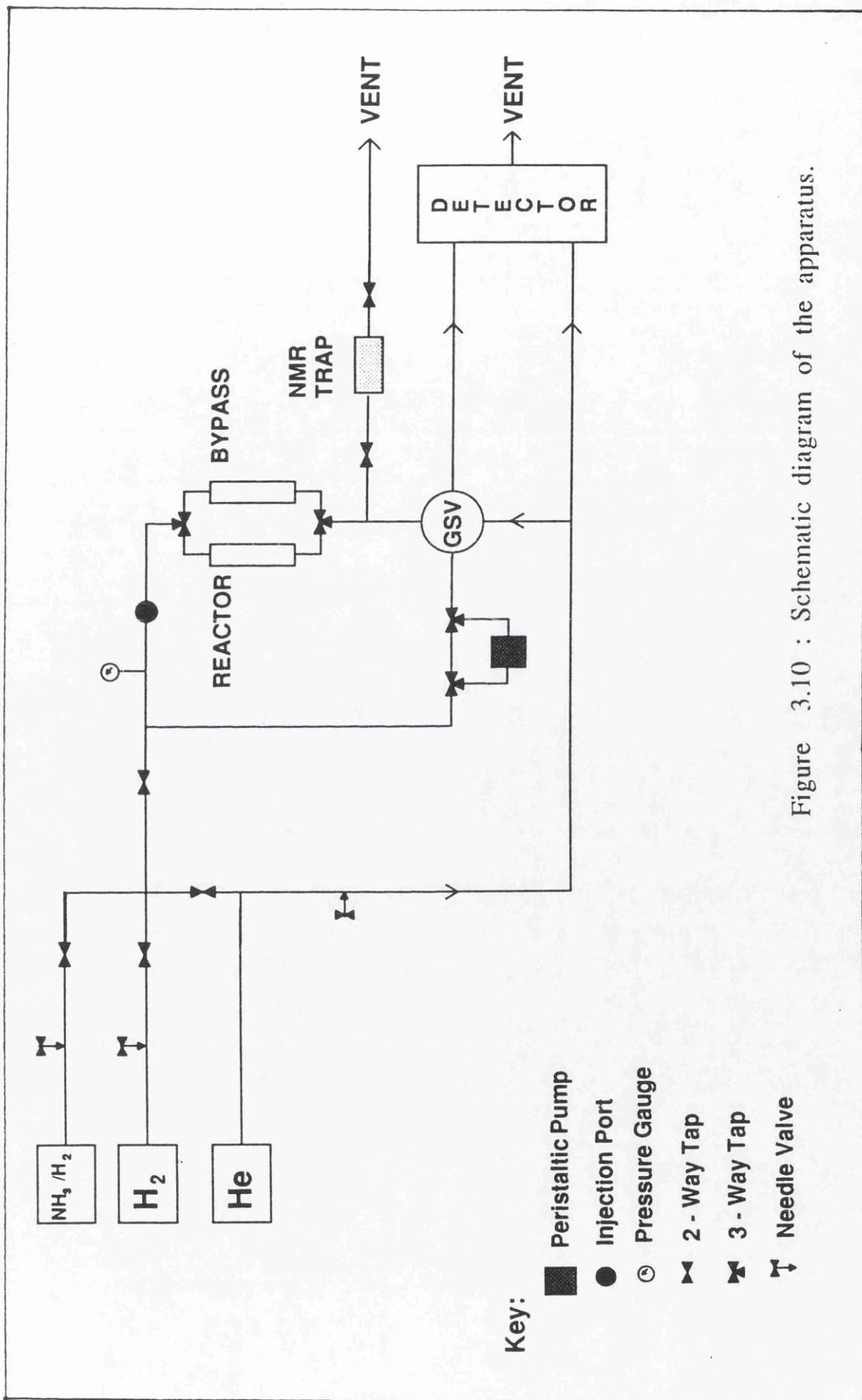


Figure 3.10 : Schematic diagram of the apparatus.

filled with 20 psi of hydrogen before it was by-passed.

3.3.5. Setting the gas chromatography PE 8500.

The gas chromatography conditions were set as follows :

- oven temperature : 373 K.
- detector temperature : 423 K.
- carrier gas flow : 25 cm³ /min.
- hydrogen pressure : 84 KPa.
- air pressure : 155 KPa.

3.3.5.1. Calibration of ethylamines , ethylalcohol, methane and ethane.

Calibration curves of peak areas against mol reactants/products were determined using the chromosorb 103 column connected to the FID over the concentration range 1 to 4 x 10⁻⁶ mol of ethylamine; 1 to 5 x 10⁻⁷ mol ethanol; 3 to 7 x 10⁻⁸ mol methane and 3 to 7 x 10⁻⁸ mol of ethane (figure 4.14 - 4.17).

3.3.6. Test reaction.

Initially, the line was heated to 383 K and swept with pure hydrogen several times. It was then filled with 5 percent ammonia in hydrogen to 20 psi.

100 μ l pure ethanol was then injected into the septum and the line turned onto the circulating mode. The gaseous mixture was circulated at 15 cm^3 /min for 15 minutes, whilst the GC was prepared for use and the catalyst-bed heated to the reaction temperature of 503 K in helium. The reaction mixture was then passed over the catalyst for 20 minutes.

3.3.7. Product analysis:

100 μ l samples were withdrawn and analysed by GC using a 1.5 m x 6 mm stainless-steel column packed with chromosorb 103 (80-100 mesh) at 373 K and the rate of helium carrier gas was adjusted to 25 cm^3 /min. The results are shown in figure 4.18 - 4.21 and table 4.11. At the end of the experiment, the reaction mixture was condensed out by cooling the trap with dry-ice/acetone. The products were dissolved in d_2 -deuteriochloroform and analysed by NMR, MS spectroscopy. The spectra obtained were used in conjunction with the FID data to determine the reaction products. Results are shown in table 4.12.

CHAPTER FOUR

RESULTS AND DISCUSSION

4.1. Chemical Analysis of the Precursors.

The nickel content of the catalyst precursors, the impregnation/ion exchange solution and the eluent from the ion exchange column were determined by atomic absorption spectroscopy (AAS) in order to assess the efficiency of each preparative route for transferring the nickel salt to the support phase.

The chemical state of the nickel ion both before and after impregnation/ion exchange was then determined by UV-vis spectroscopy. Flame photometry and elemental analysis techniques were then used to determine the purity of the precursors.

4.1.1. Studies of the precursors by atomic absorption spectroscopy.

The atomic absorption spectroscopy results are given in figure 4.1 and table 4.1. The figure shows the calibration curve of nickel concentration (1-5ppm) against absorbance. The line fits the equation :

$$Y = 8.20 X - 0.70 .$$

$$r = 0.999$$

where : Y = absorbance

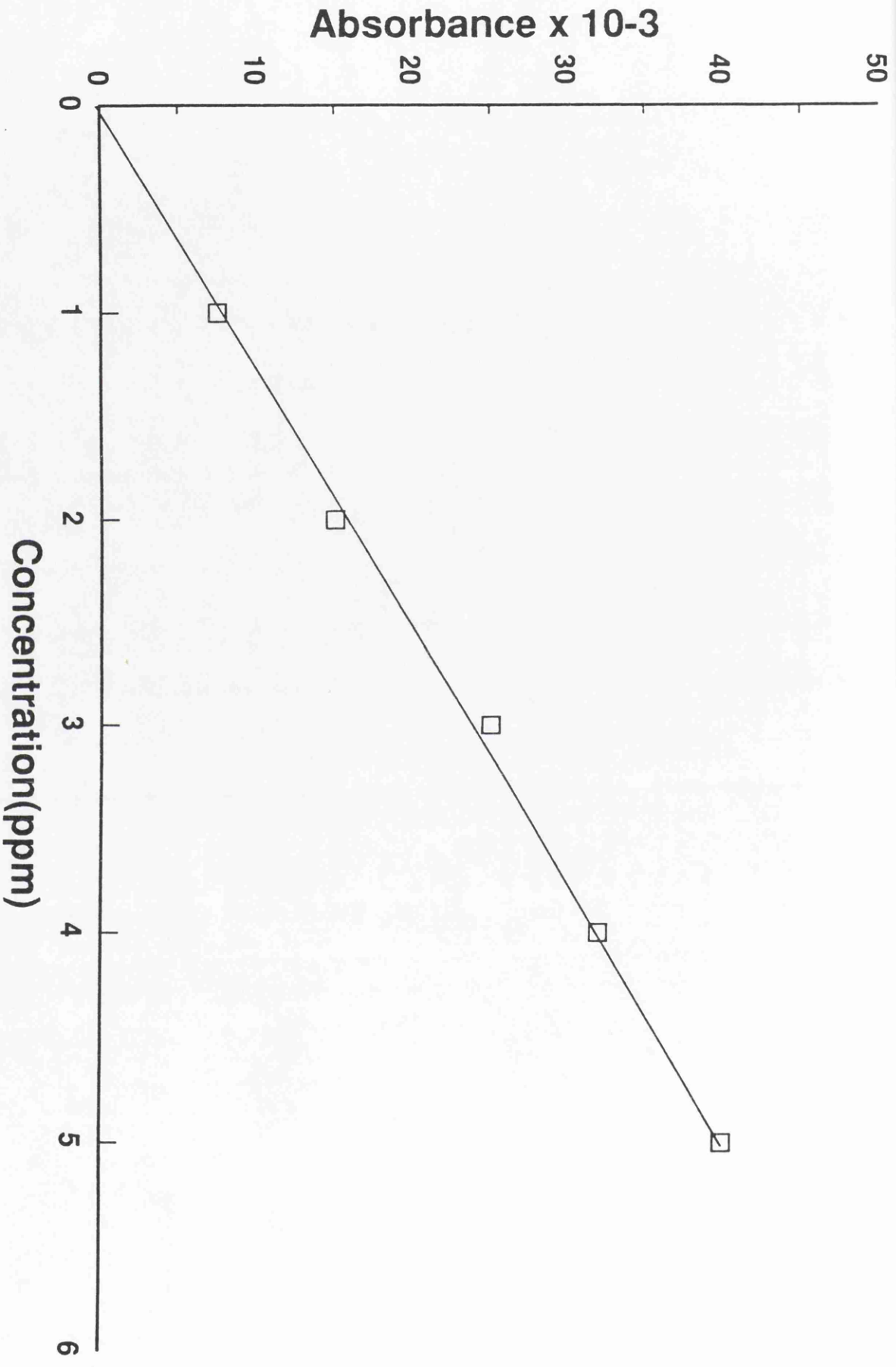


Figure 4.1. : Calibration curve of absorbances against nickel concentration.

Table 4.1.: The nickel content (%w/w) in initial solutions, solid catalyst precursors and column eluent measured by atomic absorption spectroscopy, and percentage efficiency of metal salt transfer of the methods.

Preparation Method	% Ni in Initial Solutions.	% Ni in Solid Precursors.	% Ni in Column Eluents.	% Efficiency of Metal Salt Transfer.
Impregnation	5.48	5.29	-	96.53
Ion Exchanged Sodium Hydroxide	5.36	3.37	1.46	62.87
Ion Exchanged Ammonia	5.25	4.78	0.10	91.05

X = concentration of nickel (ppm)

r = the correlation coefficient between X and Y.

This result implied that the line is quite linear with a high correlation coefficient between absorbance and concentration in the range 1-5 ppm.

The nickel content of the mother liquor, the dried precursors and the ion exchange eluents are given in table 4.1. It can be seen from the table that the impregnation technique is the most efficient at transferring the nickel salt to the support phase, the least efficient being the sodium hydroxide ion exchange technique where 27 percent of the nickel salt was left in the column eluent.

4.1.2. Studies of the eluents from the ion exchange column by UV-vis spectroscopy.

The UV-vis spectroscopy results for the ion exchange eluents are shown in figure 4.2. This figure shows that the eluents from both ion exchange routes gave a peak at 300 nm which was identified as a nitrate peak on the basis that 2 percent nitric acid was found to adsorb at 300 nm. It implied that the following ion exchange process was occurring.

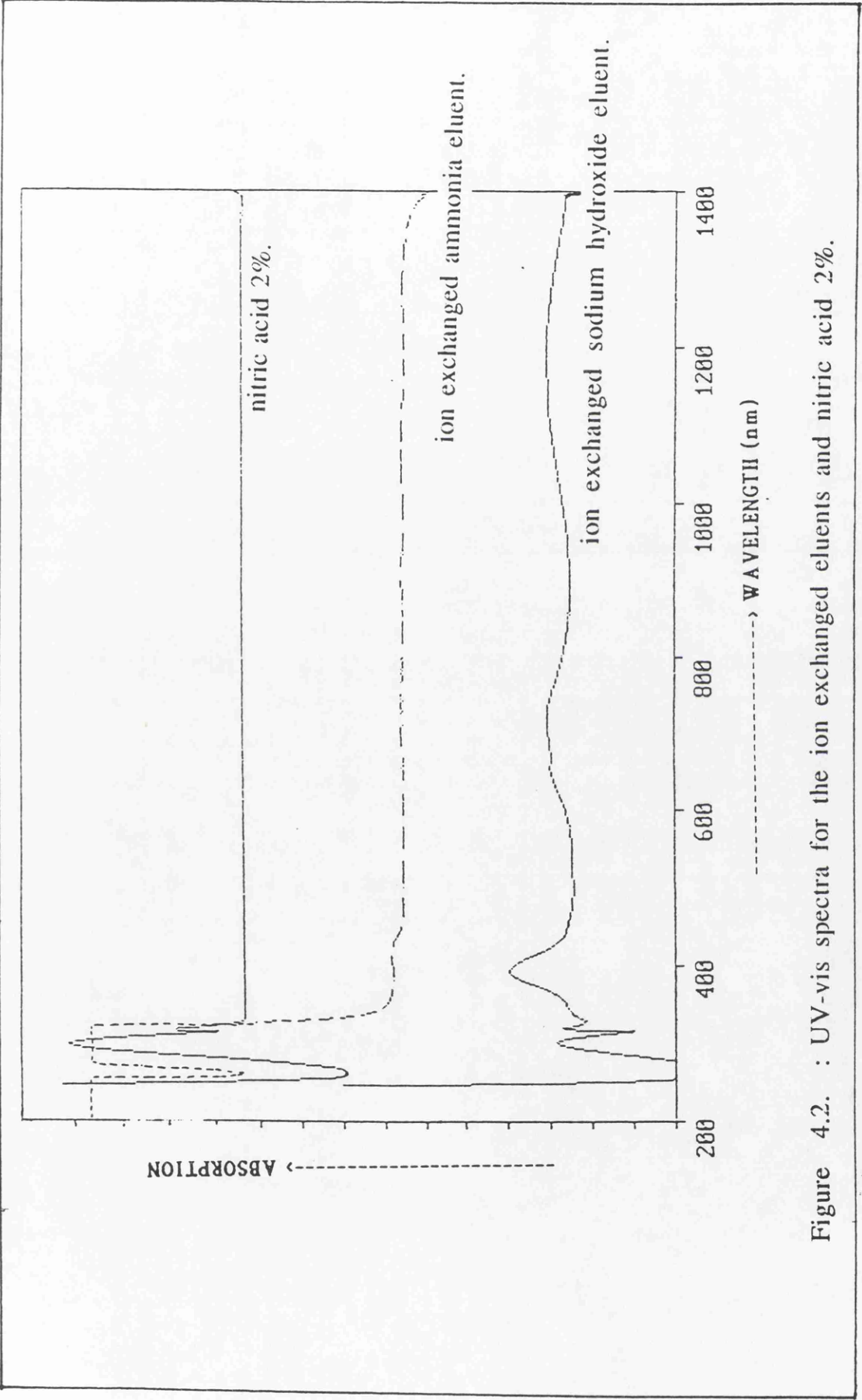
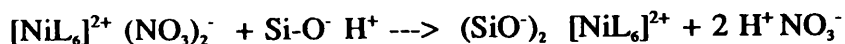


Figure 4.2. : UV-vis spectra for the ion exchanged eluents and nitric acid 2%.



where : L = H₂O or NH₃ ligands.

The eluent from the ion exchange sodium hydroxide method also produced three peaks at 1166, 718 and 398 nm which were more intense than those observed in the eluent of the ion exchange ammonia method. The peaks were due to nickel ion in an octahedral environment. The results confirm the atomic absorption results which indicates that most of nickel solution was adsorbed by silica in the ion exchange ammonia method, and that ion exchange by the sodium hydroxide method was considerably less efficient.

The low efficiency of the ion exchange produced by the sodium hydroxide method indicates that the nickel solution reached the end of the ion exchange bed during the sorption step before the surface silica was saturated with this metal ion. This was confirmed by the sodium analysis of this solid (section 4.1.3.2.) which showed that 100 g solid precursor contained 0.057 molecules of nickel and 0.004 molecules of sodium.

4.1.3. Studies of the precursors by elemental analysis and flame photometry.

The percentage nitrogen and hydrogen of the dried, calcined catalyst precursors and silica gel were determined by elemental analysis. The percentage

sodium in the calcined sodium hydroxide ion exchanged sample was examined by flame photometry. The results are presented in table 4.2.

4.1.3.1. Calcined silica gel as a reference sample.

It can be seen from table 4.2 that the calcined support contains 0.45 percent hydrogen. Lee(56) reported that silica gel contained about 4 percent water and Smith pointed out that molecular water can be strongly held even after the silica has been dried under vacuum at 623 K or higher (57). The result implied that silica gel absorbs water. This was supported by FTIR results (section 4.3.1).

4.1.3.2. Impregnated sample .

The table shows that the nitrogen and hydrogen content in the dried impregnated sample indicate that some nitrate ions and aqua ligands are retained in the catalyst precursor after drying as would be expected. No nitrogen was detected in the calcined precursor indicating that all nitrates were removed during calcination. The results were supported by FTIR (section 4.3.2) and decomposition experiments (section 4.5.1). Hydrogen detected in the calcined precursor was 0.49 %. This value is similar to that in the reference sample, thus

Table 4.2. : The hydrogen, nitrogen and sodium content (%w/w) in the dried precursors were investigated by elemental analysis and flame photometry*.

S a m p l e	% Nitrogen in Dried Precursor	% Nitrogen in Calcined precursor	% Hydrogen in Dried precursor	% Hydrogen in Calcined precursor	% Sodium* in Calcined precursor
Impregnated	1.77	n.d	1.48	0.49	-
Ion Exchanged Sodium Hydroxide	0.98	n.d.	0.83	n.d.	0.09
Ion Exchanged Ammonia	2.11	n.d.	1.04	0.71	-
Silica Gel	-	n.d.	-	0.45	-

Where : n.d. : Not detectable

- : Not measured

indicating that there was little interaction between the nickel species and the support in the calcined precursor. This was supported by XRD (section 4.4.1), thermogravimetry (section 4.5.1), TPR (section 4.6.1) and carbon monoxide chemisorption analysis (section 4.7).

4.1.3.3. Ion exchanged sodium hydroxide sample.

The dried sample ion exchanged by the sodium hydroxide method contained both nitrogen and hydrogen. Again indicating that some nitrate ions and aqua ligands are retained in the precursors. In the calcined sample neither nitrogen nor hydrogen are shown to exist. Thus the nitrate and aqua ligand in the dried sample were removed completely during calcination. The result implied that in the calcined precursor, all the hydrogen bonded hydroxyl groups were replaced by the metal indicating that a strong interaction between the nickel species and the support surface occurred. However, this result differed from the FTIR analysis (section 4.3.3), which showed that the precursor contained an hydroxyl group. This might be due to the hydrogen content being below the level of detection of elemental analysis.

The percentage of sodium in the calcined precursor was examined by flame photometry. Figure 4.3 shows the calibration curve of sodium concentration (1-4 ppm) against absorbance. The line fits the equation:

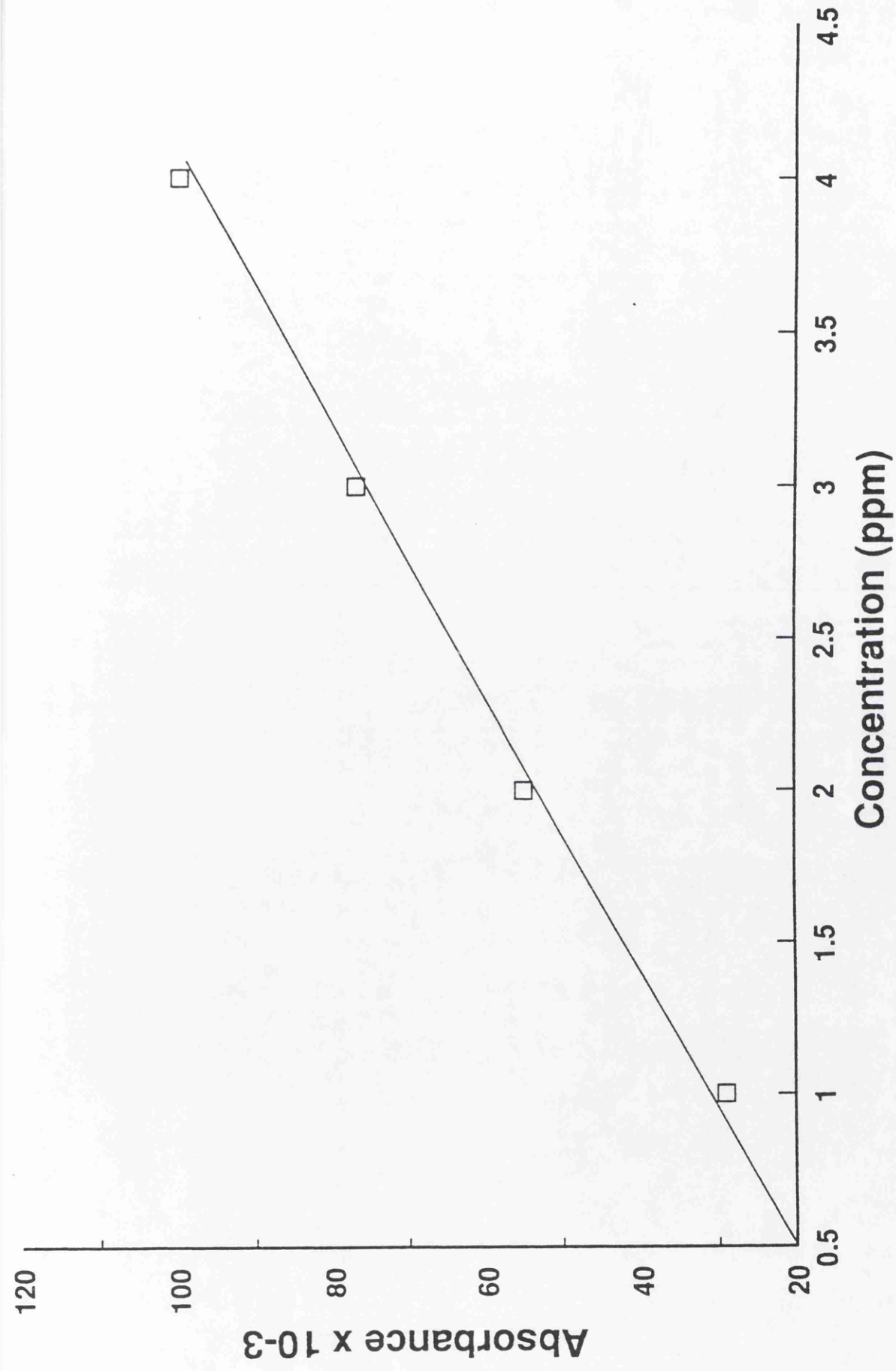


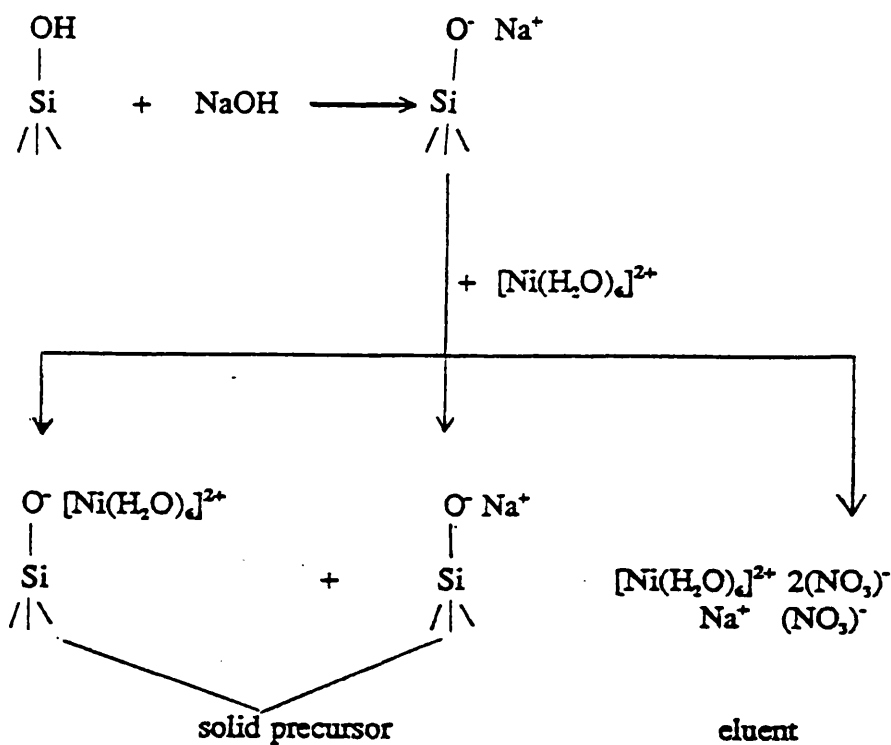
Figure 4.3. : Calibration curve of absorbances against sodium concentration.

$$Y = 21.79 X + 8.84$$

where : Y = Absorbance.

 X = Concentration of sodium(ppm).

As can be seen from the table, flame photometry analysis showed that 0.09 percent sodium was retained in the precursor prepared by this ion exchange method. This indicates that the ion exchange process occurs as follows:



Since proton surface migration, as described in section 4.2.2, can occur on the silica surface during drying, it can be predicted that the calcined precursor ion exchanged by the sodium hydroxide method contained two components i.e. nickel-hydroxide and sodium attached to the support.

4.1.3.4. Ion exchanged ammonia sample.

From table 4.2, the nitrogen content is highest in the dried sample ion exchanged by the ammonia route. This may be due to the presence of either an ammonia ligand or a nitrate ion. FTIR (section 4.3.4) and diffuse reflectance spectroscopy (section 4.2.3) supported this result. In the calcined precursor no nitrogen was detected. Again this result was supported by FTIR. This result suggested that all the nitrate ions and amine ligands in the dried precursor were totally decomposed during calcination. Hydrogen was detected in both the dried and calcined precursors, i.e., 0.71 percent hydrogen was found in the calcined precursor. This is considerably larger than that in the silica support and may be due to hydroxide ligands retained in the nickel species attached to the silica surface. This result was supported by FTIR (section 4.3.4), thermogravimetry (section 4.5.3) and TPR (section 4.6.3).

4.2. The Electronic Ground State of the Catalyst Precursors.

UV-vis spectroscopy and diffuse reflectance spectroscopy were used for the investigation of the electronic ground state of the catalyst precursors.

Figure 4.4 shows the UV-visible spectra for the prepared nickel hexaaqua and nickel hexaammine complex solutions obtained by UV-vis spectroscopy.

The solution of the octahedral complex hexaaquanickel(II) nitrate produced three main absorption bands at 1166, 718 and 394 nm. If we compare these bands with table 1.2 in section 1.4.2 which refers to the wave number for allowed transitions for the two different ligands on the nickel ion we find that the ${}^3T_2 \leftarrow {}^3A_2$ transition is at 1166 nm, the ${}^3T_1(F) \leftarrow {}^3A_2$ transition is at 718 nm and the ${}^3T_1(P) \leftarrow {}^3A_2$ transition is at 394 nm.

The octahedral complex solution, hexaaminenickel(II) nitrate, produced three main peaks at 932, 577 and 359 nm. The band at 932 nm is attributed to the ${}^3T_2 \leftarrow {}^3A_2$ transition; the band at 577 nm is assigned to the ${}^3T_1(F) \leftarrow {}^3A_2$ and the band at 359 nm is attributed to the ${}^3T_1(P) \leftarrow {}^3A_2$ transition.

Figure 4.5 shows the UV reflectance spectra of the dried catalyst precursors obtained by diffuse reflectance spectroscopy with silica gel as a reference.

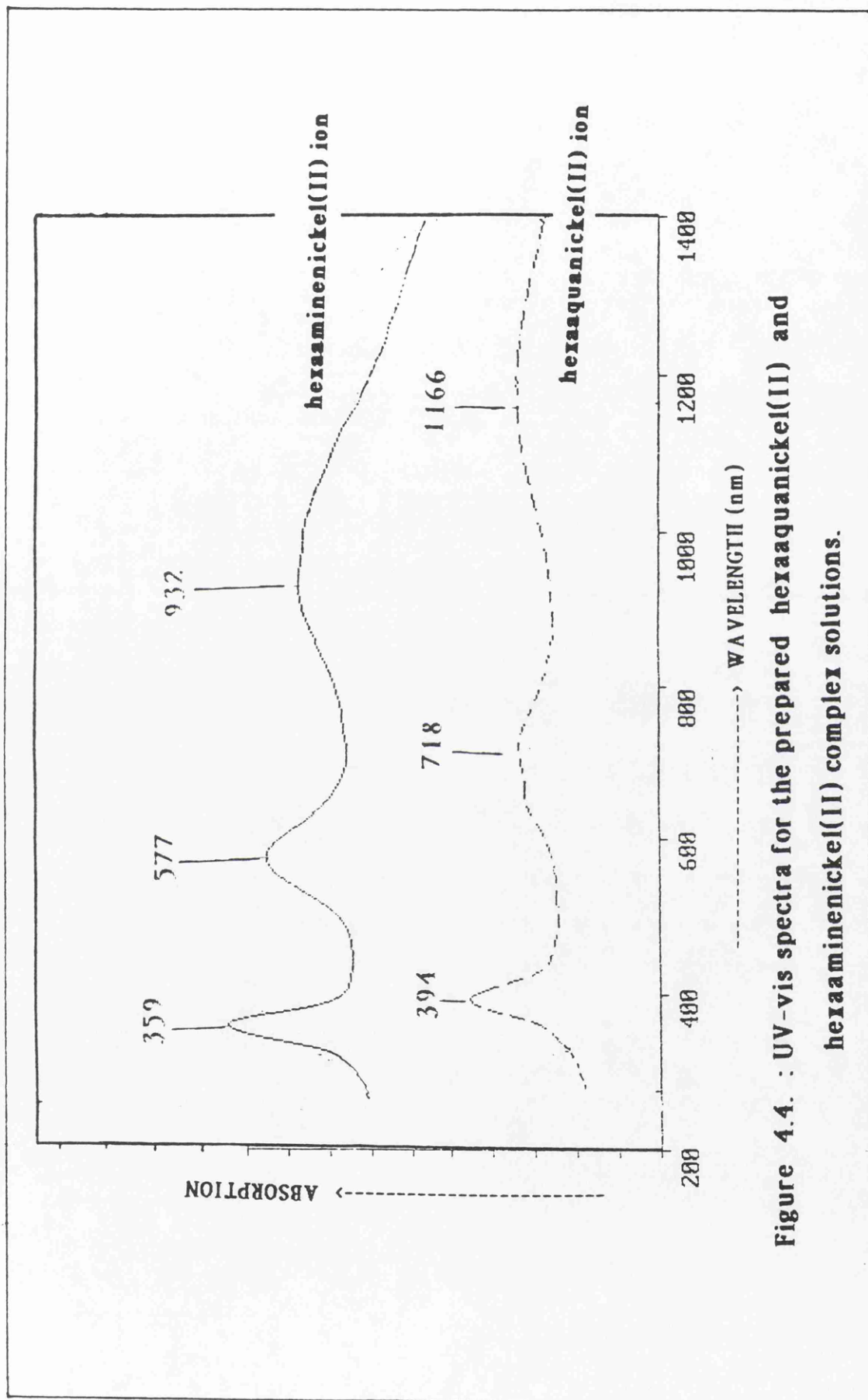
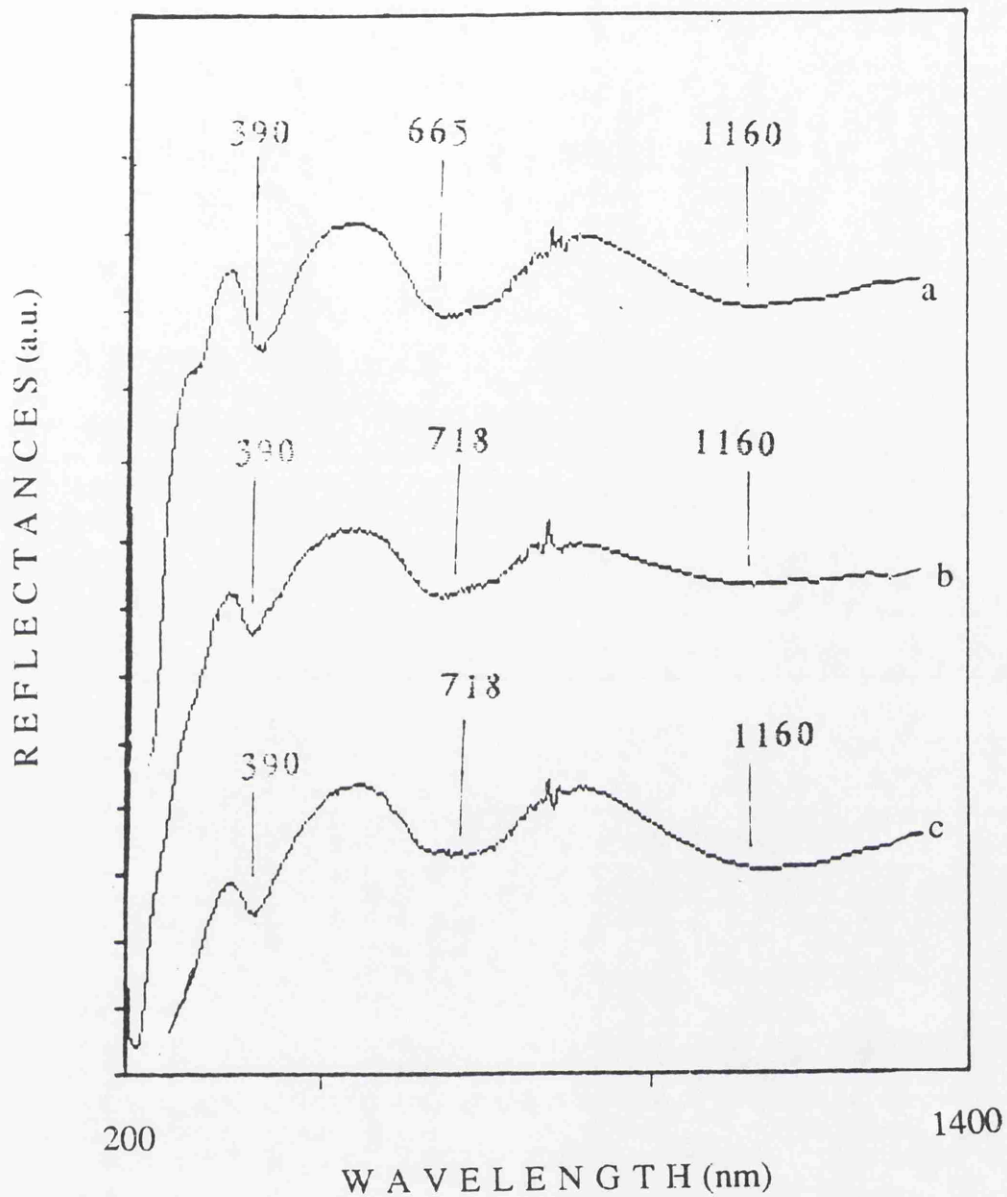


Figure 4.4. : UV-vis spectra for the prepared hexaaquanickel(II) and hexaaminenickel(II) complex solutions.



where a : ion exchanged ammonia sample.
 b : ion exchanged sodium hydroxide sample.
 c : impregnated sample.

Figure 4.5. : Reflectance spectrum of the dried catalyst precursors.

4.2.1. Impregnated precursors.

The sample gave bands at 1160, 718 and 390 nm (figure 4.5.a) corresponding to those observed in the nickel hexaqua spectra. This indicates that nickel(II) is present in the dried precursors as the octahedral complex, hexaaquanickel(II) ion.

4.2.2. Ion exchanged sodium hydroxide precursors.

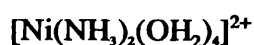
The sample gave bands at 1160, 718 and 390 nm (figure 4.5.b) which can again be assigned to nickel(II) in the octahedral coordination, hexaaquanickel(II) ion. However, the water molecules may have partially decomposed into hydroxide ions during the drying stage, since proton surface migration can occur on the silica surface during drying (7).

4.2.3. Ion exchanged ammonia precursors.

This sample gave bands at 1160, 665 and 390 nm (figure 4.5.c). The bands at 1160 and 390 nm were again similar to those in the nickel hexaqua spectra and can be attributed to the transitions ${}^3T_2 \leftarrow {}^3A_2$ and ${}^3T_1(P) \leftarrow {}^3A_2$ respectively. However the band due to the transition ${}^3T_1(F) \leftarrow {}^3A_2$ was

shifted to 665 nm. This suggests that some ammonia ligands have been retained in the dried catalyst precursor prepared by this method.

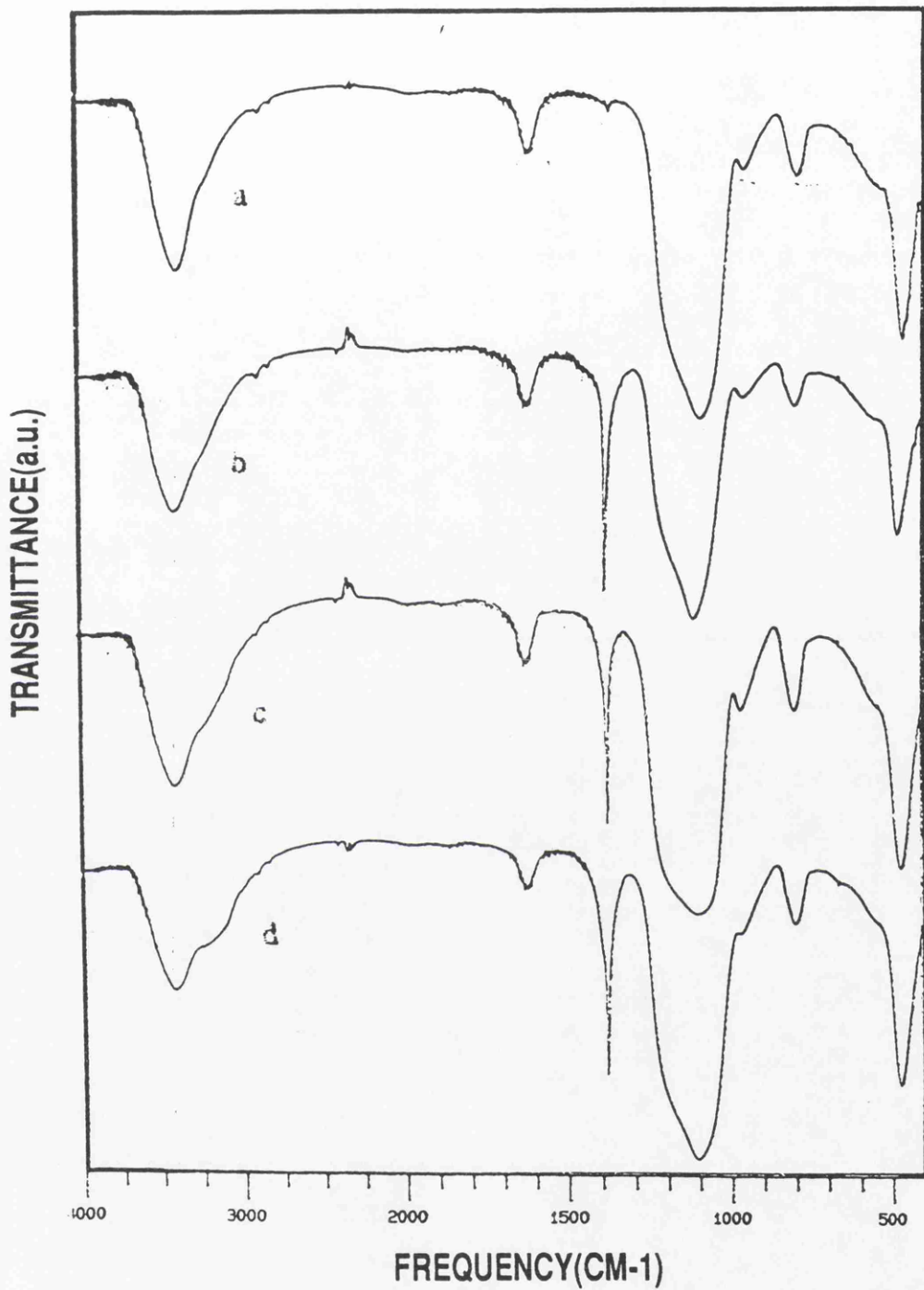
In fact, ion exchange of the silica with nickel hexaammine solution formed a blue gel which changed to a bluish-green colour on washing with water. The ${}^3T_1(F) \leftarrow {}^3A_2$ transition gave a band at 577 nm for the nickel(II) hexaammine solution. A value of 665 nm is therefore consistent with the formation of the nickel(II) diammine which would be formed by replacing the four ammonia ligands with water when the sample was washed (9). This is a good agreement with the result of percentage nitrogen contained in the sample which was measured by elemental analysis (table 4.2, section 4.1.3). The 2.11 percent nitrogen corresponds to a diamine molecule. The existence of amine was confirmed by FTIR (section 4.3.4). Once again surface migration of protons may occur to give hydroxide ions. The suggested Ni species in the sample is:



4.3. Studies of the Precursors by FTIR.

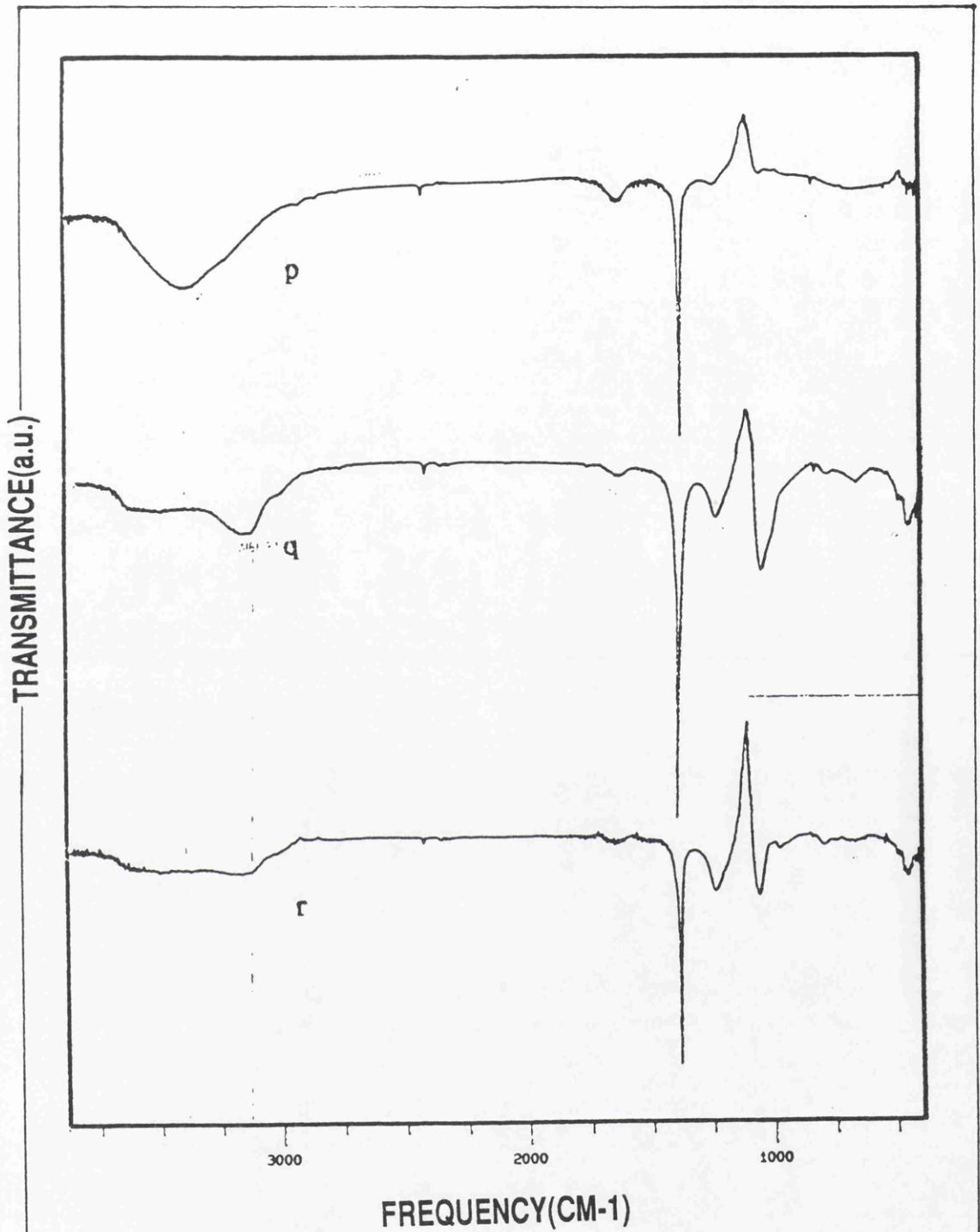
Fourier transform infrared spectroscopy (FTIR) was used to characterize the dried and calcined precursors. A pure calcined silica gel was also examined to obtain a reference spectrum.

Figure 4.6, figure 4.7 and 4.8 show the IR spectra of the dried precursors



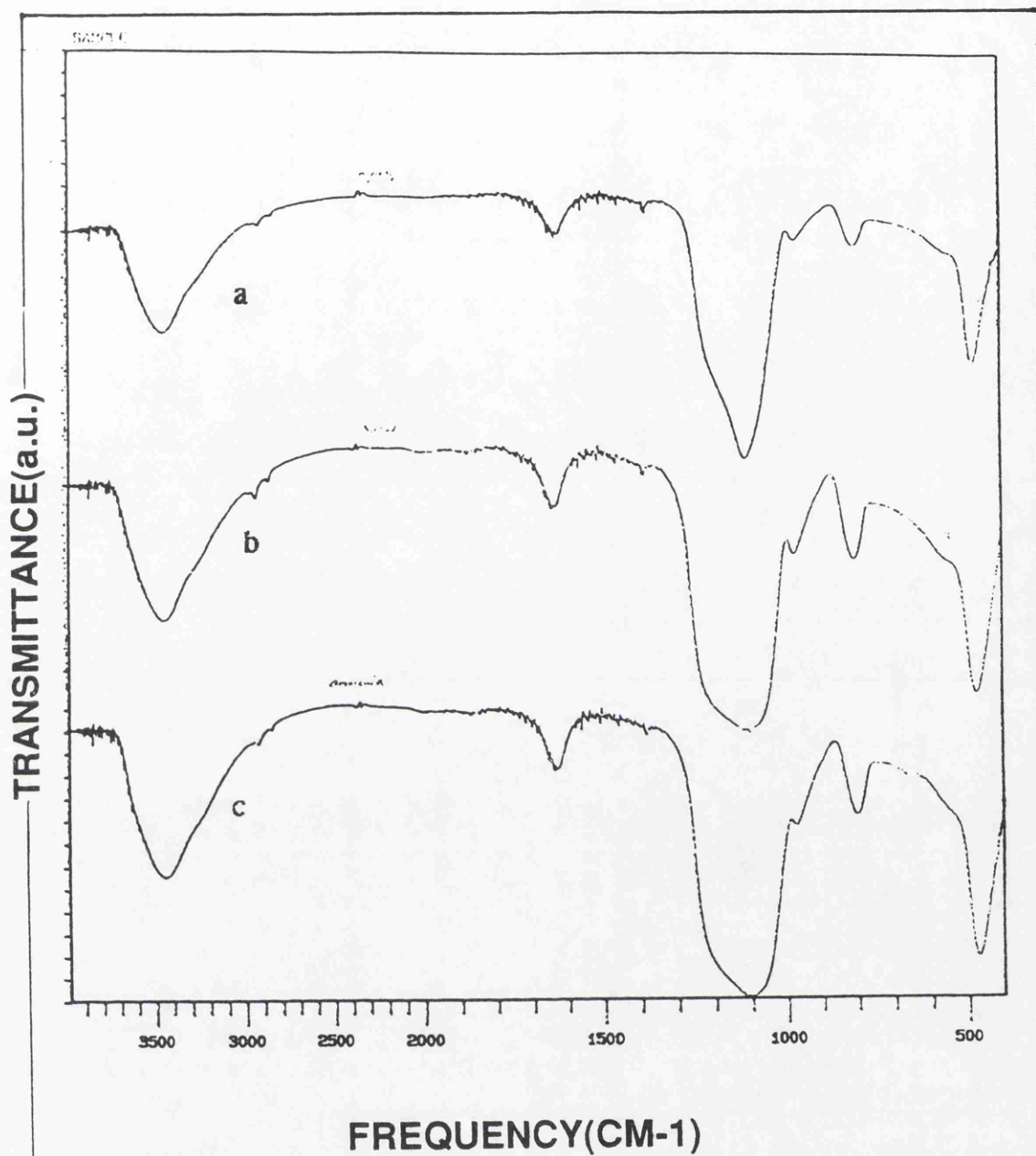
where a : silica gel
b : impregnated sample
c : ion exchange sodium hydroxide sample.
d : ion exchange ammonia sample.

Figure 4.6. : FTIR-Spectra of the dried precursors and the silica gel.



where p : impregnated sample.
q : ion exchanged ammonia sample.
r : ion exchanged sodium hydroxide sample.

Figure 4.7. : FTIR-sub traction spectra of the silica gel from the dried precursors.



where a : impregnated sample.
b: ion exchanged sodium hydroxide sample.
c: ion exchanged ammonia sample.

Figure 4.8. : FTIR-Spectra of the calcined precursors.

and the silica gel; the same spectra after subtraction of the silica gel spectrum, and the spectra of the calcined precursors respectively.

4.3.1. Reference spectra :

The reference silica gel spectrum is shown in figure 4.6.a. The silica gel gave three characteristic peaks at 3438, 1638 and 1109 cm^{-1} . The (tail) band at 3438 cm^{-1} can be attributed to strongly hydrogen bonded OH groups and/or adsorbed water; the band at 1638 cm^{-1} is assigned to OH bending in water molecules. This result confirmed the hydrogen content in the calcined silica gel (table 4, section 4.1.3) which implied that silica gel is a hygroscopic material. Molecular water can be strongly held even after silica has been dried under vacuum at 623 K or higher (57). The band at 1109 cm^{-1} is associated with the characteristic siloxane band due to asymmetric Si-O-Si stretching modes (58).

4.3.2. Impregnated method.

4.3.2.1. Dried sample :

Figure 4.6.b shows the spectra of the dried precursor and figure 4.7.p shows the

same spectra after subtraction of the reference spectra.

The peaks at 3438 and 1638 cm^{-1} in figure 4.7.p are attributed to the stretching and bending of hydrogen bonded OH groups. Since the intensity of the peak at 3438 cm^{-1} is quite high compared to that of the ion exchanged sample, the OH groups are probably in a hydrate form as implied by the elemental analysis results (section 4.1.3.1). The peak at 1385 cm^{-1} is associated with a nitrate peak. Addison et.al. (59) illustrated that the nitrate ion from hexaaquanickel(II) nitrate gave a band in the same position. Again elemental analysis(section 4.1.3.1) supported this result.

4.3.2.2. Calcined sample :

Figure 4.8.a illustrates the spectrum of the calcined precursor. The spectrum is similar to that of the reference spectra (section 4.3.1). The peak at 1385 cm^{-1} in the dried precursor spectrum has disappeared. No nitrogen was detected in the calcined precursor by elemental analysis (table 4.2, section 4.1.3) thus confirming that all the nitrate had decomposed during the calcination stage.

4.3.3. Ion exchanged sodium hydroxide method :

4.3.3.1. Dried sample:

Figure 4.6.c shows the spectrum of the dried precursor and figure 4.7.r

shows the same spectrum after subtraction of the silica spectrum. The broad peaks at 2800-3800 cm^{-1} and 1638 cm^{-1} shown in figure 4.7.r are again associated with stretching and bending modes of hydrogen bonded OH groups or some physically adsorbed water. The intensity of both peaks are very small compared to those for the impregnated sample. It is assumed that some of hydrogen bonded OH groups have been replaced by metal ions. This was supported by atomic absorption analysis (section 4.1.1), elemental analysis and flame photometry studies (section 4.1.3). The peak at 1385 cm^{-1} is once again associated with a nitrate ion.

4.3.3.2. Calcined sample :

Figure 4.8.b shows the spectrum of the calcined precursor. The spectrum is similar to that of the reference spectrum. The peak at 1385 cm^{-1} in the dried precursor spectra has disappeared, confirming that all the nitrate has decomposed during calcination as suggested by the elemental analysis results (section 4.1.3).

4.3.4. Ion exchanged ammonia method.

4.3.4.1. Dried sample:

Figure 4.6.d and figure 4.7.q show the spectra of the dried precursor and the

same spectra after subtraction of the reference spectra respectively. The broad peaks at 2800-3800 cm^{-1} and 1638 cm^{-1} are again associated with the OH group stretching and bending modes respectively. The intensity of both peaks are very small and it is assumed that the nickel ion has replaced the hydrogen bonded OH groups as was also the case for the dried ion exchanged sodium hydroxide precursor. However the spectrum of this precursor differs from its ion exchanged sodium hydroxide precursor counterpart since it contains a new peak at 3161 cm^{-1} . This new peak may interpreted as a form of NH_4^+ , since Socrates (60) found that NH_4^+ gave an IR band in the region of 3335-3030 cm^{-1} . This peak is probably the result of an interaction between hydrogen bonded OH groups or water molecules with ammonia molecules adsorbed on the precursor surface. UV-vis spectroscopy (section 4.2.3) and elemental analysis (section 4.1.3) supported this result.

4.3.4.2. Calcined sample:

Figure 4.8.c shows the spectra of ^{the} calcined precursor. The spectrum is again approximately the same as the reference spectrum. The peaks at 1385 and 3161 cm^{-1} on the dried precursor spectra have disappeared and so it can be said that all the nitrate ions and ammonia ligands have decomposed during the calcination as indicated by the elemental analysis studies (section 4.1.3).

4.4. The Bulk Structure of the Dried, Calcined and Reduced Precursors.

X-ray diffraction (XRD) was used to identify the phases present in the dried, calcined and reduced catalyst precursors. The x-ray data for the precursors and pure silica gel as a reference are reported in table 4.3. ; Powder diffraction files for nickel and its precursor salts are reported in table 4.4. and the schematic Guinier XRD patterns for the samples are shown in figure 4.9.

4.4.1. Impregnated sample :

The dried impregnated precursor gave a single x-ray line with a d value of 4.00, which corresponded in position and intensity to that of silica gel.

The calcined precursor had four lines at 3.98, 2.07, 2.40 and 1.47 with a ratio of 10 : 5 : 3 : 2 respectively. The line at 3.98(d₁) again corresponds to that of the silica gel and the d values of 2.07, 2.40 and 1.47 match those of NiO in bunsenite(table 4.4.) .

D-spacing in the reduced precursor corresponded in position and intensity to silica gel(3.97) and nickel metal(2.04, 1.77 and 1.25).

The hkl values for the above results were compiled from JCPDS files(table 4.5.). The calcined precursor, which has the composition of nickel oxide, contains both (200) and (111) planes in the ratio of 10 : 9 . The reduced precursor which has the composition of nickel metal, contains (200) and (111)

Table 4.3. : Typical X-ray diffraction line positions of the samples .

Method/Samples	d ₁	d ₂	d ₃	d ₄
Silica gel	4.04	-	-	-
DRIED SAMPLE				
Impregnation	4.00	-	-	-
Ion exchange sodium hydroxide	3.93	-	-	-
Ion exchange ammonia	4.02	-	-	-
CALCINED SAMPLE				
Impregnation	3.98 _x	2.07 ₅	2.40 ₃	1.47 ₂
Ion exchange sodium hydroxide	3.97	-	-	-
Ion exchange ammonia	4.07	-	-	-
REDUCED SAMPLE				
Impregnation	3.97 _x	2.04 ₅	1.77 ₂	1.25 ₁
Ion exchange sodium hydroxide	4.07 _x	2.17 ₁	1.88 ₁	1.44 ₁
Ion exchange ammonia	4.04 _x	2.05 ₅	1.76 ₁	1.30 ₁

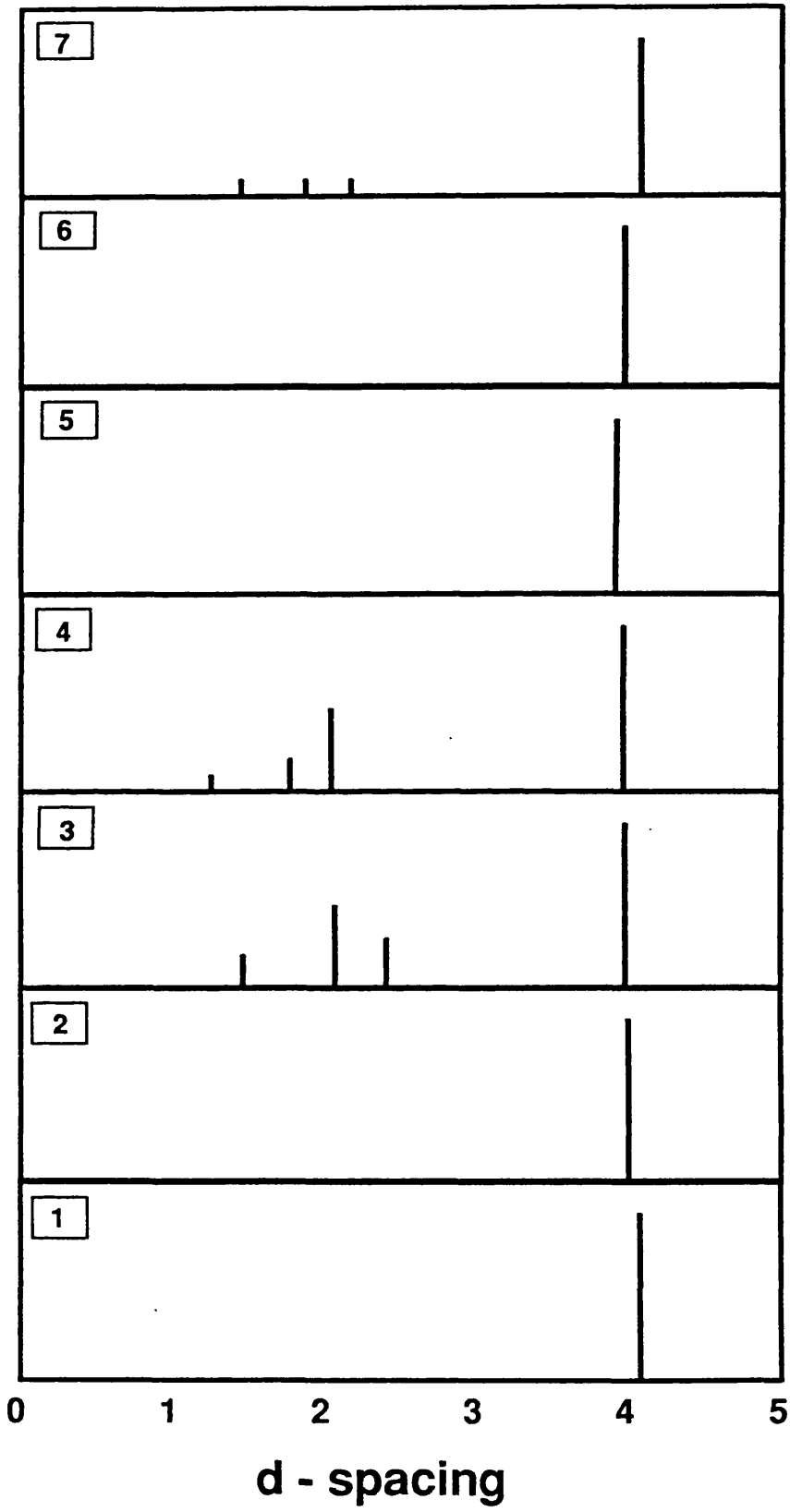
Table 4.4 : Typical XRD line positions for some nickel compounds from powder diffraction file (61).

Files data	Nickel Compound	d ₁	d ₂	d ₃
F-04-0835	Nickel Oxide, Bunsenite, syn. NiO	2.09 _x	2.41 _y	1.48 _z
F-04-0850	Nickel, syn. Ni	2.03 _x	1.76 _z	1.25 _z
F-14-0177	Nickel Hydroxide Ni(OH) ₂	4.61 _x	2.33 _x	2.71 _z
F-14-0452	Nickel Nitrate Ni(NO ₃) ₂ .6H ₂ O	2.75 _x	3.75 _y	5.49 _y
F-14-0481	Nickel Oxide (Ni ₂ O ₃)OH	2.80 _x	2.02 _x	1.77 _x
F-14-0593	Nickel Nitrate Ni(NO ₃) ₂	4.22 _x	2.20 _z	2.11 _z
F-15-0388	Nickel Silicate Liebenbergite Ni ₂ SiO ₄	2.43 _x	3.47 _y	2.74 _y

Figure 4.9. : Schematic XRD patterns (d-spacing) .

1. Silica gel.
2. Impregnated sample/dried precursor.
3. Impregnated sample/calcined precursor
4. Impregnated sample/reduced precursor.
5. Ion exchanged sodium hydroxide sample/dried precursor.
6. Ion exchanged sodium hydroxide sample/calcined precursor.
7. Ion exchanged sodium hydroxide sample/reduced precursor.
8. Ion exchanged ammonia sample/dried precursor.
9. Ion exchanged ammonia sample/calcined precursor.
10. Ion exchanged ammonia sample/reduced precursor.
11. Bunsenite,syn.
12. Nickel,syn.
13. Nickel silicate.

Intensity \updownarrow



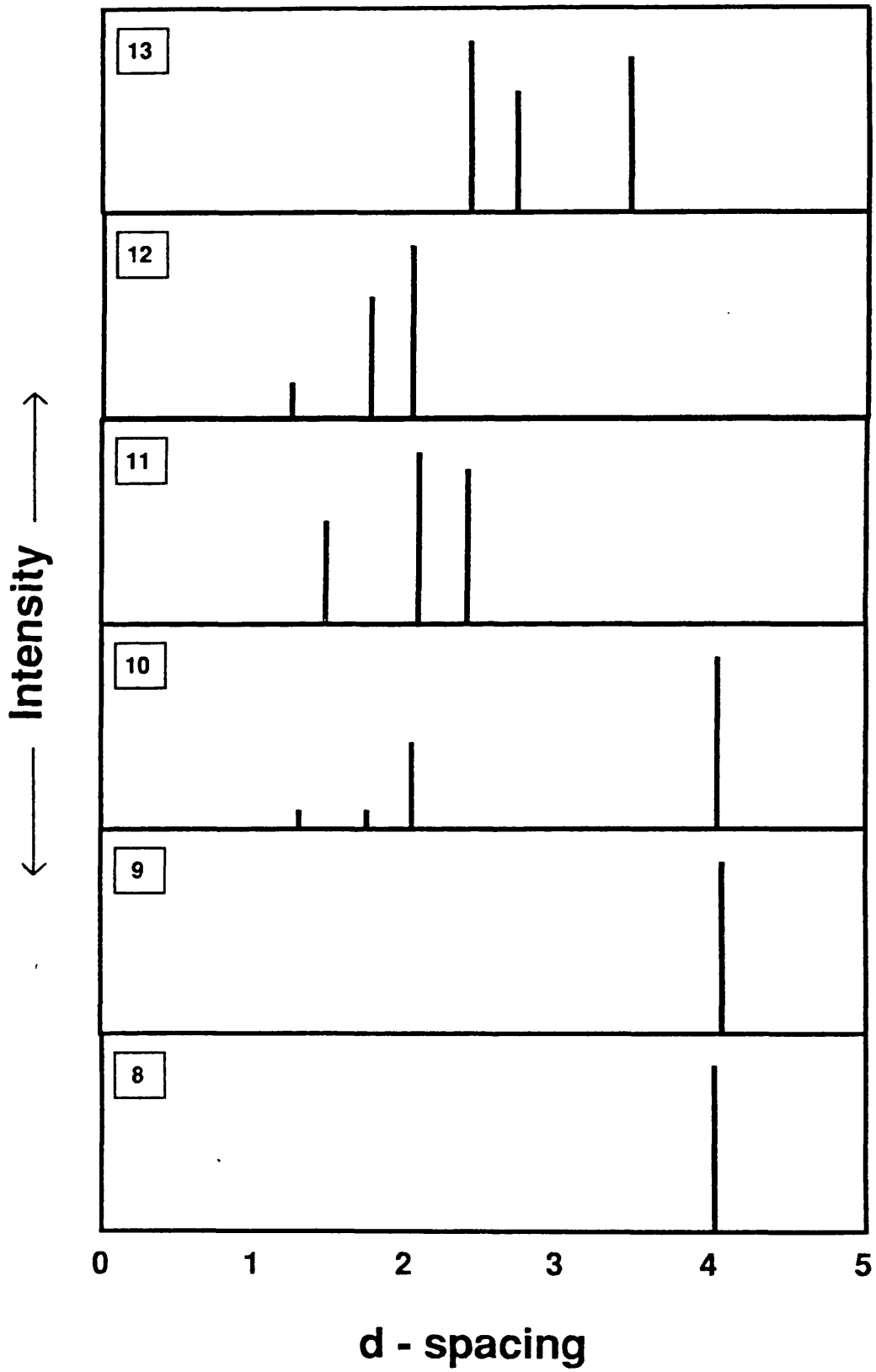


Table 4.5.: Typical hkl scales were compiled from powder diffraction files (61).

Compounds	Line position (d_n)	hkl scale
Nickel Oxide, Bunsenite,syn.	$d_1 = 2.09_x$	200
	$d_2 = 2.41_9$	111
	$d_3 = 1.48_6$	220
Nickel,syn.	$d_1 = 2.03_x$	111
	$d_2 = 1.76_4$	200
	$d_3 = 1.25_2$	222
Nickel Silicate, Liebenbergite,syn.	$d_1 = 2.43_x$	112
	$d_2 = 3.47_9$	111
	$d_3 = 2.74_7$	130

planes in the ratio of 4 : 10. Since the ratio of (200) planes decreases and (111) planes increases, it may be said that reduction involves a change from predominantly nickel(II) oxide (200) to nickel metal (111). The schematic figure for both planes is shown in figure 4.10.

4.4.2. Ion exchanged samples :

The dried and calcined precursors from both methods show a single line position about 4.0 (d_1). This line position is almost the same as that for silica gel. Both reduced precursors gave four lines, one of which corresponded to that for silica. The remaining three lines for the ion exchanged ammonia sample were at 2.05, 1.76 and 1.30 with the ratio of 5 : 1 : 1 respectively. The corresponding lines for the ion exchanged sodium hydroxide sample were at 2.17, 1.88 and 1.44 with a ratio of 1 : 1 : 1.

The hkl analysis for both reduced precursors showed that the ion exchanged sample by the ammonia method has crystals with planar spacings of (111), (200) and (222) in the ratio of 5 : 1 : 1. This result indicated that the nickel metal in this sample has a different composition from that in the nickel metal reference. The composition of the ion exchanged sample by the sodium hydroxide method could not be identified. This might be due to the nickel content being below the level of detection of the diffractometer or the influence of the retained sodium (section 4.1.3) which could probably change the crystal form.

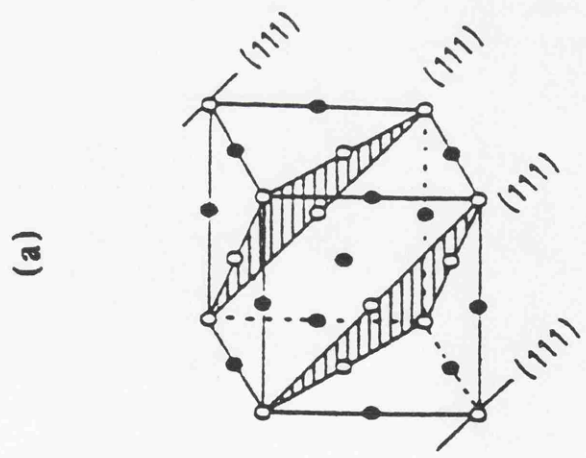
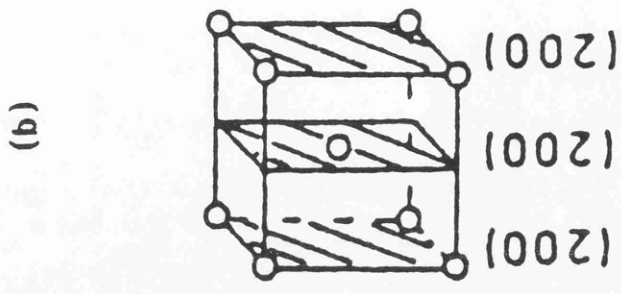


Figure 4.10. : (a) (111) planes and (b) (200) planes.

4.5. The Decomposition of the Dried Precursors.

Thermogravimetry was used to investigate the thermal decomposition of the dried precursors in air . The results are shown in Figure 4.11. The figure shows the percentage weight loss with increasing temperature from room temperature to 923 K.

4.5.1. Impregnated sample:

The TGA curve for this sample (figure 4.11), shows that increasing the temperature from room temperature to 673 K resulted in a single stage decomposition with a 19.0 percent weight loss by 673 K. No further change in weight occurred up to 923 K, indicating that the nickel species in the dried impregnated precursor had fully decomposed to nickel(II) oxide. This was confirmed by XRD analysis of this sample (section 4.4.1). Diffuse reflectance studies showed that nickel(II) ions in the dried precursor were in an octahedral configuration (section 4.2.1), but the exact stoichiometry is unlikely to be hexaaquanickel(II)nitrate due to loss of bound water on drying. The theoretical percentage decomposition in this reaction is shown in table 4.6. According to this table, the value of 19.0 % corresponds to the decomposition of nickel(II) nitrate with 5.7 molecule hydrate to nickel(II) oxide. B.Mile et.al. (37) reported that three main stages can be distinguished on the decomposition of the nickel

Heating rate : 10K/min.

atmosphere : air carrier gas rate: 50 ml/min.

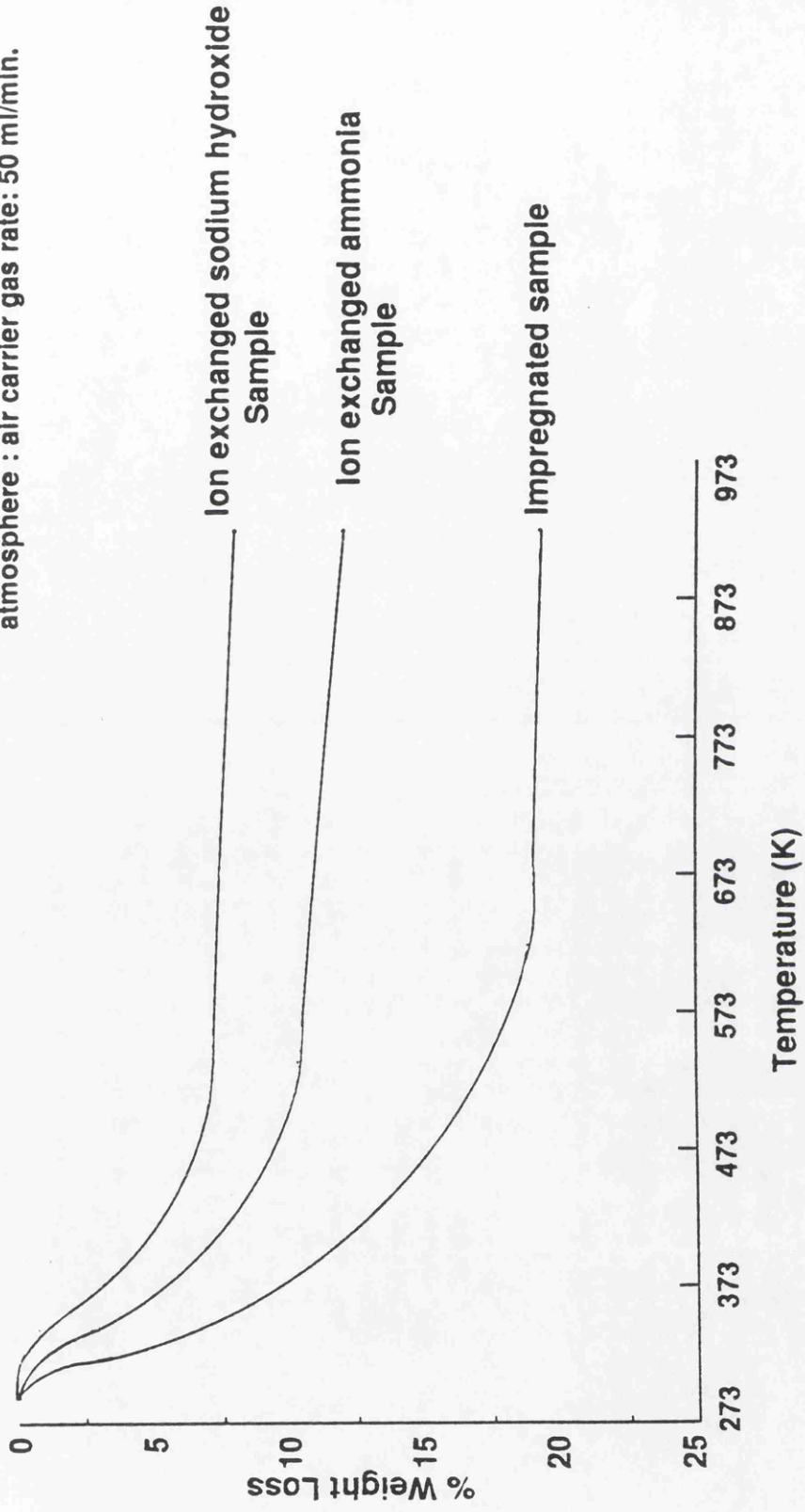


Figure 4.11. : The % weight loss of dried impregnated and ion exchanged samples with increasing temperature measured by thermobalance.

Table 4.6 : The theoretical percentage decomposition of nickel species contained in dried precursors to nickel(II)oxide at the sample which were prepared by different methods.

Preparation method/ Ni species suggested	X value	% Decomposition
Impregnation method/ $\text{Ni}(\text{NO}_3)_2 \cdot X \text{H}_2\text{O}$	X = 0	9.73
	X = 1	11.36
	X = 2	12.98
	X = 3	14.60
	X = 4	16.22
	X = 5	17.85
	X = 6	19.46
Ion exchanged sodium hydroxide method/ $\text{Ni}(\text{OH})_{2-x} (\text{NO}_3)_x \cdot (6.43 X - 1) \text{H}_2\text{O}$	X = 1	9.23
	X = 2	18.46
Ion exchange ammonia method/ $\text{Ni}[(\text{NH}_3)_6(\text{H}_2\text{O})_x](\text{OH})_2$ 6-x	X = 0	5.70
	X = 1	7.17
	X = 2	8.63
	X = 3	10.10
	X = 4	11.57
	X = 5	13.03

catalyst supported on silica prepared by ^{the} impregnation method at a 13 percent nickel loading. These stages indicated that there was a similarity with the stages created by the bulk nickel(II) nitrate hexahydrate decomposition. The last stage was at 550 K where nickel(II) salt presumably fully decomposed to form nickel(II) oxide.

4.5.2. Ion exchanged sodium hydroxide sample:

The TGA trace for this sample, (figure 4.11), shows that decomposition of the nickel salt occurred in one stage with a 7.80 percent weight loss up to 673 K. A further weight loss of 1.5 percent then occurred between 673 and 923 K. Diffuse reflectance studies of the dried precursor indicated that proton migration from the silica to the hydrated metal ion may occur on drying.

Although the decomposition of the hydroxide at 673 K did not give a diffraction pattern for nickel(II) oxide, TPR studies (section 4.6.2) indicated the presence of a nickel species which was easy to reduce. It is quite likely therefore that the decomposition of this sample includes the change from nickel hydroxide to the nickel(II) oxide attached to the silica surface.

Since elemental analysis studies (section 4.1.3.2) found that the dried precursor contained nitrogen and hydrogen which corresponds to nitrate ions and hydroxyl groups, therefore, based on the data, the nickel species in this precursor was suggested as $\text{Ni(OH)}_{2-x}(\text{NO}_3)_x \cdot (6.43 X - 1) \text{H}_2\text{O}$. The theoretical

percentage decomposition is shown in table 4.6. The value of 7.80 percent decomposition observed by 673 K from the experiment corresponds to the theoretical value at the value of $X = 0.85$. However a further weight loss was indeed measured up to 923 K corresponding to a total weight loss of 9.3 percent. Therefore the value of X is between 0.85 and 2. The stability of this precursor is indicative of a strong interaction between the nickel species and the support.

4.5.3. Ion exchanged ammonia sample :

The TGA curve for this sample (figure 4.11), shows that increasing the temperature from room temperature to 673 K resulted in a single stage decomposition corresponding to an 11.30 percent weight loss by 673 K. A further gradual weight loss (1.2 percent) was detected between 673 and 923 K indicating that decomposition of the precursor was incomplete at 673 K.

Diffuse reflectance spectroscopy studies of the dried precursor (section 4.2.3) have indicated that the nickel cation is probably $[\text{Ni}(\text{NH}_3)_2(\text{OH}_2)_4]^{2+}$ attached to the support via $\equiv\text{SiO}^-$ groups and charge compensated by OH^- rather than NO_3^- . TPR studies have also shown that the sample contains an easily reduced nickel species (section 4.6.3), so it is likely that some of the nickel salt is not in intimate contact with the support and thus readily decomposes to

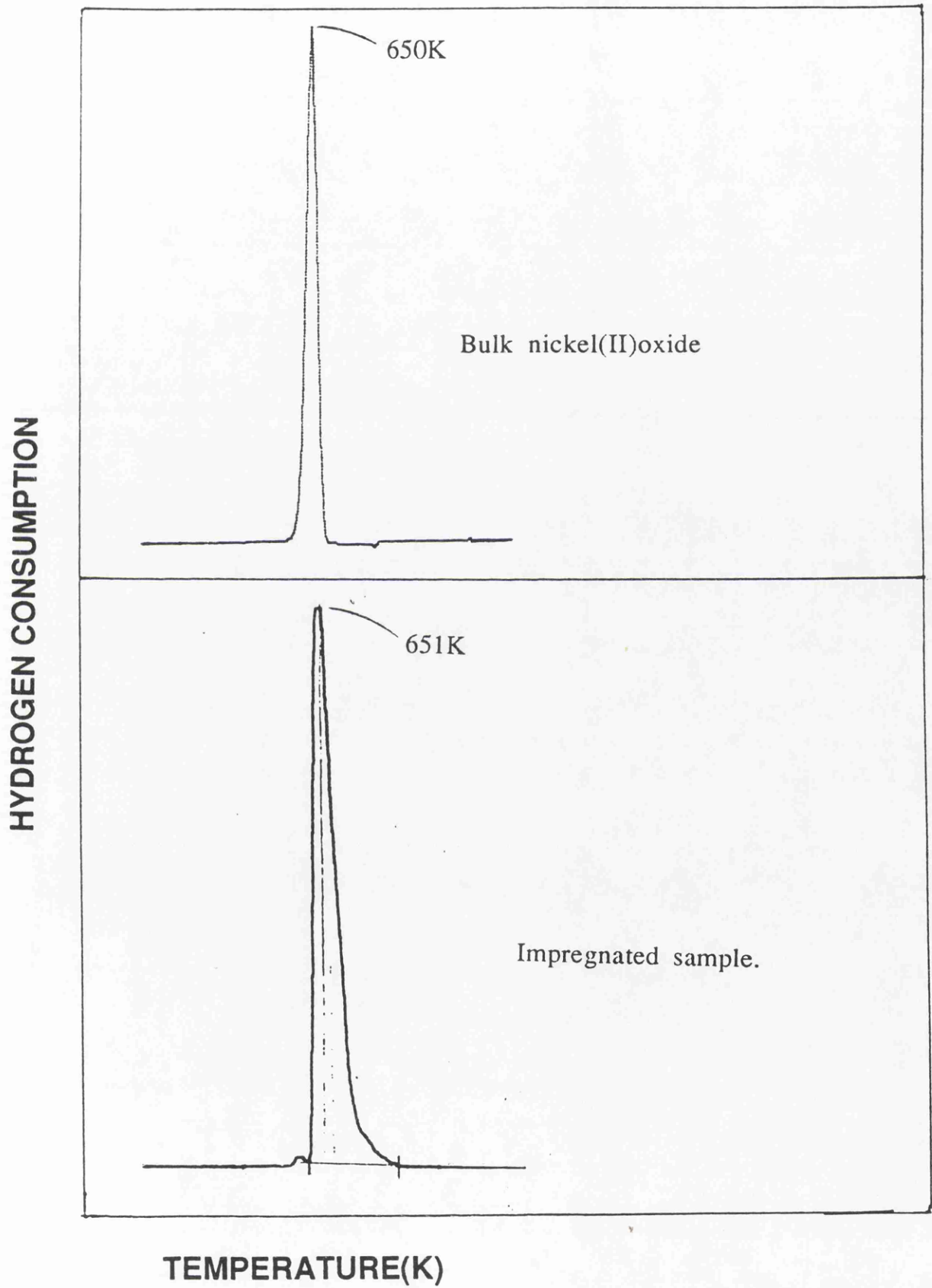
nickel(II)oxide on calcination.

The percentage theoretical decomposition was calculated assuming that no nitrate remained in the dried precursor. The result is shown in table 4.6. From the table, assuming that the nickel species in the precursor is $[\text{Ni}(\text{NH}_3)_2(\text{H}_2\text{O})_2]^{2+}(\text{OH})_2$; the theoretical percentage for decomposition to the oxide is 11.57 percent. This is in close agreement with the experimental value. The small further weight loss above 673 K may be due to the presence of small amounts of nickel hydrosilicate species which proved difficult to reduce (section 4.6.3).

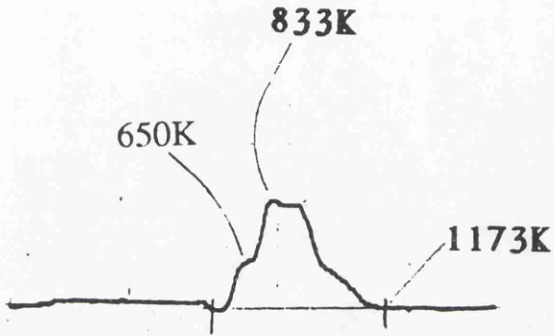
4.6. The Reducibility of the Calcined Precursors.

Temperature programmed reduction was used to investigate the reducibility of each of the calcined catalysts and nickel(II) oxide. The plot of hydrogen consumption against reduction temperature is shown in figure 4.12 and the percentage reduction estimated in table 4.7. The figure shows that bulk unsupported nickel(II) oxide gives a single TPR peak with a maximum at 651 K.

Figure 4.12 : The hydrogen consumption of calcined catalyst precursors with increasing temperature measured by temperature programmed reduction, rate :20K/min.



Ion exchanged sodium hydroxide sample



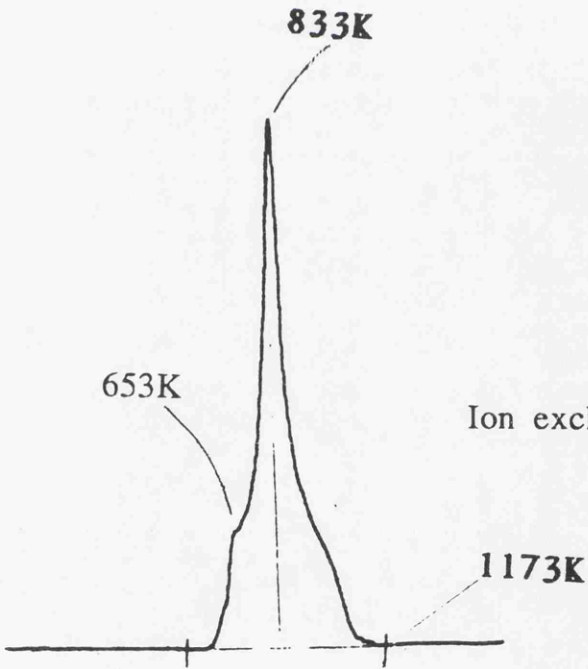
HYDROGEN CONSUMPTION

833K

653K

Ion exchanged ammonia sample

1173K



TEMPERATURE(K)

Table 4.7. : Hydrogen consumption of impregnated and ion exchanged sample

Method	Sample Weight (g)	Experiment x 10 ⁶ moles	Theoretical* x 10 ⁶ moles	% Reduction
Impregnation	0.1150	97.70	103.65	94.26
Ion exchange sodium hydroxide	0.1051	4.46	56.77	7.85
Ion exchange ammonia	0.1191	11.91	95.78	12.43

Note: * if all nickel(II)oxide reduced, refer to results of percentage nickel by atomic absorption spectrophotometer(table.4.1.)

4.6.1. Impregnated sample :

The TPR of the impregnated sample gave a single peak with a maximum at 651 K, corresponding to the bulk nickel oxide and therefore indicating that there was little interaction with the support. The peak corresponded to a reduction of 94 percent of the nickel(II) oxide (table 4.7). This is comparable to that obtained by other workers (62). This result implied that most of the nickel species in the calcined precursor was present in an easily reducible form. This result is rather different than that found in the literature (37, 63, 64) which postulated that more than one peak was found in the sample prepared by an impregnation method. This may be caused by differences in the silica support, preparative techniques and TPR operating parameters.

4.6.2. Ion exchanged sodium hydroxide sample :

The TPR profiles of this sample gave three unresolved peaks, shown as a low temperature shoulder at 650 K, a main peak at 834 K and a high temperature shoulder between 873 and 1173 K. Only 7.85 percent of this sample could be reduced. The peak at 650 K can again be assigned to bulk nickel oxide with little interaction with the support. The peak at 834 K can be assigned to a less reducible form of the nickel species. This may be due to small nickel oxide particle interacting with the support to give metastable

silicates (37). The broad high temperature shoulder peak running from 873 to 1173 K may be due to a nickel silicate compound as suggested by P.Turlier et.al (39). They found that nickel silicate can be formed at the interface of crystalline nickel(II) oxide and silica, and that the nickel(II) ions of surface silicate are more difficult to reduce than bulk nickel(II) oxide. The poor reducibility of this sample reflects the strong metal oxide-support interaction, possibly with the formation of nickel silicate (62). Furthermore alkali metals have been shown to inhibit the reduction of transition metal oxides (25) and thus the retained sodium may have contributed to this low value. This can be analogy with the work of M.Houlla et.al (62) who investigated the influence of sodium content in the nickel (II) oxide supported on aluminium(III) oxide prepared by impregnation technique. They found that increasing the sodium content resulted in the growth of the easily reduced nickel species and an increase in the intensity of the band characteristic of nickel(II) aluminate. This implied the formation of some reducible compound including sodium and nickel in a higher oxidation state.

4.6.3. Ion exchanged ammonia sample:

The TPR of this sample again gave three unresolved peaks shown as a shoulder low temperature at 653 K, a peak at 833 K and a high temperature shoulder peak between 873 and 1173 K. The peaks can be similarly interpreted

in terms of an increased interaction with the support with the possible formation of silicates. The hydrogen uptake corresponded to the reduction of only 12.43 percent of the available nickel species.

The poor reducibility of the ion exchanged samples compared with the impregnated sample is thus probably due to the stabilization of cations by interactions with the support (64). The interaction with the support is much weaker for samples prepared by impregnation.

4.7. The chemisorption of the reduced precursors.

CO chemisorption was used to estimate the total nickel metal surface area and dispersion for each catalyst. The results are shown in figure 4.13.a-4.13.c, table 4.8 and 4.9.

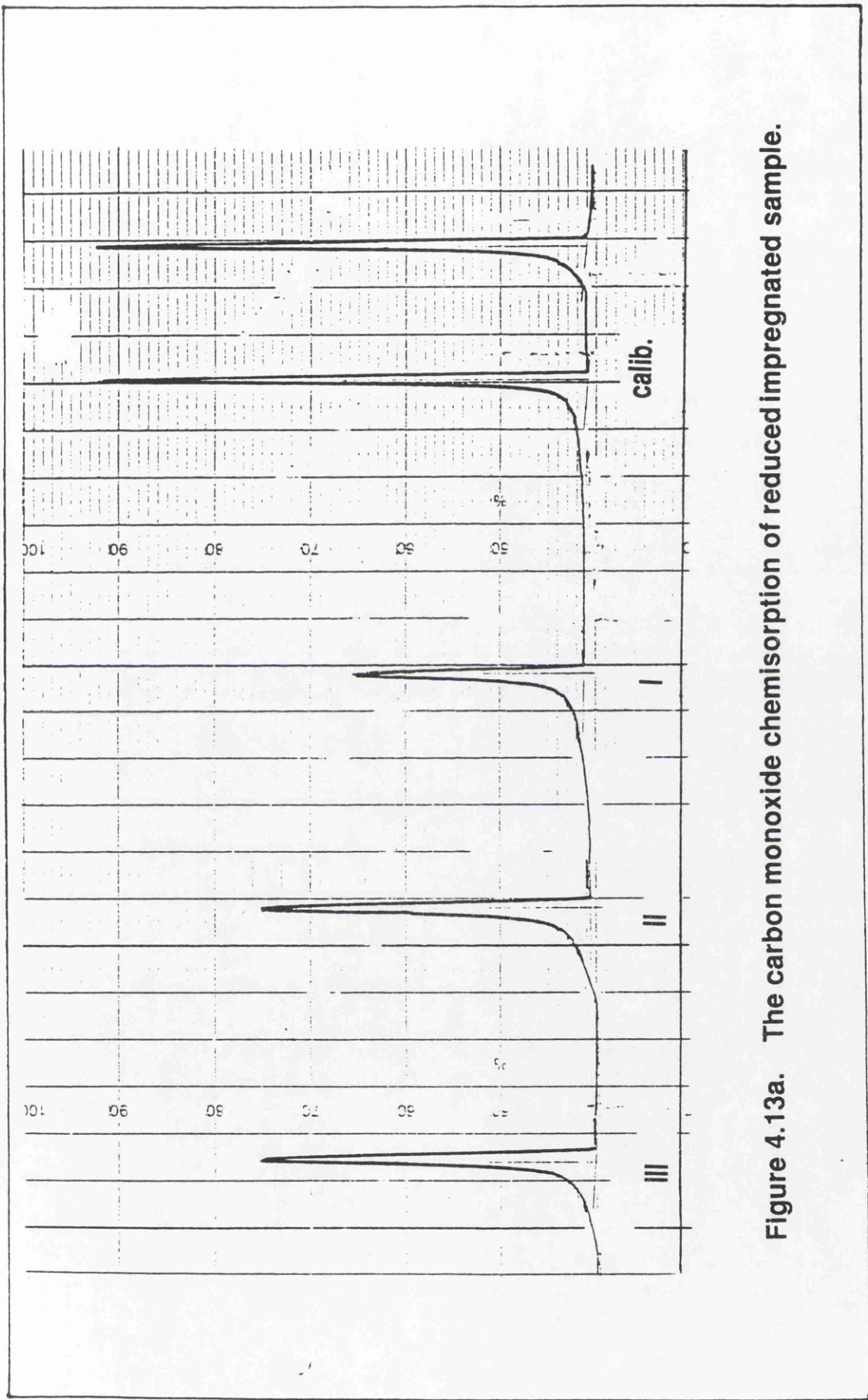


Figure 4.13a. The carbon monoxide chemisorption of reduced impregnated sample.

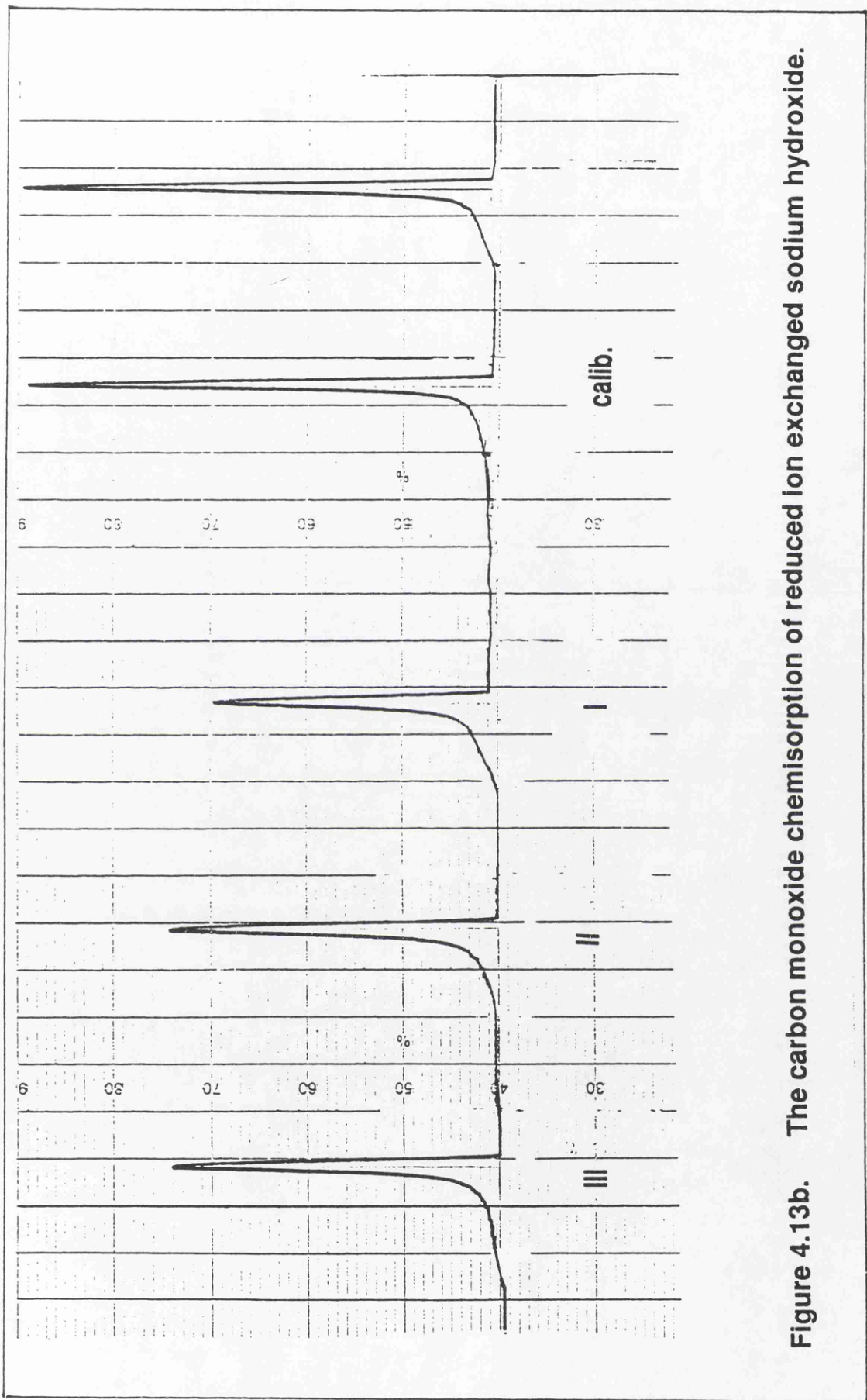


Figure 4.13b. The carbon monoxide chemisorption of reduced ion exchanged sodium hydroxide.

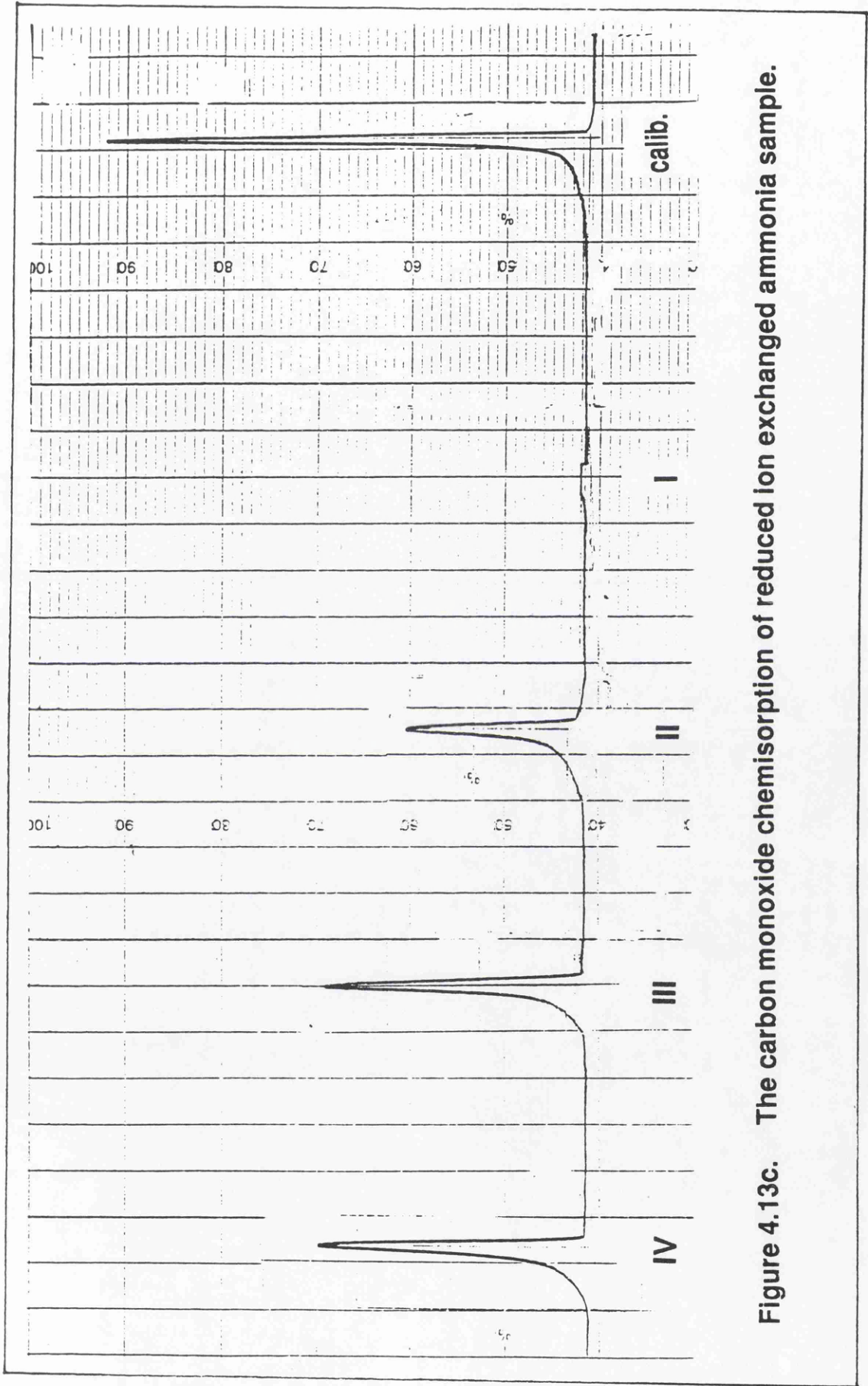


Figure 4.13c. The carbon monoxide chemisorption of reduced ion exchanged ammonia sample.

Table 4.8. : Total nickel surface area of impregnated and ion exchanged samples based on the chemisorption of carbon monoxide.

Samples	Total nickel metal surface area m ² / gr
Impregnated	14.32
Ion exchanged sodium hydroxide method	38.01
Ion exchanged ammonia method	131.24

Table 4.9. : The percentage dispersion of impregnated and ion exchanged samples based on the chemisorption of carbon monoxide

Samples	% Dispersion	
	X _m =1	X _m =2
Impregnated	2.15	1.07
Ion exchanged sodium hydroxide method	5.71	2.85
Ion exchanged ammonia method	19.70	9.85

where X_m= the average number of surface nickel metal sites associated with the

adsorption of one or two carbon monoxide molecules.

It can be seen from those tables that the ion exchanged samples have both higher total nickel metal surface areas and percentage dispersion than the impregnated sample. The ion exchanged sample prepared by the ammonia method gave the highest total nickel metal surface areas. Since only the nickel species associated with the low temperature TPR peak would be reduced under these conditions, the weak interaction with the support must give rise to very finely divided nickel. The poor reducibility and poor dispersion of the ion exchanged sample prepared by the sodium hydroxide method may be due to sodium poisoning of the metal sites (62).

4. 8. The amination reaction.

The characterised impregnated and ion exchanged supported nickel catalysts were tested for their selectivity in the amination of ethanol. The product analysis was carried out using a flame ionisation detector and a Perkin Elmer model 8500 GC with 6 m stainless steel ($d = 0.6$ cm) column packed with chromosorb 103 (mesh size 80-100) to separate the reactants and products. Initially, the system was calibrated using known volumes of ethylamine, ethanol, methane and ethane. In this manner the moles of reactant/product could be related to the peak area obtained on an integrator.

Calibration curves were then plotted for each component in order to calculate response factors. The reaction was carried out as detailed in section 3.3.6 for each of the reduced catalysts. The calibration curves for ethylamine, ethanol, methane and ethane are shown in figures 4.14, 4.15, 4.16 and 4.17 respectively.

4.8.1. Choice of the optimum conditions.

Before amination reactions could be studied it was necessary to decide on the optimum conditions for the reaction. The apparatus was based on the design used by A.P.Sharratt (52). The silicone tubing used in the peristaltic pump was found to absorb ammonia (52). It was also found that some ethanol absorbed in the tubing while the apparatus was operating in the circulating mode. The loss of ammonia could not be detected since the FID is unable to detect ammonia (65). The system was therefore initially tested by running a blank experiment in which ethanol, hydrogen and ammonia were circulated through the peristaltic pump in the absence of the catalyst. The resultant gas mixture was sampled into the G.C. via the sample valve at various time intervals. The results are shown in figure 4.18. The figure shows that the highest ethanol concentration was obtained from the system when the ethanol was circulated for between 10 and 30 minutes.

As a result of this study, the reactants were circulated for 10 minutes before being admitted to the catalyst and 20 minutes circulating over the

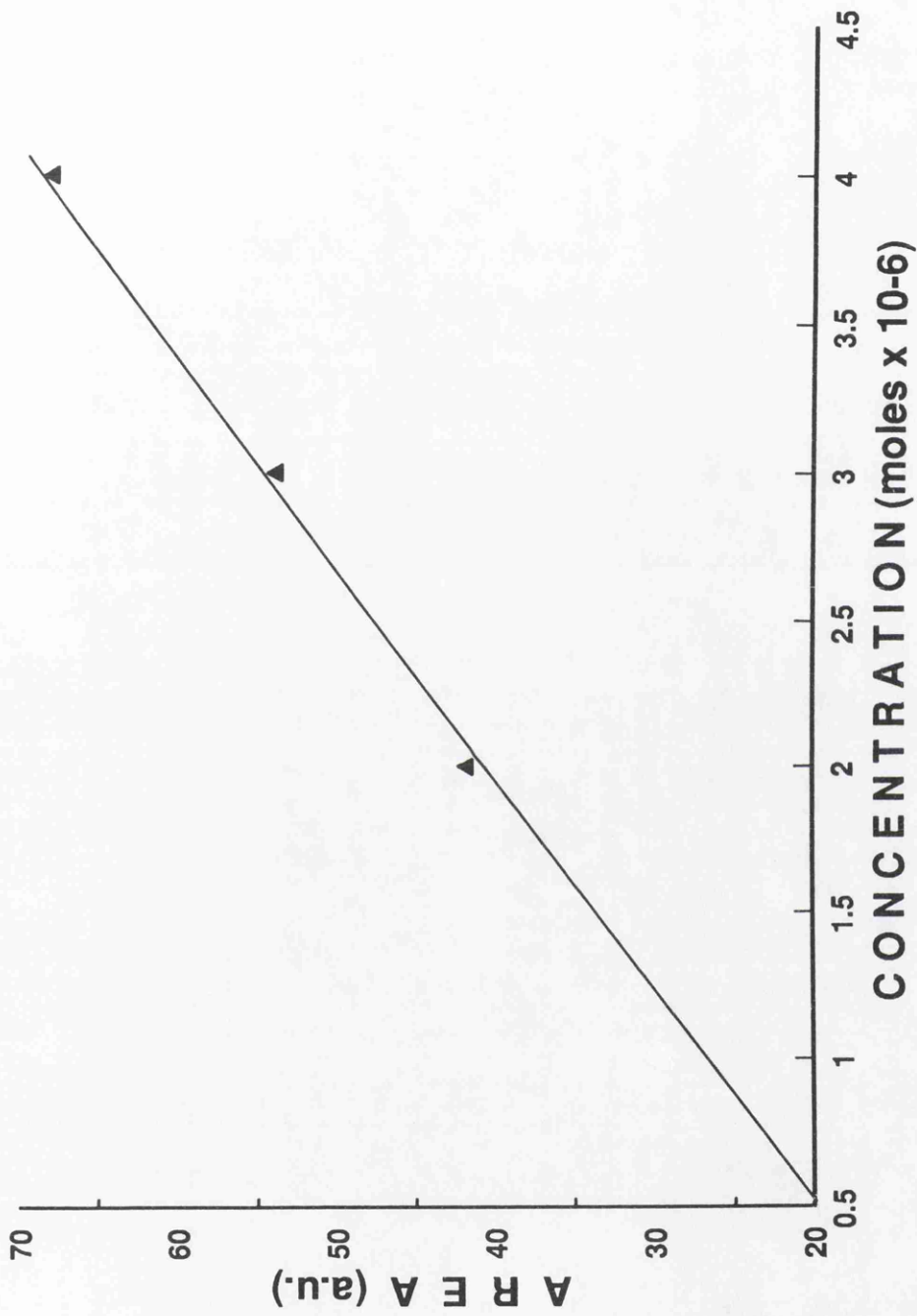


Figure 4.14.: Calibration curve of peak areas against ethylamine concentration.

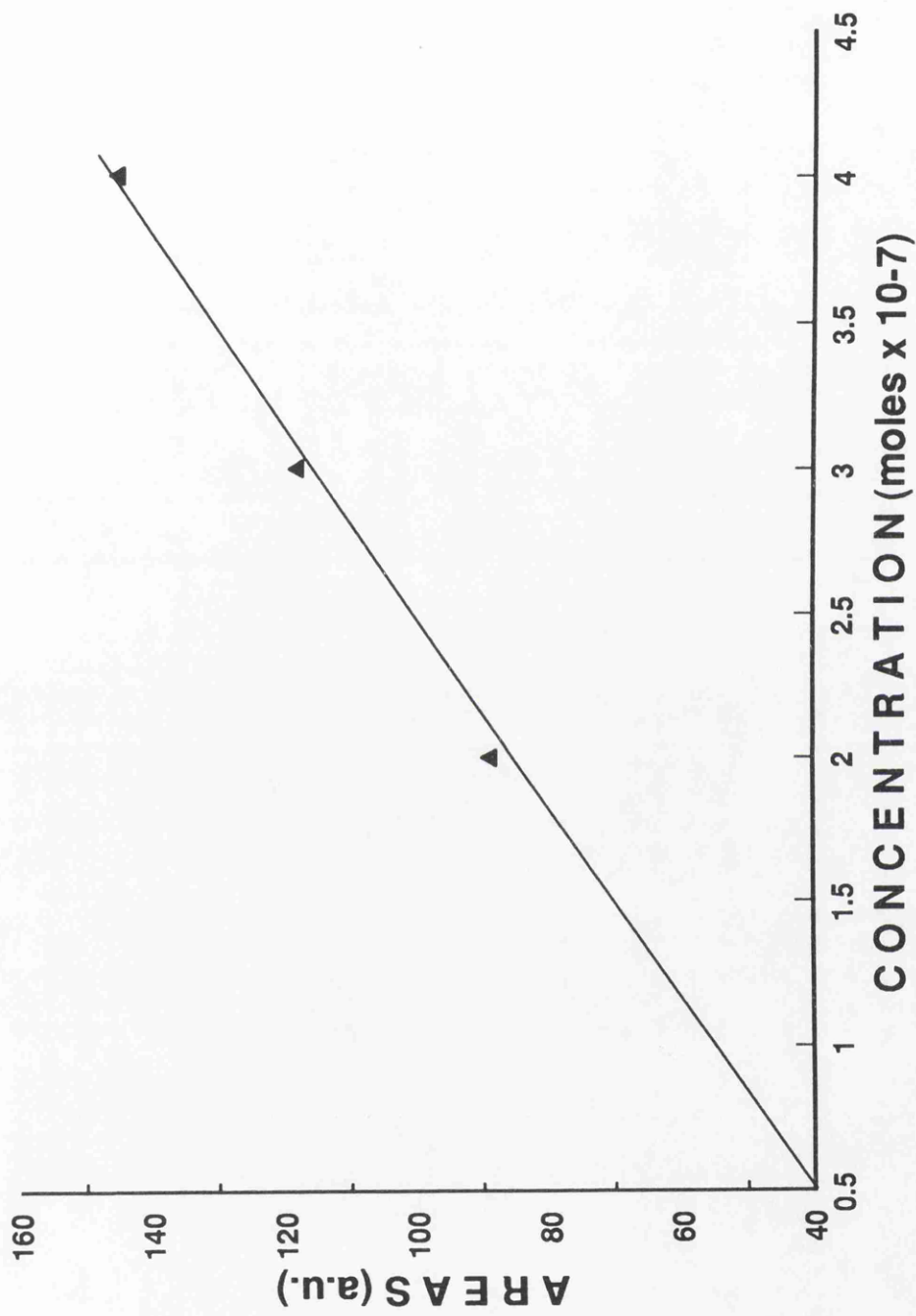


Figure 4.15. : Calibration curve of peak areas against ethanol concentration.

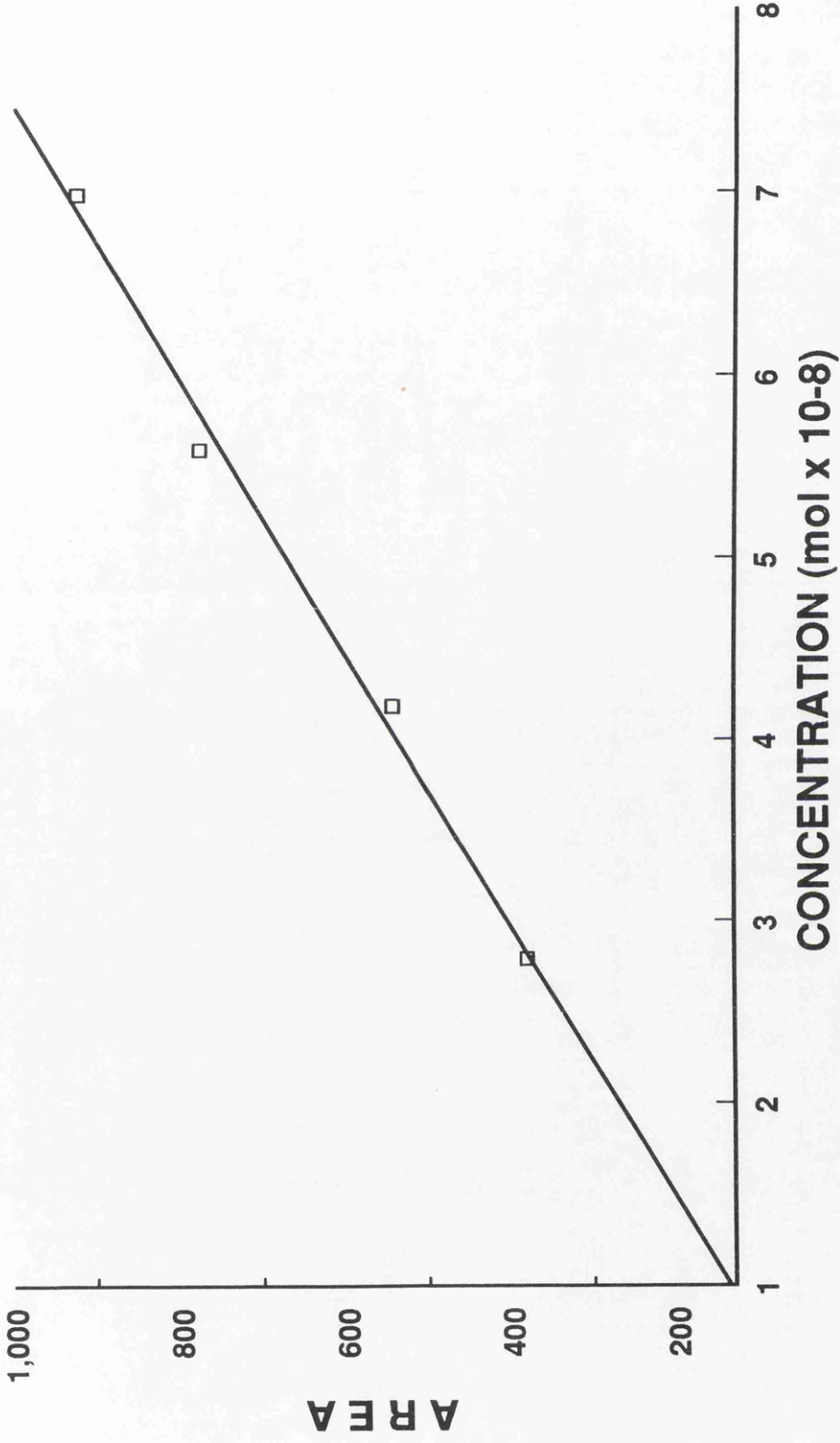


Figure 4.16. : Calibration curve of peak areas against methane concentration.

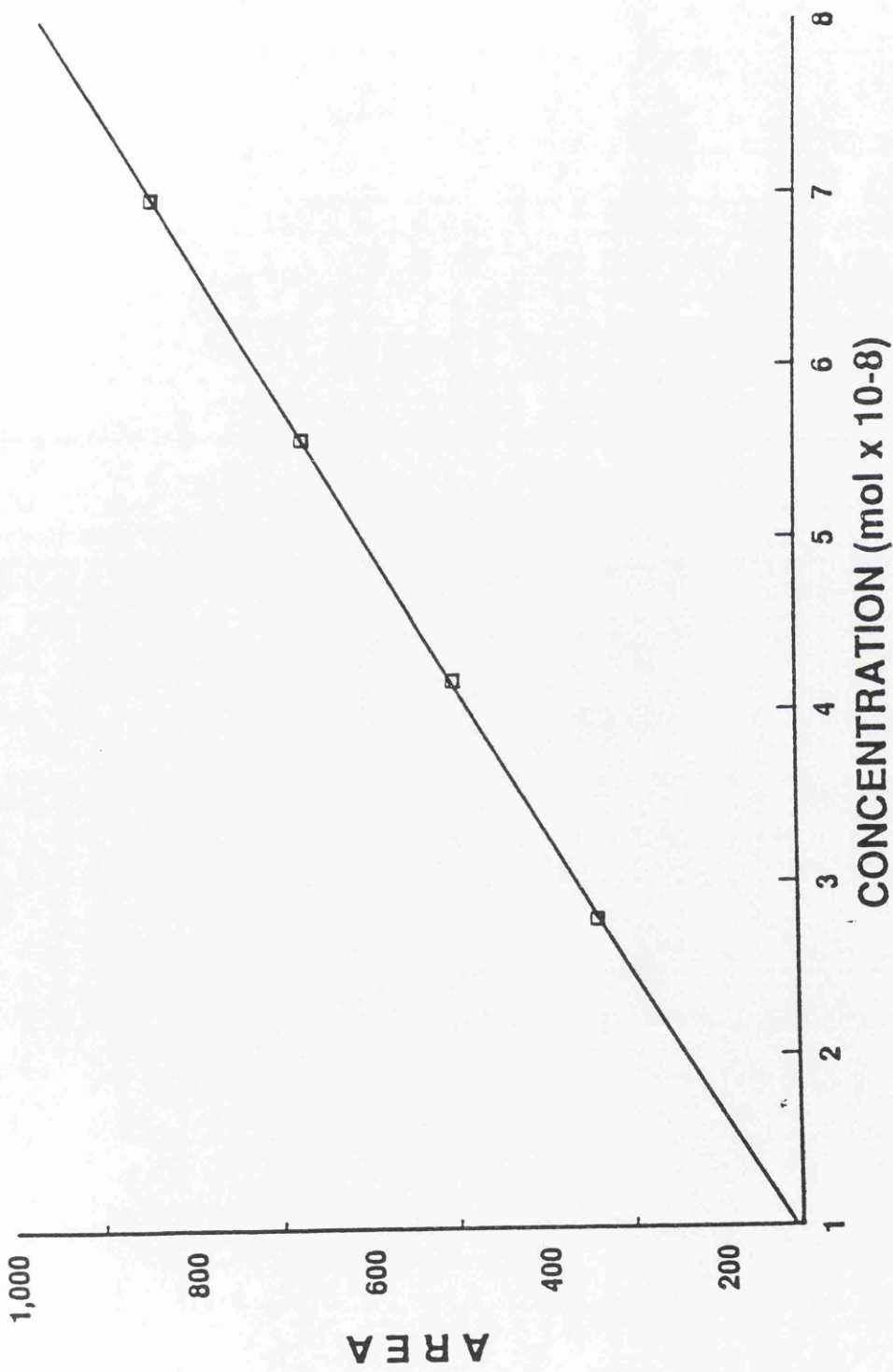


Figure 4.17. : Calibration curve of peak areas against ethane concentration.

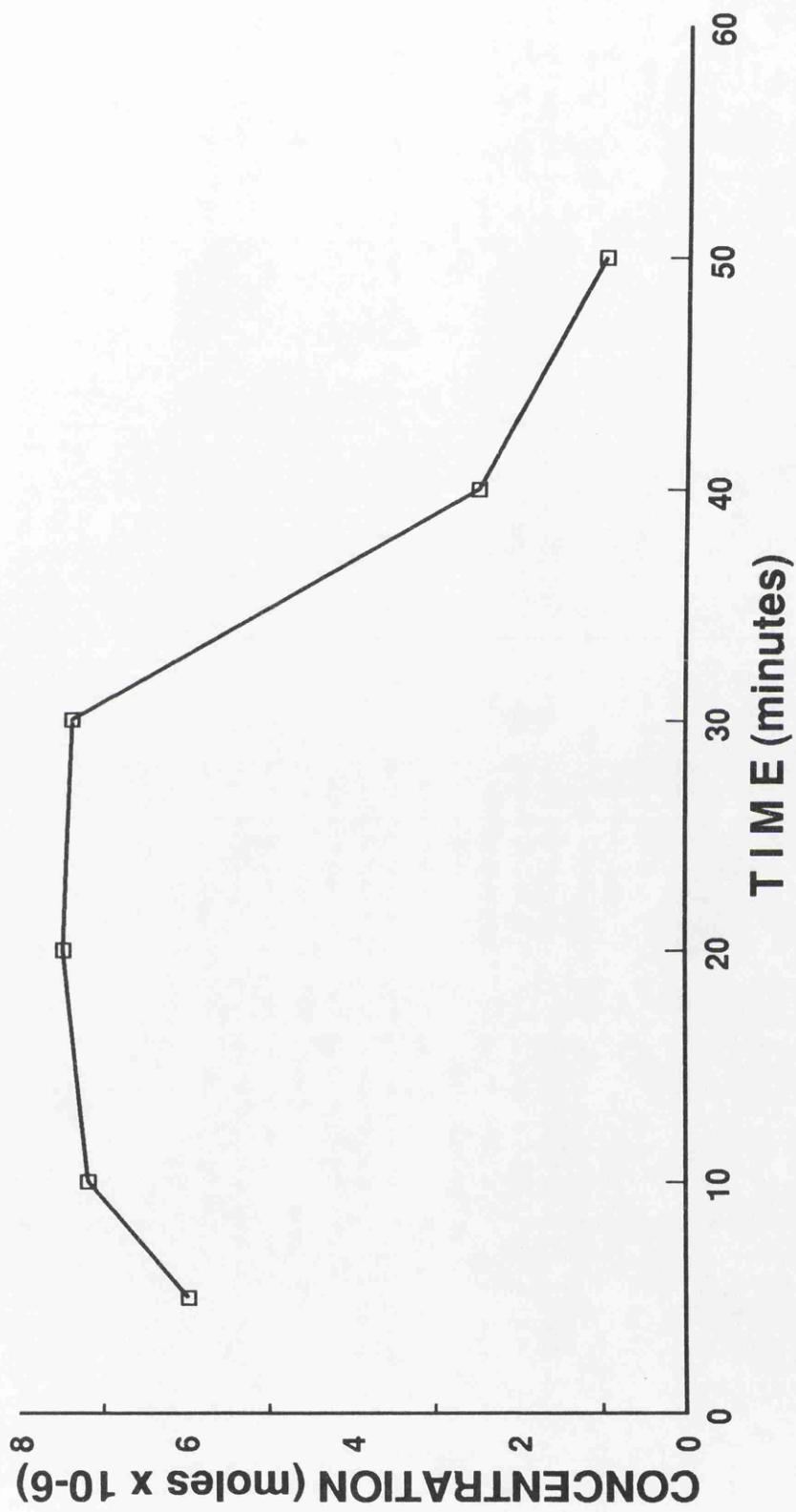


Figure 4.18. :Ethanol concentration against the circulated times.

catalyst. This is in agreement with Sharatt's work who found that circulating the reactant mixtures for 26 minutes over a 1 percent nickel on silica catalyst gave a 61 percent conversion of ethanol to ethylamine (52).

4.8.2. Ethanol amination.

The amination reaction was studied in the temperature range of 423 K to 573 K over the reduced impregnated catalyst (reduced at 673 K for 3 hours in hydrogen) as in previous work (52). The effect of varying the ethanol concentration was also determined using the impregnated catalyst, since the ratio of alcohol to ammonia is also important in determining the optimum operating conditions. 50 μ l ethanol (equivalent to 8×10^{-4} moles of ethanol) was chosen as the initial concentration and then the effect of doubling of this initial concentration was examined. Figure 4.19 and 4.20 show the results of FID analysis using concentration of 8 and 16×10^{-4} moles of ethanol respectively.

Figure 4.19 shows that with 8×10^{-4} moles of ethanol, no ethylamine was observed in the temperature range of 423 to 573 K. However, when the reaction was carried out at the higher ethanol concentration (figure 4.20) at 503 K ethylamine was formed (5.6×10^{-6} moles/g catalyst). The amount of ethylamine formed decreased however as the temperature was further increased. This observation was also reported by Baiker et.al. (42) who calculated that the dehydroamination of octanol with dimethylamine in the gas phase was an

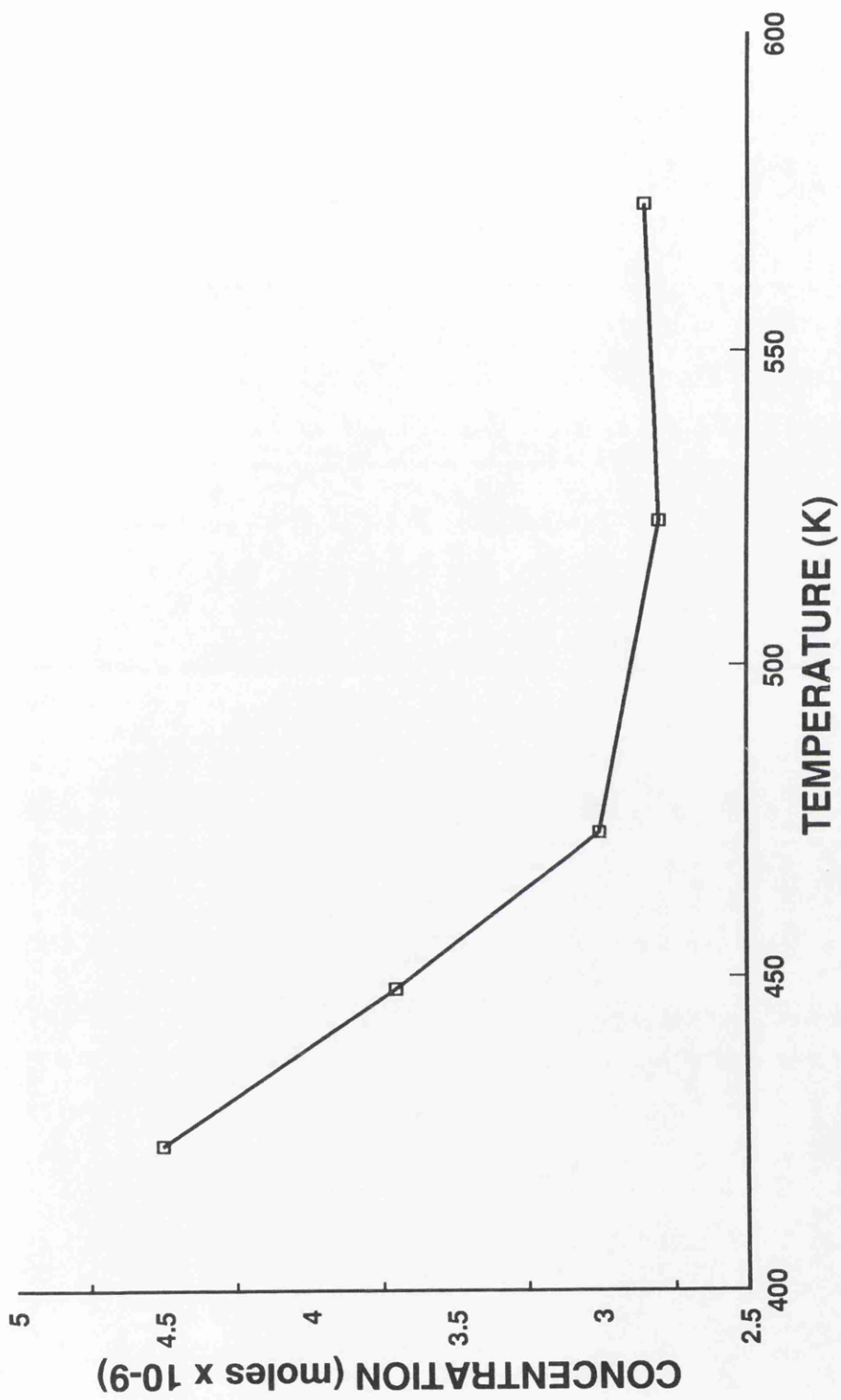


Figure 4.19.: Moles of methane produced in 100ul of the resultant gas mixture against the reaction temperatures over 0.2 g impregnated catalyst.

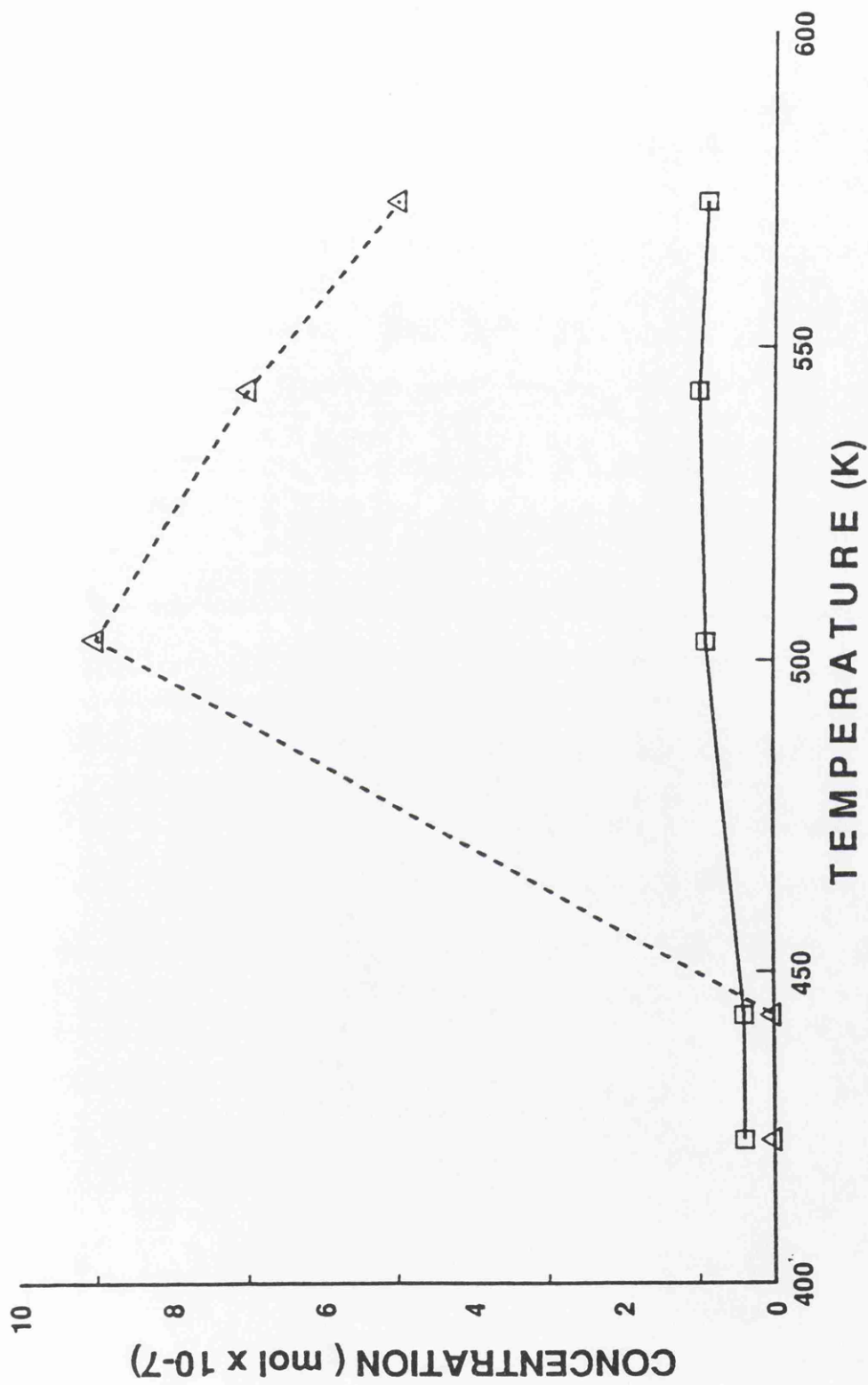


Figure 4.20. : Concentration of methane and ethylamine produced against reaction temperature of the amination of ethanol over the catalyst prepared by impregnation method.

exothermic reaction. On the basis of these results, the ethanol amination reaction was carried out at 503 K and the experiment was repeated twice to check for consistency.

The reduced ion exchanged catalysts did not form any ethylamine after the standard reduction in hydrogen gas at 673 K for 3 hours. These catalysts were therefore reduced at the higher temperature of 773 K.

A further blank experiment was carried out in which ethanol in a hydrogen atmosphere was passed over each of the catalysts in the absence of ammonia. The results of this experiment using the impregnated catalyst are shown in figure 4.21. The figure shows that the catalyst formed only methane presumably by the cracking of ethanol. Methane was also the sole by-product of the amination reaction.

The results for the ethanol amination reaction over the three catalysts prepared by either impregnation (reduced at 673 K) or ion exchange (reduced at 773 K) are shown in figures 4.22., 4.23. and 4.24.. Subsequent analysis of the trapped reaction mixture showed that the ethylamine could not be detected by NMR owing to its low concentration. The results are expressed as moles per g catalyst and moles per m² of nickel metal. Table 4.10., 4.11. and 4.12. show the number of moles of ethylamine and methane formed, percentage yield of ethylamine and percentage yield of methane respectively, calculated per g catalyst, in the ethanol amination reaction over catalysts prepared by impregnation and ion exchange methods. Table 4.13. shows the ratio of moles methane formed in the ethanol/hydrogen blank experiment and ethanol amination

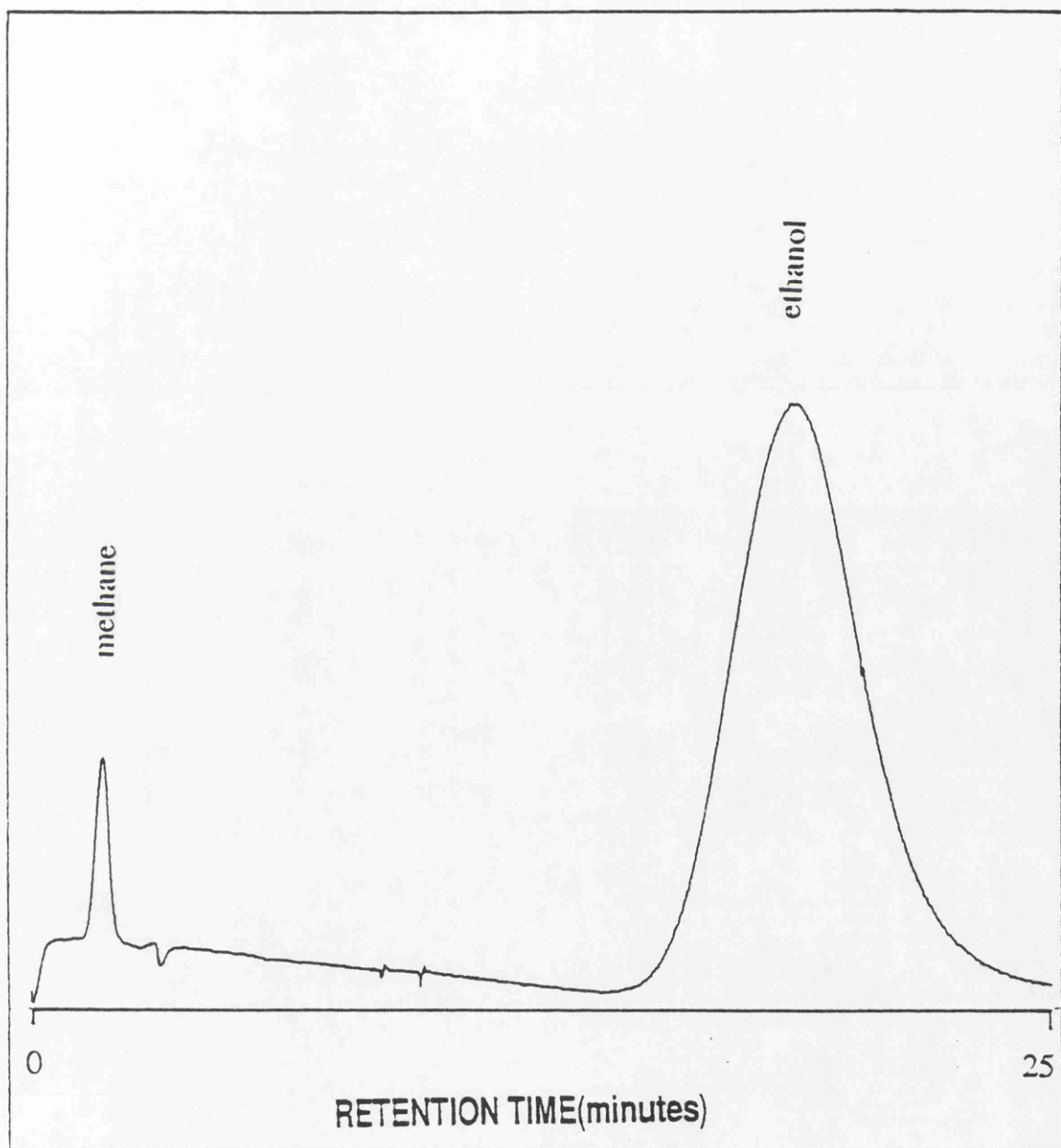


Figure 4.21. : Ethanol blank experiment (25 μ l ethanol in hydrogen over the catalyst prepared by impregnation method).

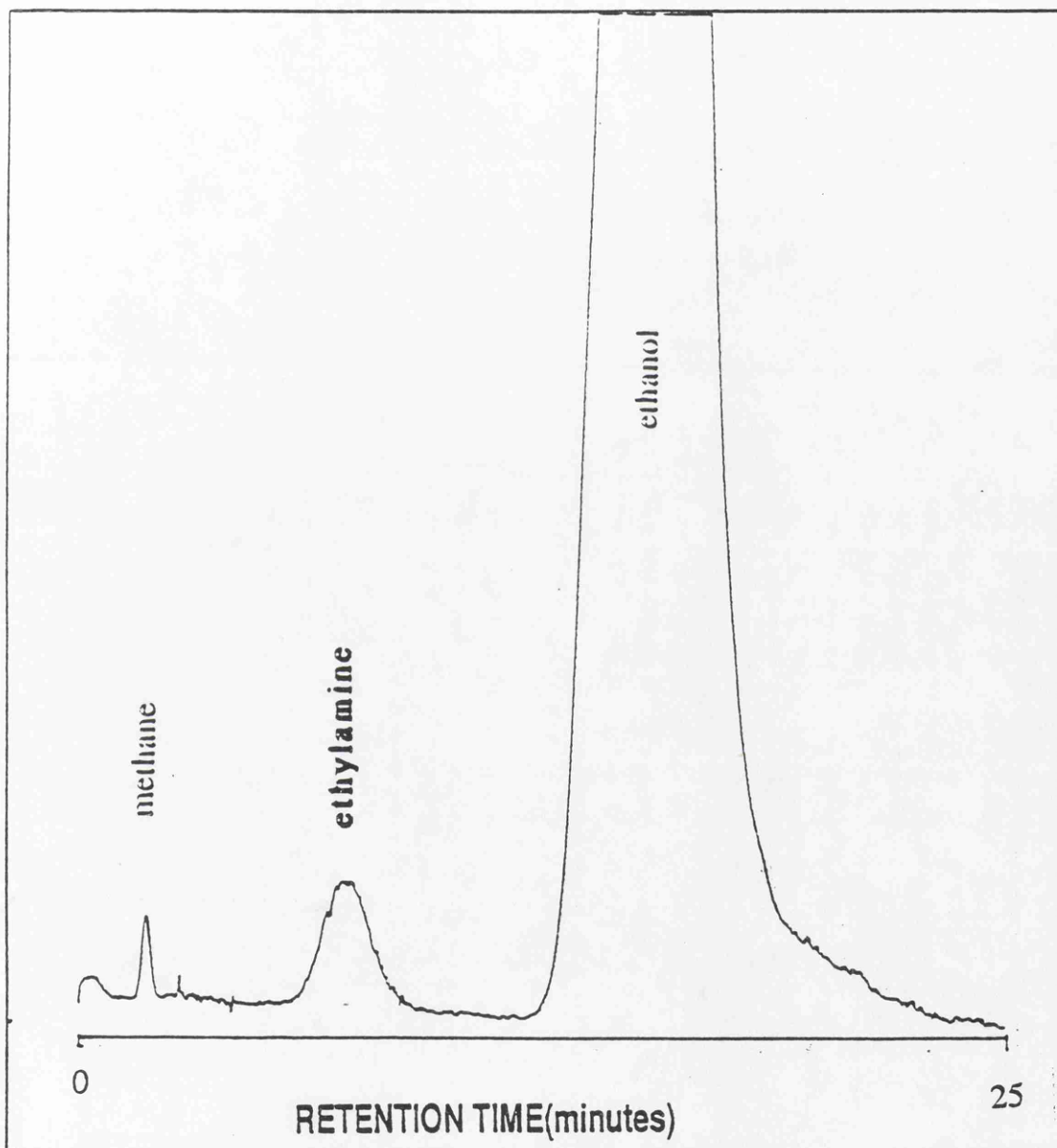


Figure 4.22. : GC chromatograph for the amination of ethanol over the impregnated catalyst.

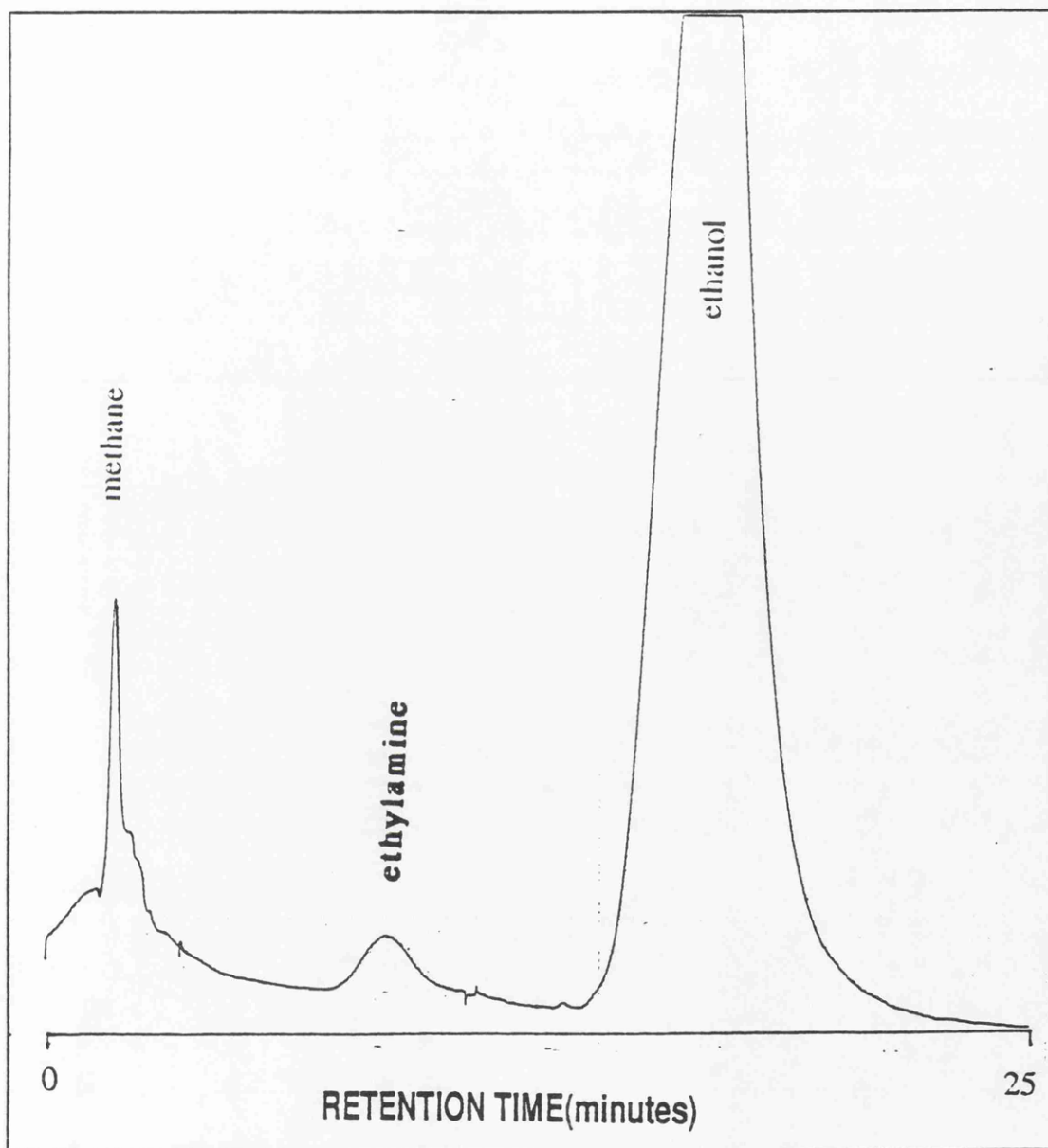


Figure 4.23. : GC chromatograph for the amination of ethanol over the ion exchanged sodium hydroxide catalyst.

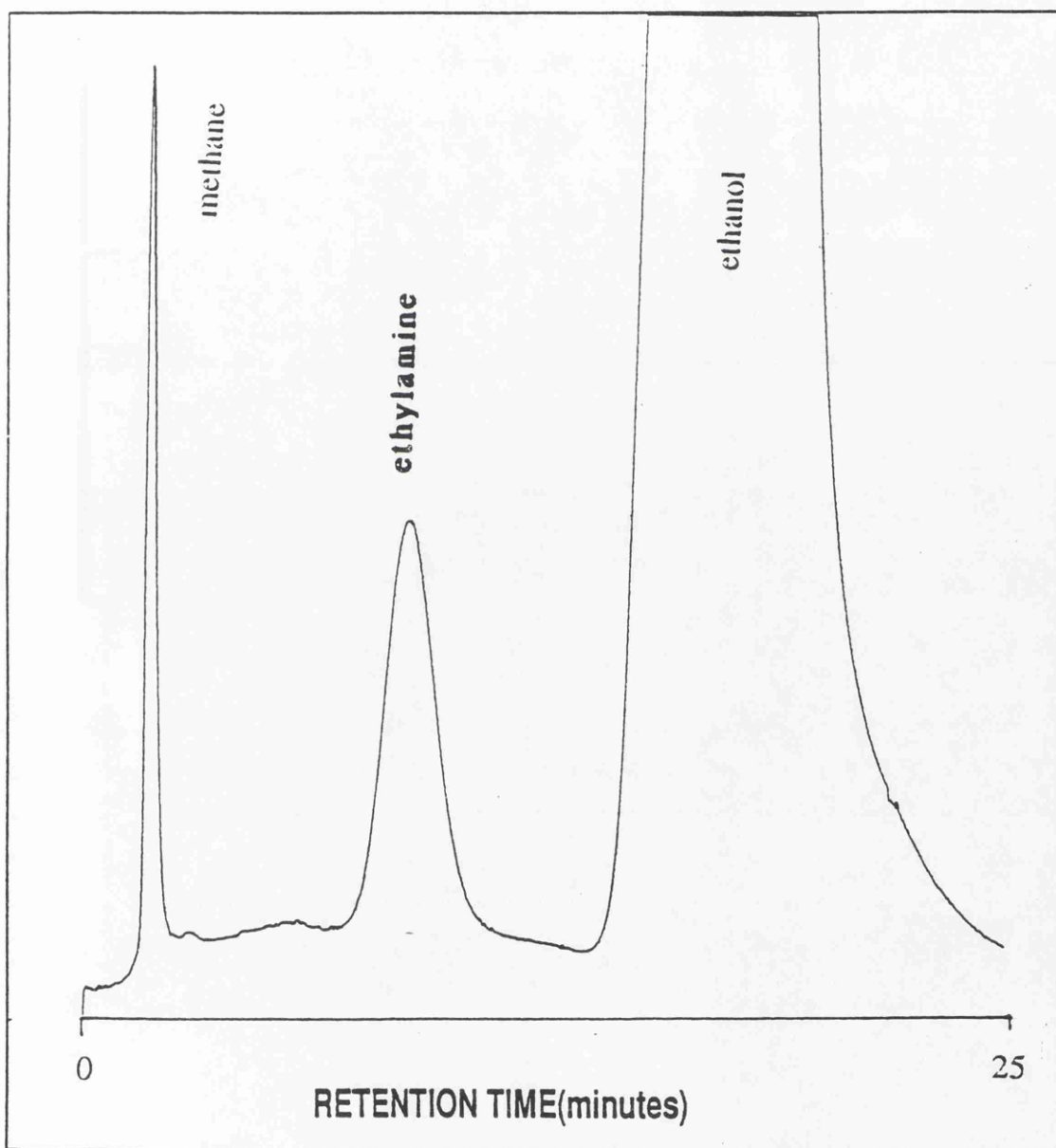


Figure 4.24. : GC chromatograph for the amination of ethanol over the ion exchanged ammonia catalyst.

Table 4.10. : Moles of ethylamine and methane per g catalyst formed in the ethanol amination reaction over catalysts prepared by impregnation and ion exchange methods.

Preparation method.	Moles of ethylamine per g catalyst.	Moles of methane per g catalyst.
Impregnation.	6.10×10^{-6}	0.4×10^{-8}
Ion exchanged sodium hydroxide.	5.80×10^{-6}	1.8×10^{-8}
Ion exchanged ammonia	59.25×10^{-6}	4.0×10^{-8}

Table 4.11. : Moles of ethylamine formed and ethanol consumed per g catalyst in the ethanol amination reaction over the catalysts prepared by impregnation and ion exchange methods.

Preparation method	Moles of ethanol consumed per g catalyst.	Moles of ethylamine produced per g catalyst.	% yield of ethylamine
Impregnation	0.22×10^{-4}	6.10×10^{-6}	27.73
Ion exchanged sodium hydroxide	0.23×10^{-4}	5.80×10^{-6}	25.22
Ion exchanged ammonia	1.04×10^{-4}	59.25×10^{-6}	56.97

Table 4.12. : Moles of ethanol consumed and methane produced per g catalyst in the ethanol amination reaction over catalysts prepared by impregnation and ion exchange methods.

Preparation method	Moles of ethanol consumed per g catalyst.	Moles of methane produced per g catalyst.	% yield for methane
Impregnation	0.22×10^{-4}	0.4×10^{-8}	0.22
Ion exchanged sodium hydroxide	0.23×10^{-4}	1.8×10^{-8}	0.08
Ion exchanged ammonia	1.04×10^{-4}	4.0×10^{-8}	0.04

Table 4.13. : The mole ratio of methane per g catalyst formed in the ethanol/hydrogen blank experiment and ethanol amination reaction over catalyst prepared by impregnation and ion exchange methods.

Preparation method	Moles of methane per g catalyst formed in the ethanol blank experiment.	Moles of methane per g catalyst formed in the ethanol amination reaction.	Ratio
Impregnation.	0.2×10^{-8}	0.4×10^{-8}	2.0
Ion exchanged sodium hydroxide	0.5×10^{-8}	1.8×10^{-8}	3.6
Ion exchanged ammonia	0.6×10^{-8}	4.0×10^{-8}	6.7

reaction over the different catalysts. Mass balance calculations indicated that the total yield of methane and ethylamine did not account for all the ethanol converted. Whilst there is some error in this calculation due to product water not being detected and possible adsorption of reactants in silica tubing, this does not account for the large discrepancy.

The results in these tables demonstrate that the ion exchanged sample prepared by the ammonia method gave the highest yield of ethylamine.

The ion exchanged sample prepared by the sodium hydroxide method only produced ethylamine, after the same catalyst sample had been tested twice with fresh ethanol in circulating ammonia/hydrogen mixture. The yield of ethylamine was similar to that obtained using the catalyst prepared by the impregnation technique. Carbon monoxide chemisorption studies (section 4.7) showed that the nickel metal dispersion was only 5.7 percent and this can be correlated with retained sodium and its effect on the reduction of the catalyst (section 4.6). The percentage yield of ethylamine obtained with the catalyst after treatment with two aliquots of reactant may be due to :

- (i) restructuring of the surface after the first exposure to the reactants resulting in the exposure of fresh active sites for the reaction,
- (ii) increased effective residence time of the reactants on the active sites,
- (iii) the reaction taking place on an adsorbed carbonaceous overlayer (2,66).

This catalyst had a nickel content of only 3.4 percent compare with 5.3 percent for the impregnated and 4.8 percent for the ion exchanged ammonia sample (table 4.1, section 4.1.1). It also contained 0.09 percent by weight of sodium.

Sodium could behave as a poison in this reaction, indeed sodium has been found to inhibit the formation of diphenylethylene carbonium ions in olefin polymerization on a silica-alumina catalyst (30).

Table 4.14 Moles of ethylamine and methane per m² nickel based on the nickel metal areas estimated by carbon monoxide chemisorption for the catalysts prepared by impregnation and ion exchange methods.

Preparation method	Moles of ethylamine per m ² nickel metal	Moles of methane per m ² nickel metal
Impregnation	4.26 x 10 ⁻⁷	2.79 x 10 ⁻¹⁰
Ion exchanged sodium hydroxide	1.53 x 10 ⁻⁷	14.74 x 10 ⁻¹⁰
Ion exchanged ammonia	4.44 x 10 ⁻⁷	3.01 x 10 ⁻¹⁰

If the product yields are calculated on a metal surface area basis (table 4.14) it can be seen that the ion exchanged sample prepared by the sodium hydroxide method was less selective for ethylamine formation and produced more methane per m² compared to the ion exchanged ammonia and impregnated

samples. The table also shows that the impregnated and ion exchanged ammonia method catalysts produce virtually equal amounts of ethylamine per m² nickel metal. This suggests that the selectivity to ethylamine in the amination reaction is related to the number of nickel sites available.

Table 4.15. shows the percentage dispersion, based on the carbon monoxide chemisorption, and the percentage selectivity calculated assuming that the ammonia and hydrogen concentrations remained effectively constant during the reaction.

Table 4.15. The yield of ethylamine for each of the prepared catalysts compare with their percentage dispersion.

Preparation method	% Dispersion	% yield to ethylamine
Impregnation	2.15	27.7
Ion exchanged sodium hydroxide	5.71	25.2
Ion exchanged ammonia	19.70	57.0

Comparison of the percentage conversion to ethylamine for the catalysts prepared by impregnation and ion exchange methods, clearly shows that the ion exchanged catalyst prepared by the ammonia method is the most selective for ethylamine formation.

CHAPTER FIVE

CONCLUSIONS

5.1. Conclusions.

The first objective of this project was to identify the ways in which the carrier may modify the properties of the active phase in the nickel(II) oxide/support system. It was found that both the nickel(II) oxide dispersion and the extent of surface/bulk compound formation between the active phase and the support are affected by the preparation method employed.

The impregnated precursor was prepared by filling the pores of the support with a solution of aqueous nickel nitrate. The nickel (II) ion adsorbed from nitrate solutions is weakly held by the carrier so that migration and aggregate formation may readily take place during drying and calcination. Ion exchanged precursors were prepared by exchange of (hexaaquo) and (hexaamine) nickel(II) ions with surface sodium ion and protons respectively. The support was then washed to remove all the free salt. The remaining metal ions were strongly bound to the carrier and could be expected to be atomically dispersed on the surface. Little migration would then be expected to occur during drying and heat treatment.

The next stage of the project involved investigating the yield of each dispersed nickel on silica catalyst for the amination of ethanol. The catalyst obtained by the ion exchanged ammonia method showed the highest yield to ethylamine for the amination of ethanol. However, with this catalyst, the activity per m^2 nickel metal for both ethylamine and methane production (table 4.11, section 4.8.1.) was similar to that of the impregnated precursor.

The ion exchanged sodium hydroxide catalyst contained a small percentage of sodium in the dried precursor, which poisoned the metal sites for ethanol amination. M.Houalla et.al. (62) found that increasing the sodium content in the catalyst precursor increased the proportion of a high temperature (1013 K) peak in temperature programmed reduction studies and this was thought to be indicative of a strong interaction of the nickel species with the support. They proposed the following reaction occurred on calcination :



(sodium nickelate)

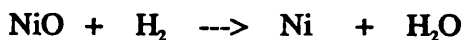
equation 5.1.

and in the reduction process, the sodium nickelate would react with hydrogen as follows :



equation 5.2.

This can be compared to the reduction of pure nickel(II)oxide i.e.



equation 5.3.

Reduction of sodium nickelate resulted in the consumption of two extra moles of H_2 per nickel atom. The increasing hydrogen consumption in this reaction was confirmed by an increase in the intensity of the peak characteristic of $NiAl_2O_4$, which corresponded to the highest temperature peak. Since the TPR curve for the ion exchanged sample prepared by the sodium hydroxide method showed a broader and more intense peak at high temperature compared to that prepared by the ammonia method, by analogy to this result, sodium nickelate may be formed together with sodium oxide and nickel silicate during calcination. This may also explain why the ion exchanged sodium hydroxide sample reduced at 627 K, examined by the amination of ethanol, was inactive.

From the results obtained in this study, it may be concluded that :

- (1). The dispersion of nickel(II), the formation of bulk nickel(II) oxide and the strength of the interaction of nickel with the support are all affected by the preparation route.
- (2). The efficiency of transferring a nickel salt to the support phase was 97, 63 and 91 percent for impregnation , ion exchange sodium hydroxide and ion exchange ammonia methods respectively.
- (3). The nickel species present in the dried impregnated and ion exchanged sodium hydroxide samples were octahedral hexaaquonickel(II) ions.

Diaminetetraaquonickel(II) ions were present in the dried ion exchanged ammonia sample. The ion exchanged sodium hydroxide sample also contained 0.09 percent sodium.

(4). The calcined impregnated sample contained mainly bulk-like nickel(II) oxide aggregates as the predominant component. The nickel(II) oxide component was easily reduced. In calcined ion exchanged samples, the nickel(II) oxide is present in small amounts attached to the support surface and is difficult to reduce.

The nickel species present in the calcined impregnated precursor had the same structure as the nickel(II) oxide-bunsenite and contained mainly (200) and (111) planes. TPR shows that this species was easily reduced. The reduction involved a change from predominantly nickel(II) oxide(200) to nickel metal(111) as determined by XRD.

Elemental analysis showed that the calcined ion exchanged ammonia sample did not contain any amine ligands. Hydroxyl groups were present, however, indicating that a hydrosilicate may be formed. TPR showed that the ion exchanged ammonia sample contained three kinds of reducible nickel species; an easily reduced nickel species similar to that found in the impregnated sample and two less reducible species interacting with the support and reducing at successively higher temperatures. A similar reduction profile was observed for the ion exchanged sodium hydroxide sample, but there was an increase in the proportion of the high temperature peak.

(5). X-ray diffraction showed that the structure of the reduced nickel species in the impregnated sample corresponded to pure nickel metal. The nickel was poorly dispersed in this impregnated sample. The diffraction pattern observed for the ion exchanged sodium hydroxide sample did not correspond to that of pure nickel, but could not be identified. It is likely that strong interactions between the metal, support and sodium oxide impurity may have given rise to species such as sodium nickelate, sodium oxide or nickel hydrosilicate but none of these species could be positively identified. This catalyst had a much lower metal surface area and percentage dispersion than the ion exchanged ammonia sample and this has been attributed to the presence of retained sodium oxide blocking the active metal sites. The d-spacings position of the ion exchanged ammonia sample corresponded to those of pure nickel, but the intensity of the (200) plane was reduced. This is possibly due to the strong nickel-support interaction resulting in embedding of some of the nickel in the silica forming meta stable nickel hydrosilicate type species. This catalyst had both the highest metal surface area and percentage dispersion of all the catalysts prepared.

(6). The catalyst precursor obtained by the ion exchanged ammonia method showed the highest selectivity for ethylamine production in the amination of ethanol. However, its activity per m² of nickel metal was similar to that of the impregnated precursor. The retained sodium in the ion exchanged sodium hydroxide catalyst poisoned metal sites as shown by carbon monoxide chemisorption and ethanol amination studies.

REFERENCES

1. Kirk-othmer Encyclopedia of Chemical Technology, 5, 3rd.ed., A Willey Interscience Pub., New York, 1978, p.272-293.
2. I.M.Campbell, "Catalysis at Surfaces"; Chapman and Hall : Cambridge, 1988.
3. G.C.Bond, "Heterogeneous Catalysis, Principles and Applications"; Clarendon Press: Oxford, 1974.
4. A.Baiker and J.Kijenski, Catal.Rev.-Sci.Eng., 27, 653 (1985).
5. M.A.Kohler, H.E.Curry-Hyde, A.E.Hughes, B.A.Sexton and N.W.Cant. J.Catal., 108, 323 (1987).
6. S.J.Thomson and G.Webb, "Heterogeneous Catalysis"; Oliver & Boyd : Edinburgh, 1968.
7. J.H. Anderson, J. Catal., 26, 277 (1972).
8. J.R.Anderson and K.C.Pratt, "Introduction to Characterization and Testing of Catalysts"; Academic Press: Sidney, London, 1985.
9. R.L.Burwell, R.G.Pearson, G.I.Tjok and S.P.Chock, Inorganic chem., 4 1123 (1965).
10. P.H.Emmet, "Catalysis, Fundamental Principles, vol.I."; Reinhold: New York, 1954.
11. F.A.Cotton and G.Wilkinson, "Advanced Inorganic chemistry, A Comprehensive Text"; Wiley: New York, Chichester, 5th ed., 1980, p 744.
12. R.K.Iler, "The Chemistry of Silica Solubility, Polymerization, Colloid and Surface Properties and Biochemistry"; Wiley: New York, Chichester, 1979.
13. D.Stirling, PhD Thesis, Liverpool Polytechnic, Liverpool, 1984.
14. N.N.Greenwood and A.A.Earnshaw, "Chemistry of the Elements"; Pergamon: Oxford, 1984.
15. W.M.Heston, R.K.Iler and G.W.Sears, J.Phys. Chem., 64, 147 (1960).
16. M.R.Basila, J.Chem.Phys., 35, 1151 (1961).

17. S.A.Greenber, J.Am.Chem.Soc., 80, 6508 (1958).
18. O.Samuelson, "Ion Exchange Separations in Analytical Chemistry"; Wiley: Stockholm, London, 1963.
19. W.G.Frankeuburg, E.K.Rideal and V.I.Komarewsky, Advances in Catalysis, III, 261-262 (1951).
20. C.B.Amphlett, "Inorganic Ion Exchangers"; Elsevier: Amsterdam, 1964.
21. L.G.Sillen and A.E.Martel, Chem.Soc., Special Pub.1, No.17, 1964.
22. R.F.Schwenker and P.D.Garn, "Thermal Analysis", vol 1; Academic Press: Sidney, London, 1964; p 284.
23. D.L.Trimm, "Design of Industrial Catalysts"; Elsevier Scientific: Amsterdam, Oxford, 1980; p 107.
24. N.W.Hurst, S.J.Gentry and A.Jones, Catal.Rev.-Sci.Eng., 24, 233 (1982).
25. F.Delannay, "Characterization of Heterogeneous Catalysts"; Marcel Dekker: New York, 1984.
26. D.A.Skoog and D.M.West, "Principles of Instrumental Analysis", 2nd ed.; Saunder College: Philadelphia, 1980.
27. D.A.Skoog, D.M.West and F.J.Holler, "Fundamental of Analytical Chemistry", 5th. ed.; Saunders College: New York, 1988; p 699.
28. I.M.Kolthoff and P.J.Elving, "Treatise on Analytical Chemistry, A Comprehensive Account in Three Part^l", Part I, vol.4; John Wiley & Sons: New York, 1984, p 520.
29. L.E.Orgel, J.Chem.Phys., 23, 1004 (1955).
30. L.H.Little, "Infrared Spectra of Adsorbed Species"; Academic Press: New York, 1966.
31. J.B.Peri, Catalysis Sciences & Technology, 5, 171 (1984).
32. R.F.Willis, "Vibrational Spectroscopy of Absorbates"; Springer: Heidelberg, New York, 1980.
33. R.S.Mc.Donald, J.Am.Chem.Soc., 79, 850 (1957).

34. A.R. West, "Basic Solid State Chemistry"; Wiley, Chichester, New York, 1988.
35. A. Jones and B.D. Mc.Nicol, "Temperature-Programmed Reduction for Solid Materials Characterization"; Marcel Dekker: New York, 1986.
36. A. Blazek, "Thermal Analysis"; Van Nostrand Reinhold: New York, London, 1972.
37. B. Mile, D. Stirling, M. Zammit, A. Lovell and M. Webb, *J. Catal.*, 114, 217 (1988).
38. C. Duval, "Inorganic Thermogravimetric Analysis", 2nd. rev.; Elsevier: Amsterdam, 1963; p 360.
39. E.E. Unmuth, L.H. Schwartz and J.B. Butt, *J. Catal.*, 61, 242 (1980).
40. M.L. Kung and H.H. Kung, *Catal. Rev.-Sci. Eng.*, 27, 425 (1985).
41. R. Pearce and W.R. Patterson, "Catalysis and Chemical Processes"; Leonard Hill: London, 1981.
42. A. Baiker and J. Kijenski, *Catal. Rev. Sci. Eng.*, 27, 653 (1985).
43. J. Carnduff, "An Introduction to Organic Chemistry"; Wiley: Chichester, New York, 1978.
44. M.V. Klyuev and M.L. Khidekel, *Russ. Chem. Revs.*, 49, 14 (1980).
45. Kirk-Othmer Encyclopedia of Chemical Technology, 2, 3rd ed., Wiley, p 16, 1978.
46. A. Baiker and W. Richarz, *Ind. Eng. Chem. Prod. Res. Dev.*, 16, 261 (1977).
47. A. Baiker, W. Caprez, and W.L. Holstein, *Ind. Eng. Chem., Prod. Res. Dev.*, (1983).
48. A. Baiker and W. Richarz, *Tetrahedron Lett.*, 22, 1937 (1977).
49. A. Baiker and W. Richarz, *Helv. Chim. Acta*, 61, 1169 (1978).
50. V.A. Nekrasova and N.I. Shuikin, *Russ. Chem. Rev.*, 34, 843 (1965).
51. E.D. Schwegler and H. Adkins, *J. Am. Chem. Soc.*, 61, 3499 (1939).
52. A.P. Sharratt, PhD Thesis, University of Surrey, Surrey, 1991.

53. A.Baiker, *Ind.Eng.Chem.Prod.Res.Dev.*, 20, 615 (1981).
54. J.R.Anderson and N.J.Clark, *J.Catal.*, 5, 250 (1966).
55. R.J.Card and JL Schmitt, *J.Org.Chem.*, 46, 754 (1981).
56. J.D.Lee, "Concise Inorganic Chemistry", 4th.ed.; Chapman & Hall: London, 1964.
57. A.L.Smith, *Spectrochem. Acta*, 16, 87 (1960).
58. N.B.Colthup, L.H.Daly and S.E.Wiberley, "Introduction to Infrared and Raman Spectroscopy", 2nd.; Academic Press: New York, London, 1975.
59. G.C.Addison and B.M.Gatehouse, *J.Chem.Soc.*, 1, 613 (1960).
60. G.Socrates, "Infrared Characteristic Group Frequencies"; John Wiley & Sons: Chichester, 1980.
61. Powder Diffraction File, Joint Committee on Powder Diffraction Standard(JCPDS)-ICDD, Copyright(C) 1986.
62. M.Houalla, F.Delannay, I.Matsuura and B.Delmon, *J.C.S. Faraday I*, 76, 2128 (1980).
63. L.Zhang, J.Lin and Y.Chen, *J.Chem.Soc.Faraday Trans*, 88, 2075 (1992).
64. S.A.Stevenson, J.A.Dumesic, R.T.K. Baker and E.Ruckenstein, "Metal-support Interactions in Catalysis, Sintering and Redispersion"; Van Nostrand: New York, 1987.
65. A.B.Littlewood, "Gas Chromatographic, Principles, Technique and Applications"; Academic Press: New York, London, 1962; p 294.
66. G.Webb., *Catal. Today*, 7(2), 139 (1990).

